personal buildup for

Force Motors Ltd.

ATZ .worldwide 12/2008 released on n.a.

ATZ

WORLDWIDE

12 | December 2008 Volume 110

www.ATZonline.com

Dual-clutch Transmissions in Transaxle Design

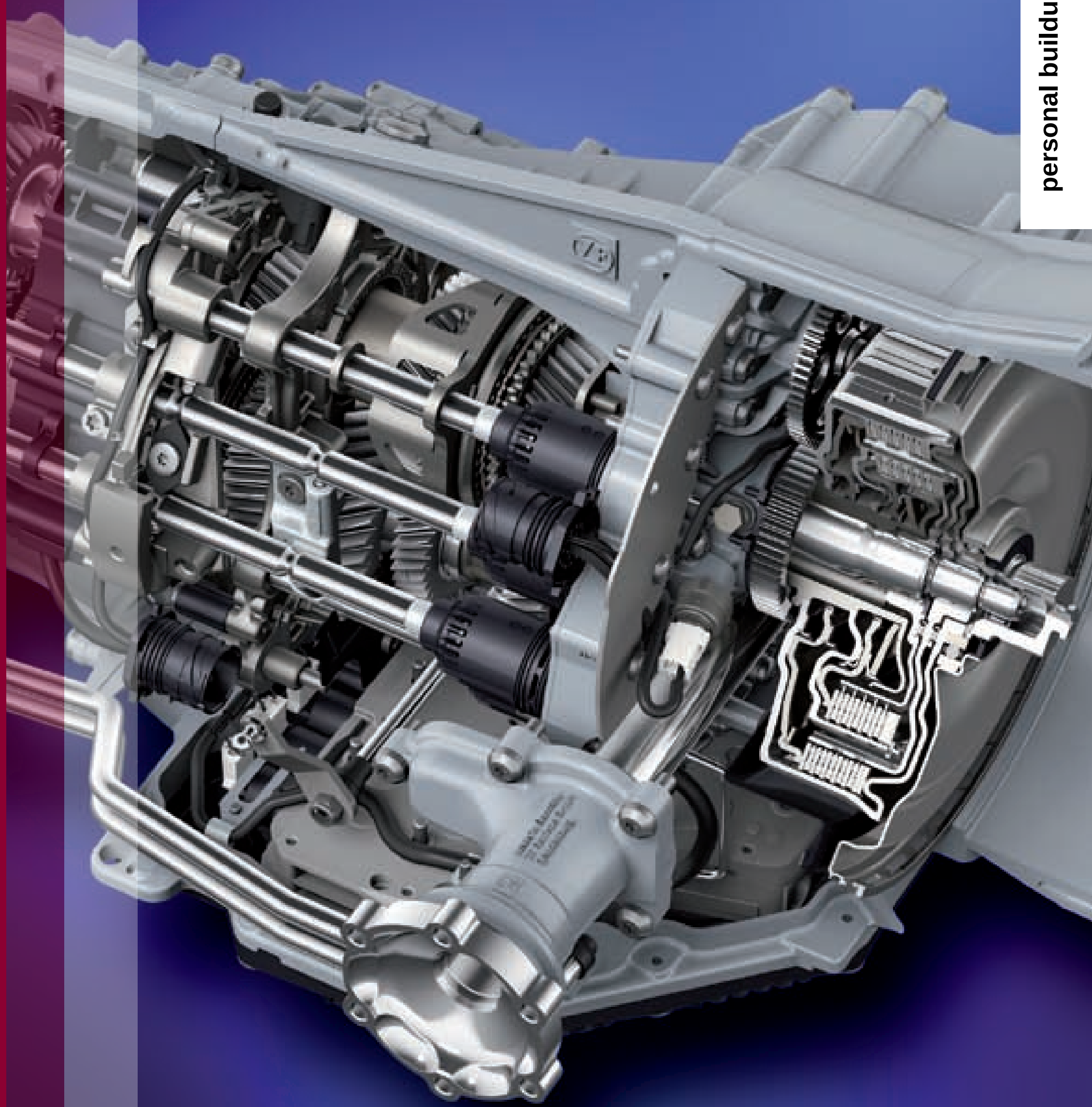

Torque Vectoring with Electro-hydraulic Actuation

Micro-mild Hybrids Using Ultra-cap Technology

Torque Optimized Spur Gear Differential – Perspective for Reduced Size and Weight

SEA Modelling for Sound Package Development

Analysis of Driver Behaviour and Implementation Strategies of Assistance Systems

Prediction of Virtual Interior Noise

INTERVIEW

»Emerging Economies are Characterised by Dynamic Growth«
Dr.-Ing. Bernd Bohr, Bosch

For more information visit:
www.ATZonline.com

COVER STORY

Dual-clutch Transmissions in Transaxle Design

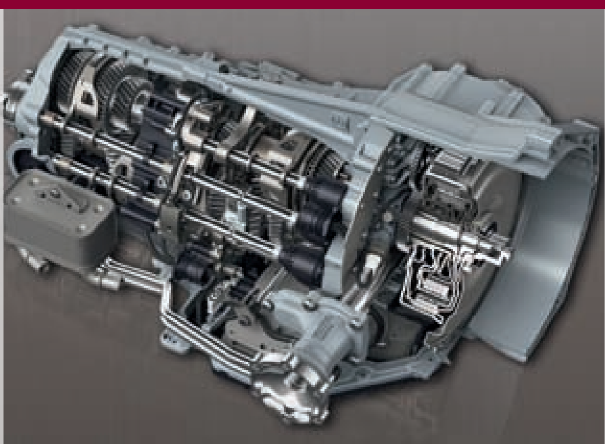

4

The wellknown seven-speed **Dual-clutch Transmission** by ZF has been extended and now forms a transaxle kit for various installation positions and torque categories. The kit comprises automatic transmissions as well as the correspondingly derived manual transmissions. Gear set structure, bearing concept, and structure are illustrated.

Reached Your Goal?

Dear Reader,

It's so reassuring, at the end of a car journey, to hear my navigation system say "You have reached your destination". In life, however, such confirmation of having reached a certain goal is often lacking. As Christmas draws near at the end of this turbulent automotive year, I have to admit, like many others in our industry, that I haven't achieved everything I wanted to.

Is that already failure? It would certainly be hubris if someone were to claim that they had totally foreseen the dramatic events that have taken place since the summer. Life teaches us again and again that goals are set in certain framework conditions. And in such an interwoven world as ours, no-one can achieve their goals all by themselves. As soon as conditions change – and this is something that we are currently experiencing in every aspect of our business: purchasing behaviour, the economy, political constraints – it is no longer the absolute goal itself that matters, but how much closer we have come to our long-term vision.

Keeping a number 1 position, closing in on the technology leaders or simply helping a company to survive in difficult times – sometimes this requires even greater achievements than those expressed in performance figures like EBIT.

This year, ATZ has initiated many new projects. Our Worldwide edition is no longer published as a printed supplement but in real time as an e-magazine, complete with all the images. Our new magazine ATZproduktion now offers valuable support to production engineers. At the same time, we have further consolidated the scientific standard of our magazines by introducing a peer review process.

I am sure that this will help to keep us in pole position when it comes to providing technical information in the automotive sector. Thank you for your constructive support. See you again in 2009!

Johannes Winterhagen
Frankfurt/Main, 16 November 2008

Johannes Winterhagen
Editor-in-Chief

ATZ WORLDWIDE
12|2008

Organ of the VDI-Gesellschaft Fahrzeug- und Verkehrstechnik (FVT)

Organ of the Forschungsvereinigung Automobiltechnik e. V. (FAT) and of the Normenausschuss Kraftfahrzeuge (FAKRA) in the DIN Deutsches Institut für Normung e. V.

Organ of the Wissenschaftliche Gesellschaft für Kraftfahrzeug- und Motorentechnik e. V. (WKM)

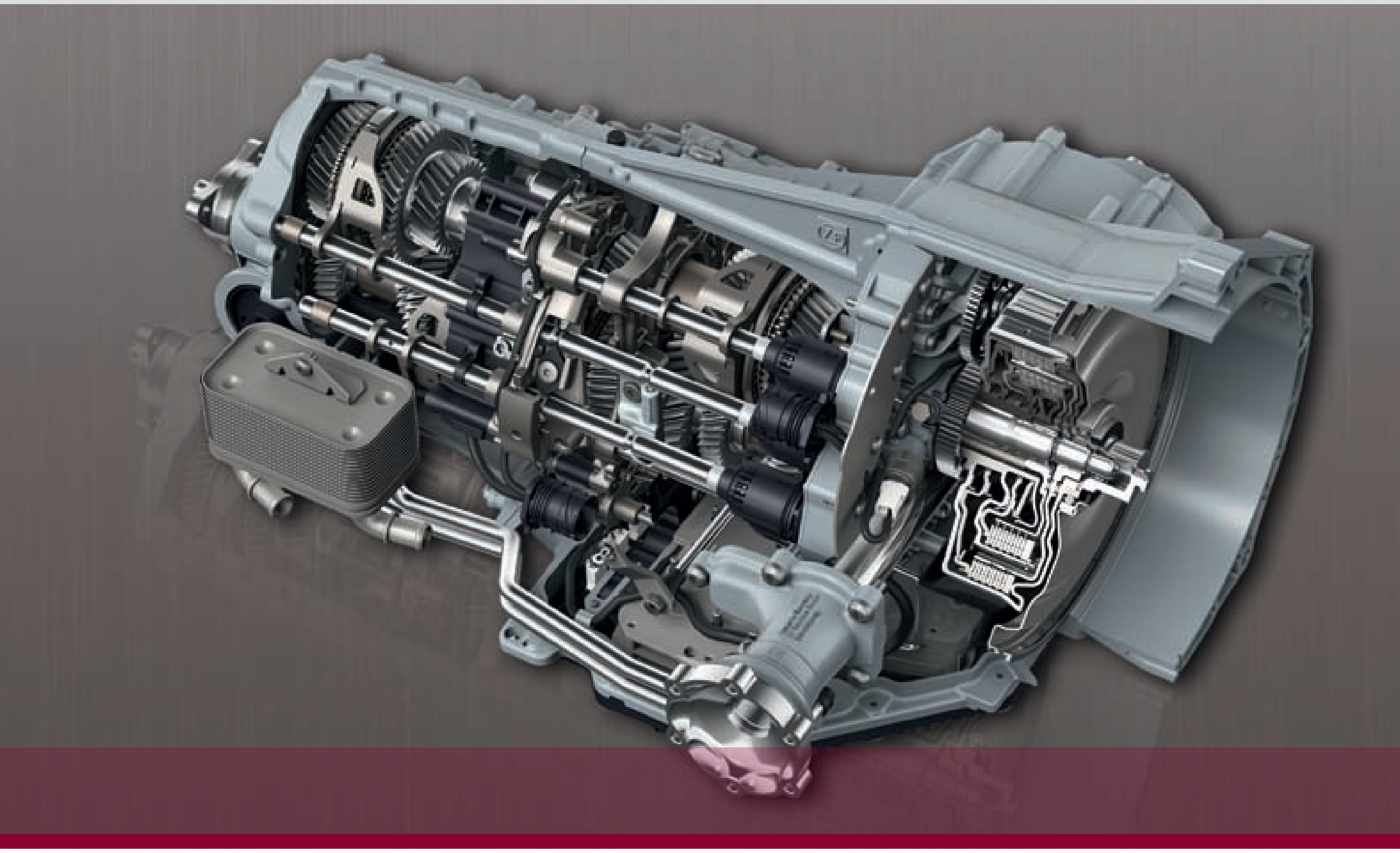

New Seven-speed Dual-clutch Transmissions in Transaxle Design

The transaxle construction is actually the designation for a transmission model where the vehicle transmission, the differential transmission, and the axle drive are located in one housing. It is primarily used with sports cars. The well-known seven-speed dual-clutch transmission by ZF has been extended and now forms a transaxle kit for various installation positions and torque categories. The kit comprises automatic transmissions as well as the correspondingly derived manual transmissions. Gear set structure, bearing concept, as well as the structure of the transmission are illustrated. Special requirements of a transmission intended for high dynamics and the respective shift times are presented. The scope of application is presented for these transmissions vis-à-vis the converter planetary transmissions developed by ZF.

1 Introduction

Today, car buyers can choose from different transmission variants. If they want a full automatic transmission, the offer will comprise a multi-ratio automatic transmission with planetary gear sets, a CVT, or a dual-clutch transmission, depending on the vehicle manufacturer. In sporty applications, dual-clutch transmissions feature benefits that have led to corresponding demand and an individual product range at ZF. With the new modular kit for dual-clutch transmissions, together with the also newly engineered automatic planetary transmission, ZF is able to offer the suitable transmission to suit the vehicle characteristics, providing optimal performance and lowest possible fuel consumption.

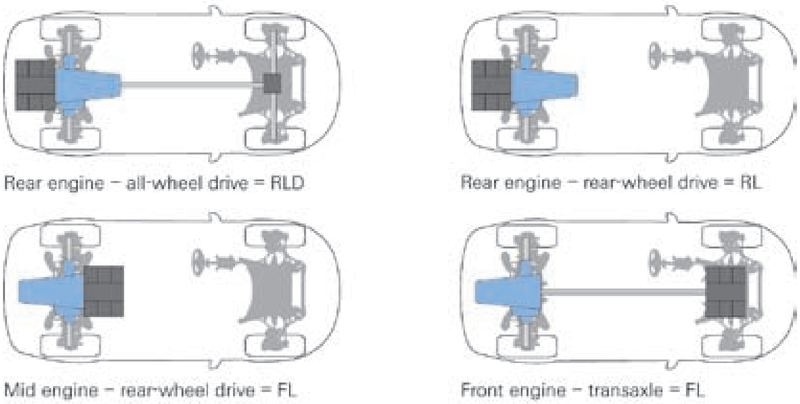

Figure 1: Schematic illustration of the modular concept for various powertrain concepts and installation positions of the dual-clutch transmission – the dual-clutch transmission of ZF can be used for all drive concepts, from middle engine / rear wheel drive to front-longitudinal engine with rear-wheel drive

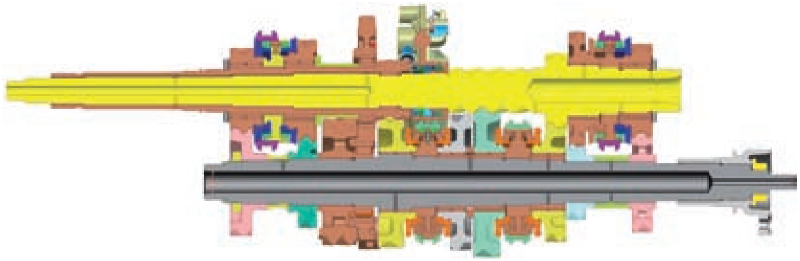

Figure 2: Section view of the gear set

2 Modular Concept

Particularly in the sports car sector, in addition to the transmission for the standard drive described under [1], there is a demand for transaxle transmissions (designation for a transmission design where the vehicle transmission, differential transmission, and axle drive are located in a housing) in longitudinal installation for both, pure rear wheel drive as well as all-wheel drive. The engine can either be located in front of or behind the transmission. In addition to these installation variants, they are also designed for various torque classes. ZF meets these complex requirements by offering a modular principle. A gear set which has been optimized for the torque limit and an axle drive are combined with a housing which is adapted to the installation and a standard control unit. Depending on the torque category, two variants of the dual-clutch transmission are available with the same structure but different diameters. If necessary, a manual transmission can be derived from the kit, using identical parts from the dual-clutch transmission for gear set and axle drive. Some of the possible combinations (modular concept) are illustrated in **Figure 1**. First series application was in 2008 with the 7DT45 HL in the torque category of up to 450 Nm.

3 Gear Set Concept

The center distances and installation lengths of the gear set, **Figure 2**, were selected for a maximum engine torque of 700 Nm and a maximum input speed of 8000 rpm. Differentiation between both torque classes is done via material selection and gear finishing. The ratings for both transmission ranges 7DT45 and 7DT70 can be found in the data sheet in the **Table**, the gear set pattern is illustrated in **Figure 3**. As it is required with dual-clutch transmissions, the even and uneven gears are distributed among one sub-transmission each [2].

The reverse gear is in the same sub-transmission as the 1st gear and the extension of the first gear is used as a fixed gear [3]. This has the advantage that reversing can also be initiated with the big clutch and, without extending the transmission, a ratio can be implemented which nearly corresponds to that of 1st gear. This leads to the same starting quality in reverse gear as in the forwards gear and the driver is not surprised by different tractive power even though the accelerator pedal may be in the same position. A disadvantage, however, is that when reversing D-R or R-D, one process is required each for deselecting, synchronizing, and selecting, which leads to slightly increased shift times with a pure comfort calibration.

Figure 3 also shows that a center support became necessary for the shafts due to the high torques and large installation length. An additional bearing plate in the level surface next to the output con-

The Authors

Dr.-Ing.
Ulrich Remmlinger
is head of product engineering dual-clutch transmissions at ZF Getriebe GmbH in Kressbronn (Germany).

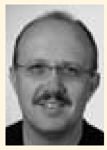

Dipl.-Ing. (FH)
Manfred Fischer
is project manager dual-clutch transmissions at ZF Getriebe GmbH in Kressbronn (Germany).

Dipl.-Ing.
Jens Patzner
is head of product engineering manual shift transmissions and basic transmissions for dual-clutch transmissions at ZF Getriebe GmbH in the production plant Brandenburg (Germany).

stant reduces forcing back of the shaft, thus preventing gearing noise which would result from mal-positioning due to shaft deformation. The constructive design of the tubular shafts can be seen in **Figure 4**. It also becomes obvious in the section view, Figure 2, that all free spinning gears of the gear set run on needle bearings with a separate inner race. This design was chosen because the axial play of the free spinning gears then only depends on the longitudinal tolerance of the inner race and can thus be kept small. If the needles ran directly on the shaft, this would lead to axial clearance which is the sum of the tolerances across the entire shaft length. The reduction of axial clearance and thus backlash is an important contribution to the sportiness behaviour of the transmission. As shown later on, small angular clearance is a decisive factor for the subjective impression that the vehicle is very responsive.

To attain a high level of power density, the gears and shafts are produced according to special ZF supply specifications from case-hardened steels, for which the over years at ZF established SIN curves are available. The counter shaft for the rear-longitudinal (RL) transmission is cold-extruded from a tube and the material is thereby stretched both in radial and axial direction. In the all-wheel drive version with an additional output, the shaft is too long to use this new technology. Therefore, the all-wheel drive version is manufactured conventionally with deep-hole drilling.

When selecting the synchronizers, the requirement for sportiness with short shifting times was met by using linings with a high admissible synchronizer performance. For gears 1, 2, 3, and reverse (R) gear, these are triple synchronizers with powder sinter linings. For gears 4, 5, 6, and 7, simple synchronizers with carbon linings are used. Moreover, to protect the linings, the energy input due to drag torques during the synchronizing process is kept at a small level. This is ensured by a continuous, requirement-based control of the coolant flow, which flows through the open clutch. During the synchronizing procedure, the cooling oil flow is interrupted for a short time.

Table: Data sheet of the new seven-speed dual-clutch transmission – models 7DT45 with 450 Nm and 7DT70 with 700 Nm input torque (all data is based on ZF design cycle)

Feature	Value or item		
Übertragungsfähigkeit		7DT 45	7DT 70
Torque capacity	$T_{max,\ engine}$ at 4200 rpm	450 Nm	700 Nm
	n_{max}	8000 rpm	7500 rpm
Starting element	Dual clutch ND 2014 to 450 Nm and ND2216 to 700 Nm		
Gears	7		
Center distance	85 mm		
Spreading	6.335		
Ratios	3.909 – 2.929 – 1.654 – 1.303 – 1.081 – 0.881 – 0.617 ; R = -3.545		
Transmission steps	1.335 – 1.771 – 1.269 – 1.205 – 1.227 – 1.428		
Axle ratio	3.444		
Selector lever positions	P, R, N, D; electric shift mechanism, cable-controlled parking lock		
Control system	Hydraulics with external ECU; controlled powershifts; various shift programs		
Weight with oil	RL 450 Nm 115 kg / RL 700 Nm 121 kg		

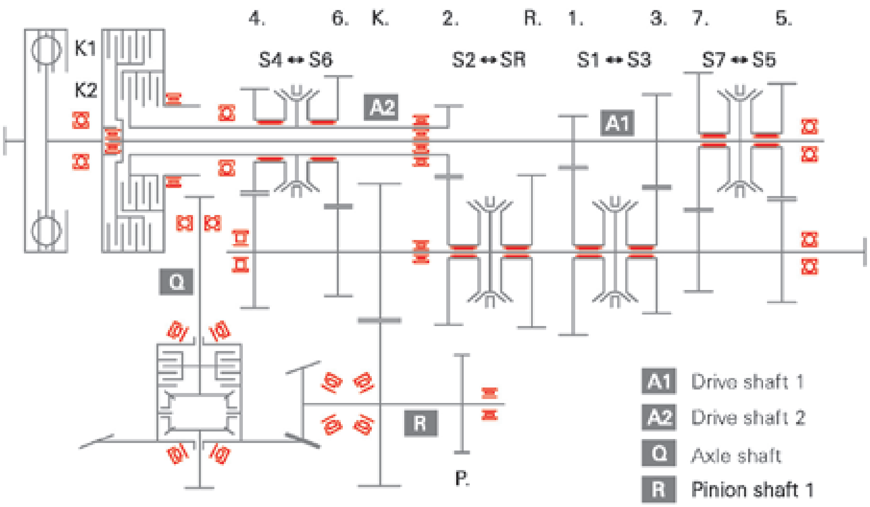

Figure 3: Gear set and bearing pattern

4 Transmission Structure

Figure 5 shows a cutaway view of the entire transmission. The two concentric drive shafts are at the top, the counter shaft with the output constant is underneath, and the pinion shaft with engagement in the ring gear is at the side. The parking lock is located at the end of the pinion shaft. The axle drive with differential and flange shafts is located transversal to transmission, through the ring gear. Optionally, the transmission can also be supplied with a mechanical differential lock. For transmissions for all-wheel drives, the additional output is implemented at the end of the main shaft. The control unit is at the bottom of the transmission.

Since the axle drive with the bevel gear set requires the use of a hypoid oil, which is not suitable for use with the starting clutch, however, two separate oil chambers had to be designed. Both oil chambers with separation are illustrated in **Figure 6**. The clutch oil was selected in combination with the friction linings of the starting clutch. This first oil chamber with 5.5 liters

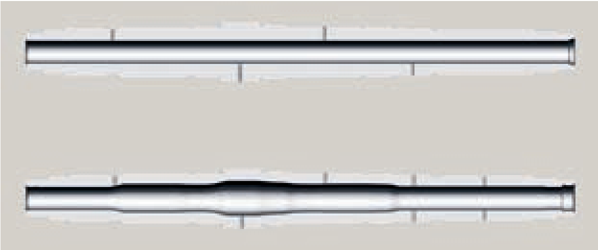

Figure 4: Tubular shafts as main shaft in all-wheel drive version as well as the main shaft, cold-extruded in the version without additional output

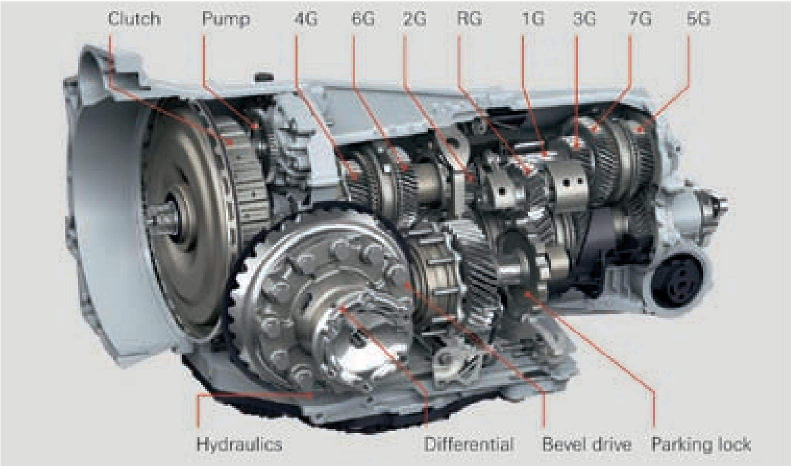

Figure 5: Dual-clutch transmission (all-wheel drive version) with seven gears 1G to 7G and reverse gear RG

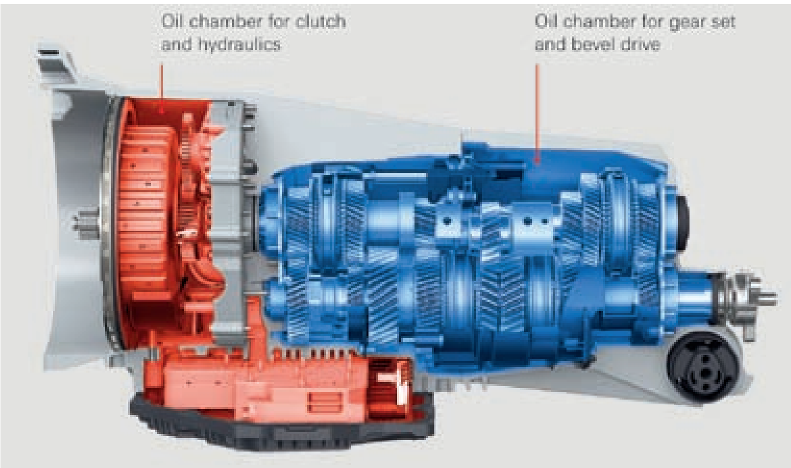

Figure 6: Oil chamber separation

comprises the clutch, pump, hydraulic control unit, gearshift rod cylinder, oil filter, and oil pan. A second oil chamber is in the housing part which contains the gear set and bevel gear. It is filled with 3.0 liters of hypoid oil. Double radial shaft seals with relief bore ensure safe separation of the oil chambers. No additional pump is planned for the second oil chamber. Therefore, the oil drip channels and oil baffles, **Figure 7**, known from the manual transmission must be used in order to ensure sufficient lubrication and cooling of the gear set.

Additional components, such as the dual clutch, the pump, and the valves of the hydraulic control unit are identical to those of other ZF dual-clutch transmissions and have already been described in [1]. Regarding the clutch, it must be mentioned that the control of the cooling oil flow in line with the requirements provides the enormous cooling power required for a racing start, but also reduces the oil flow in constant operation to such an extent that drag torques, splash losses, and splash of oil are minimized. The cooling power required is continuously calculated in the software by means of an online temperature model.

5 Design for High Level of Dynamics

In addition to a low power-to-weight ratio of the vehicle, the following features must be available among others, so that the driver rates the driveline response as being sporty:

1. Fast acceleration change with transient changes of drive power („vehicle is responsive“)
2. Smallest possible backlash, meaning no lag time in the case of traction/thrust changes
3. Short shifting times
4. Sporty shift program which allows for driving in low gear with high traction reserve, if the driver wishes to do so
5. Upshift prevention before bends and with delayed overtaking maneuvers.

The quick response claimed in item 1 requires a dynamic driveline with a high natural frequency. The latter is determined by the mass moments of inertia which are shown in **Figure 8** for a sporty sedan. Even in the first gear, the masses which can be influenced by the transmission are low compared with the vehicle mass relating to the input shaft. The limitation in transmission installation length in the sports car exacts the alignment of both clutches one above the other in the transmission. This means that further reduction of rotating mass in the dual clutch is not possible. With the dual-mass flywheel (DMF), a reduction would be allowed if it was possible to reduce irregularities in terms of engine excitation. Furthermore, the natural frequency of the driveline is determined by its spring stiffness. Here, for the first natural frequency, exclusively the drive shafts have an impact on the wheels, the rest of the driveline is stiff. When selecting the stiffness of the drive shafts, however, their impact on the longitudinal and pitching natural frequency in particular is to be considered in combination with the transmission sus-

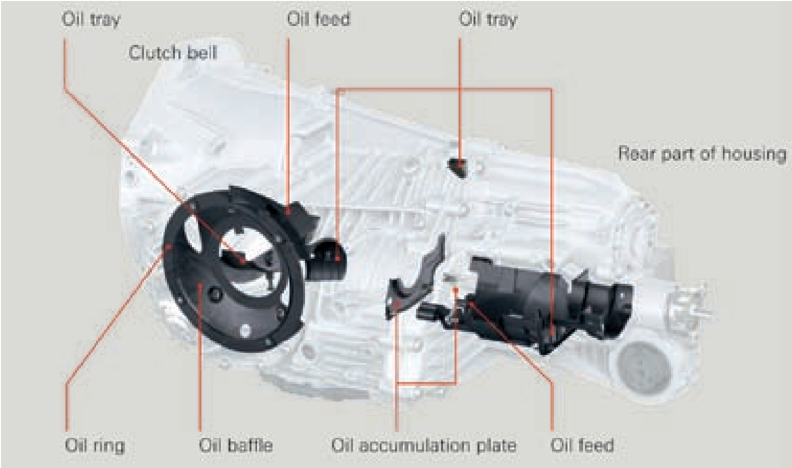

Figure 7: Oil baffles

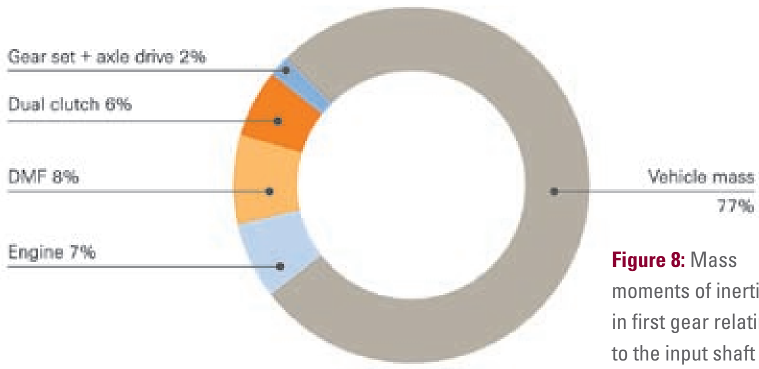

Figure 8: Mass moments of inertia in first gear relating to the input shaft

pension. If it is designed incorrectly, this can lead to unpleasant vibrations during starting with a resonance peak [4]. In terms of spring stiffness, the second natural frequency is dominated by the torsional damper. Here again, slight engine excitations allow for the design of a dynamic driveline with a stiff torsion spring.

The dynamics achieved by the dual-clutch transmission is compared in **Figure 9** with that of a converter transmission. Here, the torsion angle between transmission input and output was calculated for a specified rev-up with a vibration simulation and standardized to the value of the dual-clutch transmission. It can be seen immediately that the slip in the converter decisively worsens the dynamics, which is perceived by the driver as a „spongy" response. Thus, after starting, the lock-up clutch would have to remain permanently closed to ensure that the converter transmission achieves the dynamics of a dual-clutch transmission. This is not possible with the converter transmissions currently available on the market because the damping element in the converter clutch does not have the quality of a dual-mass fly wheel and there are driving situations in which the open converter is required to decouple vibrations. The measures to reduce clearance as mentioned in item 2 have already been described in Chapter 3 for the gear set. The backlash in the bevel gear is set with a narrow tolerance during assembly. The other backlash settings in the drive shafts are determined by the OEM irrespective of the transmission.

The short shifting times demanded in item 3 constitute the most important criterion for a sporty transmission. For the first time, a new speed control concept is used with the 7DT45 in series, to achieve even shorter shifting times. In multiratio automatic transmissions, the engine torque during shifting is usually influenced in the speed adaptation phase by a CAN signal sent to the engine control so that the desired speed gradient is realized. With the 7DT45, control in this phase is transferred to the engine control unit, which will set a prescribed target rpm for the engine. The hydraulic control unit with pre-controlled valves also contributes to the short shifting times described in [1]. Very short shifting times are realized by the interaction with the four position sensors on the gearshift rods and the cumulative effect of these measures, which are compared in **Figure 10** with measurement values from competitor transmissions. When comparing shift times, it must be considered that these depend strongly on the selected setup. The differences between a comfort shift and a sporty upshift with peak traction have already been illustrated in [1]. Sporty shifts with similar rpm gradients are taken for this comparison. It immediately becomes obvious that with the traction upshifts, the dual-clutch transmissions and modern automatic transmissions from ZF have a head start compared to the competitors' conventional converter transmissions. A system-inherent disadvantage of dual-clutch transmissions makes itself felt during downshifts across two gears with the competitors' transmission. The new gear cannot be pre-synchronized because it is located in the same sub-transmission as the driving gear, which results in longer shifting times. With the 7DT45, this drawback is largely compensated by the described rpm control measures. In the sports and supersports program, the high rpm gradients which are possible with the 7DT45 control unit are fully utilized. All gear changes run equally quickly without any difference and thus set a new reference for sportiness.

The functions and features demanded under item 4 and item 5 must be considered in the driving strategy. Here, the dual-clutch transmission benefits from the experience made with the 5HP and 6HP transmissions by ZF and can take over the software functions for the driving strategy and hill detection with only few changes. Especially the upshift prevention by the „fast off" function, which processes the gradient of the accelerator pedal change, suits the character of a sports car very well. Since the software design is modular, an individual driving strategy program of the OEM can be incorporated upon request. The racing start, another function to support the sportiness offered by the transmission, has already been described in [1].

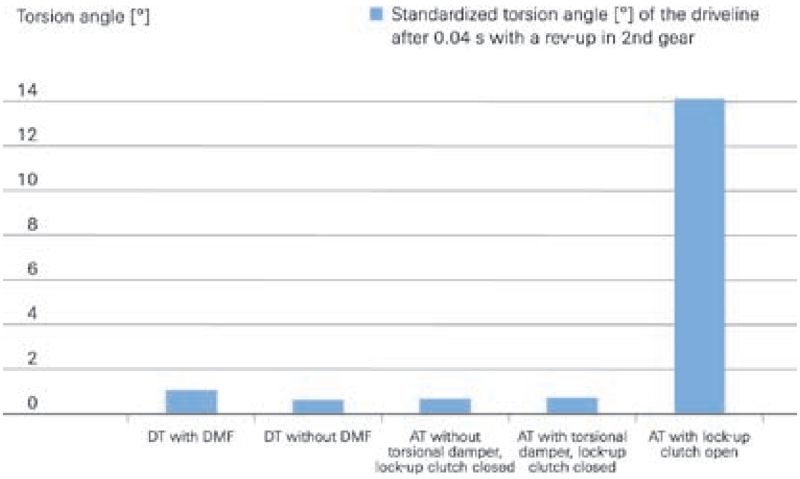

Figure 9: Standardized torsion angle of the driveline after 0.04 s with a rev-up in second gear

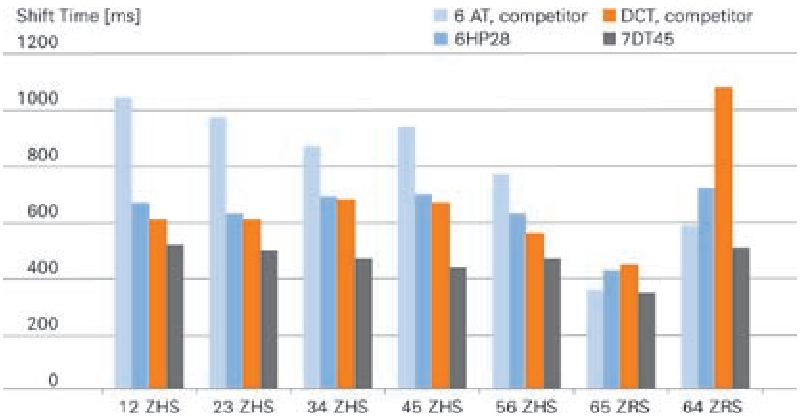

Figure 10: Comparison of different sports program shifting times (example: 12 ZHS means: traction upshift from gear 1 to 2)

6 Transmission Losses

The future legislation on CO_2 emissions will make no exceptions for sports cars, so the demand for a high transmission efficiency will gain even more importance. The dual-clutch transmission has the potential of achieving the same high level of efficiency in all gears, similar to the characteristics of a manual transmission. However, this requires careful optimization of the details of all individual components. In contrast to the manual transmission, the dual-clutch transmission requires an oil pump, which is designed as an axially parallel internal-gear pump with small diameters and the smallest possible play in order to achieve good efficiency. Moreover, compared with manual transmissions, there is an additional open clutch with the dual-clutch transmission which generates drag torque. This loss can be kept at a small level if a sufficient air gap is provided for and the coolant flow can be controlled in terms of time and quantity.

With the dual-clutch transmission, the efficiency not only depends on the selected gear, rpm, and oil temperature, but also on the gear pre-selected in the other sub-transmission. For the measurement, the next highest gear was pre-selected at 1500 rpm; for lower engine speeds and in seventh gear, the downshift was prepared. Especially in second gear it becomes clear how the pre-selection of the lower gear below 1500 rpm leads to higher speeds in the other sub-transmission due to the high gear step, thus generating higher drag torques. In general it can be said that the losses in gears 2 to 6 are very close together, similar those of a manual transmission, and they do not exceed the relevant area of 8 % for the fuel cycle.

With a planetary transmission, the gear-dependent losses vary more strongly, depending on the design versions and the gear set system used. In addition, compared with the planetary transmissions, it becomes obvious for similar performance ranges that the transmission losses above the speed only rise slightly with dual-clutch transmissions. When using the transmission with a sporty driving style in a vehicle with a high-revving engine, this behavior has a very favorable impact on consumption.

7 Summary

According to these explanations, there is a clear delimitation for the use of dual-clutch transmissions with a longitudinal design. Dual-clutch transmissions have advantages when used with high-revving engines, in terms of shift times and the stiffness of the driveline. Compared with converter transmissions, they lead to smaller losses, which allow for more favorable fuel consumption and better acceleration values in the vehicle. In terms of travel after 4 s, converter transmissions are still unbeatable due to their gain in traction in the torque converter, especially when it comes to vehicles which are weakly motorized. With the new generation of ZF's 8HP transmissions, the converter transmission will catch up in terms of performance and consumption. Therefore, it is in the market segment for sports cars and sporty sedans where the benefits of dual-clutch transmissions take effect. Since the volumes in this segment are limited, a kit with a high share of equal parts was the right response to the requirements of the different vehicle concepts.

References

[1] Kubalczyk, R.; Ebenhoch, M.; Schneider, H-J.: 7-Gang-Doppelkupplungsgetriebe für sportliche Anwendung. [7-Speed Dual-Clutch Transmission for Sporty Applications.] VDI-Berichte Nr. 1943, Düsseldorf, 2006

[2] Patentanmeldung DE 10 2005 058 946 A1

[3] Patentanmeldung DE 10 2005 005 163 A1

[4] Böger, T.; Pfingst, J.; Kurrle, F.; Krüger, A.: Entwicklungsmethodik zur Optimierung des Anfahrkomforts bezüglich Gesamtfahrzeugschwingungen. [Development Method on the Optimization of Starting Comfort in Terms of Overall Vehicle Vibrations,] VDI-Berichte Nr. 1987, Düsseldorf, 2007

Dr.-Ing. Bernd Bohr
Chairman of the Automotive Group, Bosch

"Emerging Economies are Characterised by Dynamic Growth"

Regarding the segment of low-price vehicles, how does Bosch plan to achieve comparatively lower prices while maintaining the high quality required? This is only one topic ATZ discussed with Dr.-Ing. Bernd Bohr, Chairman of the Automotive Group, Bosch. Further topics of the debate were emerging markets, lithium-ion batteries and the future prospects of the internal combustion engine.

ATZ How would you describe the ideal cooperation between an OEM and a supplier?

Bohr I can put it into three words: early, intensive and collaborative. Very close cooperation with our customers during the early development phase results in innovative, cost-effective and efficient technical solutions. In particular, the OEM benefits not only from our experience in automotive technology but also from our knowledge of the markets in different regions worldwide. Good examples are projects such as the Tata Nano, which not involved meeting new market requirements but also demanded a high level of local content in development and manufacturing. The experience of our Indian engineers and their worldwide networking with other development centres are the basis for meeting these challenges regarding quality at very low costs.

ATZ Are you developing completely new products or are you redesigning existing concepts for the low-cost market?

Bohr We are currently pursuing three different approaches. Firstly, the "top down" approach is the quickest and simplest solution. It involves a targeted simplification of standard products. It is often the case that certain components and functions that will not be used in low-price vehicles anyway can be completely eliminated. Secondly, the "bottom up" approach – for example expanding the scope of functions and systems of a motor cycle engine management unit in order to adapt it to the requirements of a car. Thirdly, we supply the market with new products that are specifically designed for low-price vehicles.

"We can manage the short development times with our corresponding capacities"

ATZ How will the comparatively lower price be achieved while still maintaining the high quality required?

Bohr It will certainly not be achieved by reducing quality. But definitely with specifications that have been adapted by the OEM to suit the requirements of the market. Furthermore, we can only achieve that with innovative technology concepts that concentrate on what is absolutely necessary. Local manufacturing and local procurement are important elements. In such cases, we can make use of locations with decades of experience in countries like India, Brazil or China. And ultimately we will achieve it with the prospect of large production volumes in a highly interesting market. With this strategy, we will also succeed in achieving similar returns in the low-price segment as we do in supplying established markets.

ATZ What are the special requirements of the growing markets in India and China?

Bohr Including our software activities, we employ more than 18,000 people in India. In China, the figure is around 19,500. We have significant growth in these markets in particular – in 2007, our sales in India rose by 15 % and in China by 35 %. The increasingly strict emissions limits require state-of-the-art automotive technology, which means that our sales will increase even further. In addition, car makers in these markets – to a greater extent than OEMs in established markets – expect Bosch to supply complete concepts and not only components and applications. In this context, time-to-market also plays a key role, as emerging economies are characterised by particularly dynamic growth. We can manage the short development times with our corresponding capacities in the region and with the appropriate market knowledge.

ATZ What influence do the rising raw material prices have on profits in your sector?

Bohr The rapid and high increase in raw material prices has a major influence on our earnings. As 2008 was the third year in succession with rising prices, we are forced to pass on a part of these extra costs – and in some cases all of them – to our customers. It goes without saying that such discussions are not easy.

ATZ Your joint venture with Samsung produces lithium-ion batteries. For which OEM is the battery pack being produced?

Bohr Our 50:50 joint venture with Samsung started work under the name SB Limotive on September 1, 2008. It combines the expertise of Samsung as one of the world's leading manufacturers of lithium-ion batteries for consumer electronics with the comprehensive experience of Bosch in automotive and hybrid technology. In 2010, we plan to start large-scale production of lithium-ion batteries and to produce complete battery packs from 2011 onwards. We are already talking to our later customers, but we won't be able to talk about them until later.

ATZ Some well-known OEMs have announced that they plan to launch electric cars by 2012. You have said that a range of between 200 km and 300 km is possible without recharging the battery. How and by when do you want to achieve this?

Bohr Our forecasts for electric vehicles are conservative. For 2015, we expect a worldwide market of just over 350,000 electric vehicles and plug-in hybrids, and for 2020 we are expecting the figure to be 1.5 million units. These are vehicles with an electric drive system or with an additional internal combustion engine as a range extender. The preconditions for achieving these targets are a significant increase in the energy and power density of lithium-ion batteries, lightweight vehicles and, not least, car buyers for whom a range of 200 km to 300 km before recharging is sufficient.

"Engine technology for petrol and diesel still has considerable potential"

ATZ With your lithium-ion batteries you are focusing on electric drive systems. Together with Mahle you have entered the turbocharger business. Which drive technology has the greater perspective for you?

Bohr We are convinced that the electric drive system will dominate in the long term, particularly when it uses electricity from regenerative energy sources. Until then, however – and we are talking about time periods over the next twenty years – the internal combustion engine will be dominant in vehicles, particularly from a worldwide perspective. Engine technology for petrol and diesel still has considerable potential regarding fuel consumption and emissions, and Bosch engineers will implement this in series production over the next few years. Bosch Mahle Turbo Systems can look confidently into the future.

ATZ Dr. Bohr, it has been a pleasure talking to you.

The interview was conducted by Roland Schedel.

Dr.-Ing. Bernd Bohr

has been a member of the Board of Management of Robert Bosch GmbH since July 1, 1999. He has corporate responsibility for quality, and divisional responsibility for the Chassis Systems Brakes, Chassis Systems Control, Diesel Systems, and Gasoline Systems divisions. He has been chairman of the Automotive Group since mid-2003. He also has regional responsibility for India. Bernd Bohr was born in Mannheim (Germany) on September 7, 1956, and is married. After leaving school in 1975, he studied Production Engineering at the University of Aachen, taking his diploma examination in 1982. He received his doctorate in Engineering at the same university in 1983.

Micro-mild Hybrids Using Ultra-cap Technology

Hybridization requires energy storage elements even for the first steps like micro-hybrids. The level of hybridization determines directly the energy storage solution. Furthermore, the energy storage solution influences strongly the global cost of the system. For electrical vehicles, the cost of the battery exceeds 70 % of the hybridization costs. This fact has pushed the choice of Valeo to offer a intermediate micro-mild solution based on ultra-capacitors in order to optimize the costs of the system.

1 Global Warming and the Concern of Rising Oil Prices

Awareness of global warming due to CO_2 emission has been rising in developed countries since the 1990's. In particular, road traffic is often cited by public opinion as one of the most responsible of CO_2 emissions. If we consider recent figures, private cars generate 12 to 16 % of the total CO_2 emissions in Western developed countries. At world levels, this ratio goes significantly down due to a lower global equipment level and the large use of fossil energy as the main energy source in emerging countries. The significant share of CO_2 emissions linked to road transportation in developed countries and the economic impact of recently rising oil prices justifies the efforts made to improve fuel economy in automotive applications.

2 CO_2 Reduction and Regulations

CO_2 reduction has also become a concern for governments due to environmental concerns and oil dependency. Developed countries have or are preparing regulations to accelerate this movement. As displayed in **Figure 1**. despite of different fuel consumption targets in Europe, the United States and in Japan, the targets are ambitious compared to the present situation and represent CO_2 reductions of up to 30 % over the next five years.

Hybridization of the powertrain is one solution towards improving the overall vehicle fuel economy. This technology has introduced new functions at vehicle level.

3 New Functions Introduced by Hybridization

3.1 Stop-Start

This function can be summarized as the possibility to stop the engine during idle mode and to restart it quickly when required. By implementing this function, the engine can be stopped for short periods of time in urban traffic when the vehicle is stopped. Stop-Start is the first step of hybridization and is common to all hybrid systems. The end user is able to appreciate directly this function since no engine noise or vibration is produced at idle.

3.2 Regenerative Braking

This function recovers energy during vehicle coasting or braking phases. An electrical machine is used to slow the vehicle and the energy recovered is stored in energy storage elements like batteries or ultra-capacitors. Energy is saved instead of being lost in the brakes (transformed to heat). Energy recovered by regenerative braking can be used to supply the electrical network of the vehicle or to supply the torque assistance function. This function may not be fully perceived by the end user since it may not be possible to distinguish the effect of classical braking using either the friction brakes or engine brake from braking with the electrical machine.

Figure 1: CO_2 regulations

3.3 Torque Assistance

Since hybridization has been introduced through an electrical machine in the powertrain, this electrical machine can be used to act in motor mode and provide extra torque and power to the thermal engine. Torque assistance and regenerative braking are often introduced together on the vehicle. This function can be used for example to increase the available torque at low engine speeds and thus to improve the fun to drive by offering improved acceleration. For the energy balance, torque assistance uses the available energy coming from regenerative braking.

In classical cars, the size of the engine is given by the peak power or the peak torque requirement. This peak power is used only during short periods of time so that the engine runs a low partial load for most of the time. In these conditions, the efficiency of the engine is low due to the friction losses of the large engine. Decreasing the engine size to use the engine at a higher load will improve significantly the engine efficiency and will lower the fuel consumption. This trend of downsizing the engine displacements has started years ago with the implementation of turbo-chargers. Hybridization can now offer to go further in the direction of smaller displacement engines (and also different combustion cycles) by offering the possibility to reduce the peak power of the engine and to complement the engine power by electrical means when the peak power is needed.

3.4 Electrical Drive

In this configuration, the vehicle can move by means of an electrical motor while the thermal engine is off. Energy is provided by energy storage elements and the thermal engine may either not exist (case of electrical cars) or only be turned on when the battery state of charge is too low or when more power is required.

4 Hybridization: a Scalable Approach

Hybrid functions can be classified as shown in **Table 1**. Hybridization functions can be introduced one at a time as the hybrid systems are scaled up to meet greater demand for fuel economy. The advantage of a progressive introduction of hybrid functions is a better management of the cost to performance ratio. The car manufacturer can select up to which level of hybridization it makes sense, compared to other fuel economy solutions. Increasing the hybridization level increases the system costs, in particular the cost associated with energy storage elements (such as batteries).

5 Market Analysis – Interest and Penetration of Hybridization

Anticipating the market share of hybrid vehicles in the future is a difficult exercise as there are any market drivers such as: government regulations, government incentives, the price of oil and vehicle

Table 1: Classification of hybrid vehicles

Naming	Function
Micro-hybrid	Stop-Start function Regenerative braking up to 2 kW
Micro-mild-hybrid	Stop-Start Regenerative braking 4 to 8 kW Torque assistance 3 to 8 kW
Mild-hybrid	Stop-Start, Regenerative braking 8 to 15 kW Torque assistance 6 to 15 kW
Full-hybrid	Stop-Start Regenerative braking 20 to 100 kW Torque assistance 20 to 100 kW Vehicle capable of electrical driving with a limited range
Electrical vehicle	Electrical vehicle with significant range capability (> 100km). Optionally, the vehicle may include a range extension with a thermal engine or a fuel cell

The Authors

Jean-Claude Matt
is P2 R&D Director at Valeo Electric Systems in Créteil (France).

Derek De-Bono
is Marketing Director at Valeo Electric Systems in Créteil (France).

Table 2: Market penetration – CO_2 reduction potential

	Western Europe (2015)			
	Market share (2015)	Fuel economy NEDC	Fleet CO_2 reduction	Pay back distance (km) [(1)]
No hybridization	25,0 %	0 %	0,0 %	0
Micro-hybrids	55,0 %	6 %	3,3 %	48000
Micro-mild-hybrids	10,0 %	10 %	1,0 %	86000
Mild-hybrids	3,0 %	20 %	0,6 %	111000
Full-hybrids	1,7 %	30 %	0,5 %	121000
Electrical vehicles	0,3 %	100 %	0,3 %	462000
		Total	**5,7 %**	

(1) Pay back distance is the distance after which the initial over-cost is recovered by the end customer through fuel savings. Computations have been made for a medium sized gasoline vehicle with a mean consumption of 7 l/100km and a gasoline price of 1.50 €. For mild hybrids, full hybrids and electrical vehicles, cost of battery maintenance is deducted from the savings with an hypothesis of a battery life time of 100000 km. Cost of electrical energy is deducted from the savings of the electrical vehicle.

on-cost influencing the overall trend. Many publications have been made on the subject and in order to evaluate the CO_2 reduction potential, a rough synthesis for Europe is presented in **Table 2**. It can be seen that the likely global fuel economy in 2015 coming from hybridization can reach aver 5 % in Europe. The two first steps of hybridization (micro and micro-mild hybrids) should allow 4.3 % total fuel economy and will concern more than 65 % of all vehicles. These two first steps represent also by far the best performance to cost ratio. Pay back distance is short with a micro-hybrid solution and initial costs are recovered after about 60000 km. For mild hybrids and full hybrids, the pay back distance exceeds 110000 km. And for electrical vehicles the pay back distance even exceeds 400000 kms due to high acquisition costs and high maintenance costs of batteries.

6 Valeo Bottom up Approach for Hybridization

The Valeo strategy towards hybridization is focused on providing solutions for the micro and micro-mild segments first. As shown in the previous section, these two segments provide the best performance to cost ratio and are anticipated to be the segments entering mass production with a high equipment rate. In terms of global fuel economy on a fleet, the best medium term results will be obtained by a large deployment of the first steps of hybridization. This is driven by the good fuel economy to cost ratio of these solutions.

7 The Valeo Road Map towards Hybridization

The Valeo road map, illustrated in **Figure 2**, has started with micro-hybrid solutions composed of the „StARS“ and „i-StARS“ products dedicated to Stop-Start function.

"StARS", based on a classical claw pole machine and a separate power control unit, has been in mass production since 2004. The second generation called "i-STARS" integrates the power inverter on the rear of the machine thanks to a breakthrough in mechatronic technology. Mass production is scheduled for 2010.

For the micro-mild segment, Valeo offers the „StARS+X“ system with a power handling capacity of up to 4 kW. This micro-mild system uses ultra-capacitors as energy storage element and will be detailed in the next sections. Start of production of "StARS+X" is foreseen in 2011.

For the mild hybrid segment, at power levels of up to 10 kW, advanced products have already been evaluated. The market adoption has been slower, due to the less favorable performance to cost ratio of this segment. This will change as battery technologies and costs improve and as different architectures appear on the market.

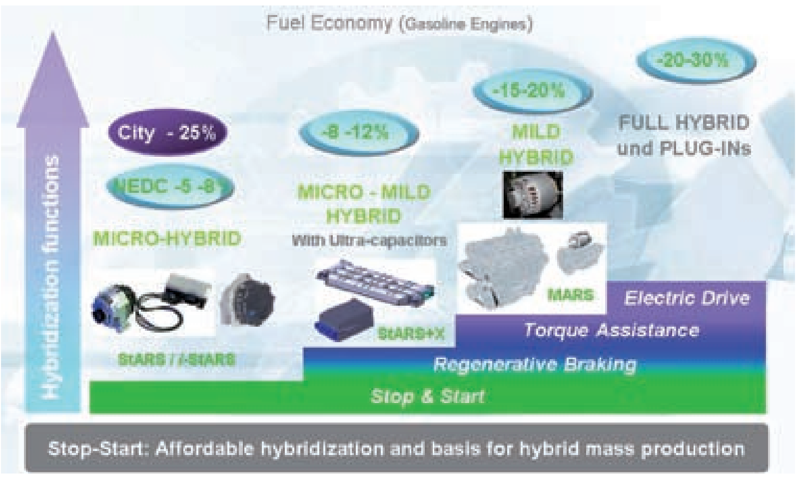

Figure 2: Valeo road map

8 Energy Storage Elements in Micro and Micro-mild Hybrids

Hybridization requires energy storage elements even for the first steps like micro-hybrids. The level of hybridization determines directly the energy storage solution, **Table 3**. Furthermore, the energy storage solution influences strongly the global cost of the system. For electrical vehicles, the cost of the battery exceeds 70 % of the hybridization costs. This fact has pushed the choice of Valeo to offer a intermediate micro-mild solution based on ultra-capacitors in order to optimize the costs of the system.

Table 3: Energy storage solutions

Hybridization	Power	Energy storage
Micro-hybrid	1.5 – 3 kW	Lead acid battery
Micro-mild-hybrid	3 – 5 kW	Ultra Caps
Mild-hybrid	5 – 15 kW	Li-ion Battery or Ultra Caps
Full-hybrid	> 20 kW	Small Li-ion battery
Electrical vehicle	> 20 kW	Large Li-ion battery

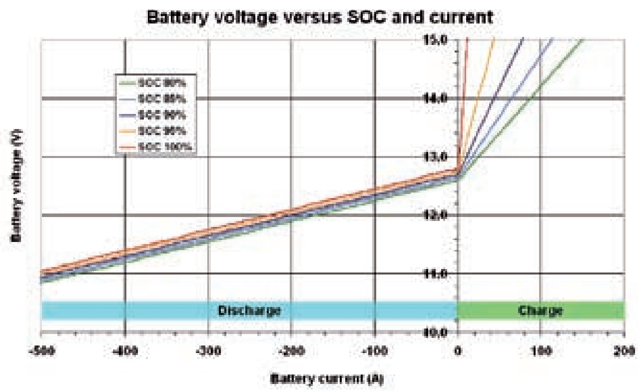

Figure 3: Lead-acid battery (70 Ah/3.5 mΩ)

8.1 Lead Acid Batteries

Lead acid batteries are the standard in automotive applications and will continue to be used as basic storage elements in micro hybrids. Nevertheless, the Stop-Start function introduces new requirements for this battery and in particular:

1. a better behavior in current cycling as the battery will see discharge phases during the stop mode
2. a need for low internal impedance to limit board net voltage drops during restarts
3. a good behavior during regenerative braking phases where high charging currents are produced.

The first two points can be addressed with existing lead acid battery technology for example the AGM (Absorbent Glass Mat) technology which is more robust in current cycling and offers lower internal resistance than the classical flooded lead-acid batteries.

Nevertheless, lead-acid batteries do not allow high charging currents and therefore limit the possible regenerative braking power. This is due to the fact that lead-acid batteries must be maintained at a high state of charge in order to avoid lead sulfate generation and accelerated aging. Unfortunately, at high state of charge, the charging impedance is high and does not allow the use of high charging current without generation of board net over-voltages. Therefore the practical peak power density in charging mode of lead acid batteries is very low and limited to 100 to 300 W/kg. **Figure 3** illustrates this behavior. It can be noticed that the charging current is limited to a low value when the state of charge is close to 100 %. For a state of charge of 90 % for example and a maximum board net voltage of 15 V the displayed battery will only accept about 60 A which represents only 900 W. Therefore, regenerative braking on a lead acid battery is very limited.

8.2 Ultra-capacitors or Electrolytic Double Layer Capacitors

An Electrolytic Double Layer Capacitor (EDLC) is basically a capacitor and can be designed with very low internal resistance. For example, the internal resistance of a 2000 F cell can be as low as 0.3 mΩ thus allowing very high charging or discharging currents. The peak power capability is in the range of 15 to 20 kW/kg. Unlike batteries, the voltage on an ultra-capacitor is variable and proportional to the state of charge (SOC). At 0 % of SOC the voltage on a cell is 0 V and 100 % of SOC the cell voltage is at 2.7 V to 3.1 V depending on the cell voltage rating.

The main advantage of ultra-capacitors is that the charging or discharging impedance is not dependant on the state of charge. Ultra-capacitors accept very high charging currents up to the maximum rated voltage. Therefore, charging currents of 500-1000 A on a 1000-3000 F EDLC cell are possible making them well suited for regenerative braking – which is often a small burst of power.

Ultra-capacitors accept a large number of charging/discharging cycles. The main aging effects are a slow decrease of the capacitance and a limited increase of the internal resistance. Reliability tests performed in automotive cycling conditions have demonstrated a cycling capability of more than 1 million cycles with less than a 30 % loss of capacitance. This characteristic is a major advantage for the use of this storage technology for regenerative braking.

8.3 Li-ion Batteries

Li-ion batteries have been developed initially to supply power to mobile electronic devices like mobile phones or PCs; small sized Li-ion batteries are now used by billions of people the world over.

Li-ion batteries show excellent energy density in the range of 100 to 200 Wh/kg. Peak power capability is limited to 1 to 3 kW/kg and cycling capability is typically 2000 cycles of 100 % of depth of discharge. To reach a cycling capability of 500,000 to 1 million cycles like for regenerative braking, the depth of discharge must be limited to 2 to 3 % which leads to the use of a large battery. Therefore, Li-ion batteries are more suited for mild and full hybrids or electrical vehicles.

8.4 Need for a DC to DC Converter

A DC/DC converter is required to connect the ultra-capacitor storage pack to the 14 V board net of the vehicle. This is due to the fact that the voltage on the ultra-capacitors floats in a large voltage range since the state of charge of an ultra-capacitor is proportional to the voltage. This voltage converter will transform the variable voltage on the ultra-capacitors to a fixed and very stable voltage for the board net.

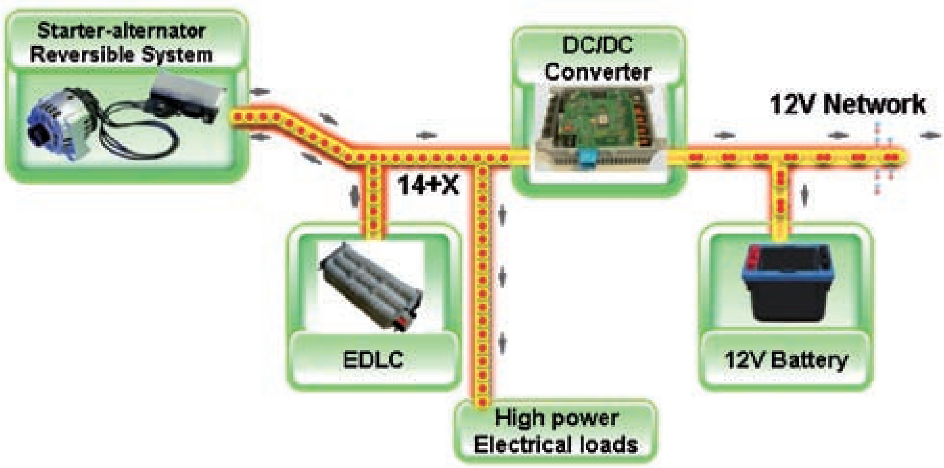

Figure 4: "StARS +X" system layout

9 The Valeo "StARS+X" system

The "StARS+X" system developed by Valeo is a system offer for the micro-mild hybrid segment. This system is built around an ultra-capacitor storage system with an energy capacity of 72 kJ. It allows Stop-Start, regenerative braking and torque assistance with a power level of up to 4 kW.

As addressed in the previous sections, this system uses the high power handling capability of EDLC's without compromising the life time of the energy storage system. The energy storage system needs no replacement during the life time of the vehicle.

Fuel saving provided by the system is 8 to 12 % on NEDC cycle and thus "StARS+X" allows a further step in the Valeo hybridization road map beyond i-"StARS". "StARS+X" offers the functions of a mild-hybrid but with reduced initial costs and very limited maintenance costs. This achievement was made possible thanks to the use of ultra-capacitors as storage elements.

9.1 System Layout

The system layout is given in **Figure 4**. The following components can be seen:
- a claw pole machine similar to an alternator with the associated inverter unit to drive the machine in generator or motor mode
- a power pack based on ultra-capacitors for energy storage. The capacity of the power pack is of 200 F which represents 35 kJ of energy when the pack is cycled from 18 to 26 V
- a DC to DC converter required to supply the vehicle's 14 V board net.

9.2 Operation Modes of the System

9.2.1 Stand by Mode

The car is in parking mode and the inverter and the DC/DC converter are switched off. The power pack is at the voltage reached when the system was switched off. As self discharge of the power is low, power is available in the pack for at least ten days. During the parking mode, the lead acid battery supplies the equipment requiring permanent power.

9.2.2 First Cranking of the Engine

The DC/DC and the inverter are switched on. If the power pack voltage is too low (due to the vehicle being parked for a long time, for example), the power pack is charged by the DC/DC converter in reverse mode. This charging mode may take a few seconds. Cranking is then done by the classical starter powered by the lead-acid battery.

9.2.3 Generator Mode

Here the engine is running, the claw pole machine is driven by the inverter and operates in generator mode. The output current of the claw pole machine charges the power pack up to the nominal operating voltage (16 to 20 V). Once the nominal voltage is reached, the inverter regulates the excitation of the claw pole machine in order to maintain the power pack voltage at nominal value. The DC/DC converter operates in direct mode and supplies the 14 V board net by taking power from the power pack.

9.2.4 Regenerative Braking

When the vehicle decelerates either due to vehicle coasting or braking, the inverter operates the machine in generator mode at a high power level. The output power can reach 4 to 5 kW and the recovered energy is stored in the ultra-capacitors. During regenerative braking, the voltage of the power pack increases up to the maximum voltage of 27 V. During this phase the DC/DC converter continues normal operation and supplies the 14 V board net ensuring that no voltage variations occur on the 14 V net.

9.2.5 Stop Mode

In urban traffic, the regenerative braking phase is often followed by a stop phase. In this phase the engine is turned off and the DC/DC converter keeps on supplying the 14 V net by taking energy from the power pack. The voltage of the power pack decreases during this phase. If the power pack was fully charged by regenerative braking, then the energy recovered is sufficient to supply 1 kW to the board net for 30 to 40 s. During this time, the 14 V voltage is stable. If the stop phase is longer, then the lead acid battery will take over the supply of the 14 V and a small decrease of the net voltage will be seen. If the stop is short, the power pack remains over the nominal voltage of 16 to 18 V.

9.2.6 Re-start

After the stop phase, the engine is restarted by the claw pole machine which is driven by the inverter in motor mode.

During this phase, energy is taken from the ultra-capacitors only for re-cranking so that no voltage drop occurs on the 14 V board net due to the high cranking currents. Cranking with a starter generator reversible system (SGR) is very quick especially with a "StARS+X" where the injected mechanical power reaches 3 to 4 kW in cranking mode. Cranking duration is of less than 350 ms which appears for the driver as a spontaneous and noiseless restart.

9.2.7 Torque Assist

If residual energy is available in the ultra-capacitors, it is possible to decide to use this energy either to supply the board net during driving or to the use the torque assist function to inject this energy into the powertrain. The torque assist ancecan help to run the combustion engine more efficiently. It also maximizes the energy which can be recovered during next regenerative braking (by discharging the power pack).

Figure 5: "StARS +X" machine

9.3 Machine

The machine proposed with the system is a high performance claw pole machine using a rotor with mixed magnet and winded field excitation, **Figure 5**. The machine associates a 144 mm lamination diameter stator with an eight pole pair rotor. A benefit of this machine technology is that it is an electrical design that has been already validated in mass production for alternators. The performance of the machine is improved due to the variable output voltage. In terms of efficiency, this machine benefits from an increased output voltage (16 to 27 V) and of the synchronous rectifying performed by the separate inverter.

9.4 Inverter

The inverter, **Figure 6**, has been dimensioned to drive the machine in generator and motor modes. The current capability of the inverter is of 1000 A on the supply line for the cranking mode and of 250 A continuous in generator mode. The driving principle is an enhanced full wave mode allowing accurate and continuous angular phasing of the stator voltage associated with bridge aperture modulation. Linear sensors have been fitted on the machine to allow the continuous measurement of the rotor position with a resolution of less than 0.2 mechanical degrees. This, together with optimized control algorithms, maximizes the starting torque.

In generator mode, the inverter operates as a synchronous rectifier which greatly reduces rectification losses. Drop voltage due to rectification is decreased to less than 100 mV instead of 1.4 V with classical diodes. Synchronous rectification contributes to the global efficiency of the system by raising the generator efficiency seven points. The inverter accepts ambient temperatures up to 85 °C and is air cooled. Operation of the inverter is controlled through the CAN network.

9.5 DC to DC Converter

The DC/DC converter, **Figure 7**, has a power capability of 2.2 kW and is designed to be reversible. Nominal mode of operation is to supply the 14 V network by tak-

Figure 6: "StARS+X" inverter

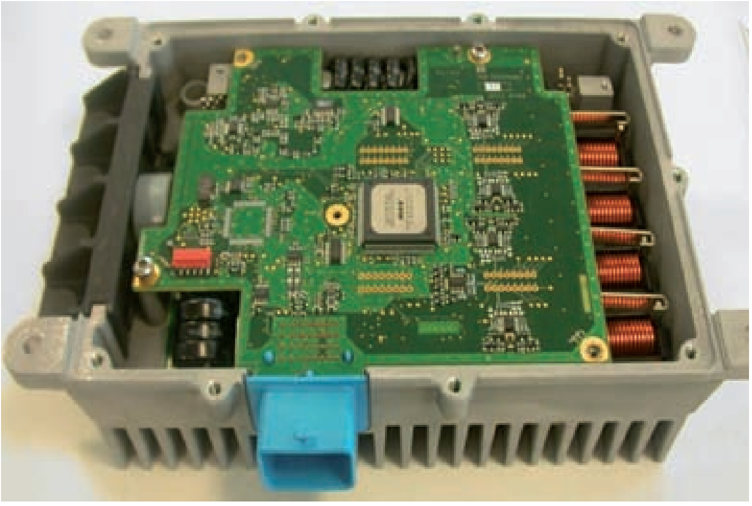

Figure 7: DC/DC converter

Figure 8: Power pack 200 F/27 V

ing power from the ultra-capacitors. But the DC/DC converter is also able to charge the ultra-capacitors by transferring power from the lead acid battery to the power pack. This second mode of operation is only used in particular situations like starting after the vehicle has been parked for an extended period or after maintenance operations.

The converter is designed to be air cooled and accepts an environment temperature up to 85 °C with a minimum air flow of 2 m/s. The converter is connected to the CAN network for operation and for diagnosis.

9.6 Ultra-capacitor Power Pack

The power pack is a 200 F pack with a voltage rating of 0 to 27 V, **Figure 8**. The pack is built around ten cells of 2000 F/2.7 V and contains the diagnosis and balancing electronics for the pack.

Total stored energy is of 72 kJ at maximum voltage. The operational voltage range is of 16 to 26 V, which allows to store and recover up to 42 kJ per cycle. The metallic housing ensures good thermal homogeneity for the pack and protects in an optimum way the internal cells. Operating temperature is limited to 50 °C and storage temperature must not exceed 60 °C. Dimensions are: 510 x 210 x 70 mm, weight is of 9 kg.

9.7 Re-cranking Capability

"StARS+X" is able to crank gasoline engines up to 4 l of displacement and diesel engines up to 3 l. Torque characteristics are given in the **Figure 9**. Low speed torque is in the range of 60 to 80 Nm depending on the voltage available in the ultra-capacitors. The available mechanical cranking power at 800 rpm (about 300 rpm on the engine) is of 2.4 kW with 18 V supply and reaches 4 kW with 24 V supply. The minimum available power of 2.4 kW at 18 V allows a very fast re-start of the engine.

9.8 Regenerative Braking

Figure 10 displays the output current at 18 V on the power pack. It can be seen that the output current reaches 220 A at 5000 rpm on the machine (1600 to 2000 rpm on the engine). This output level corresponds to 4 kW of generated electrical power. This power level can be used during regenerative braking. Within 10 s of braking at this level, the ultra-capacitors are charged up to maximum voltage.

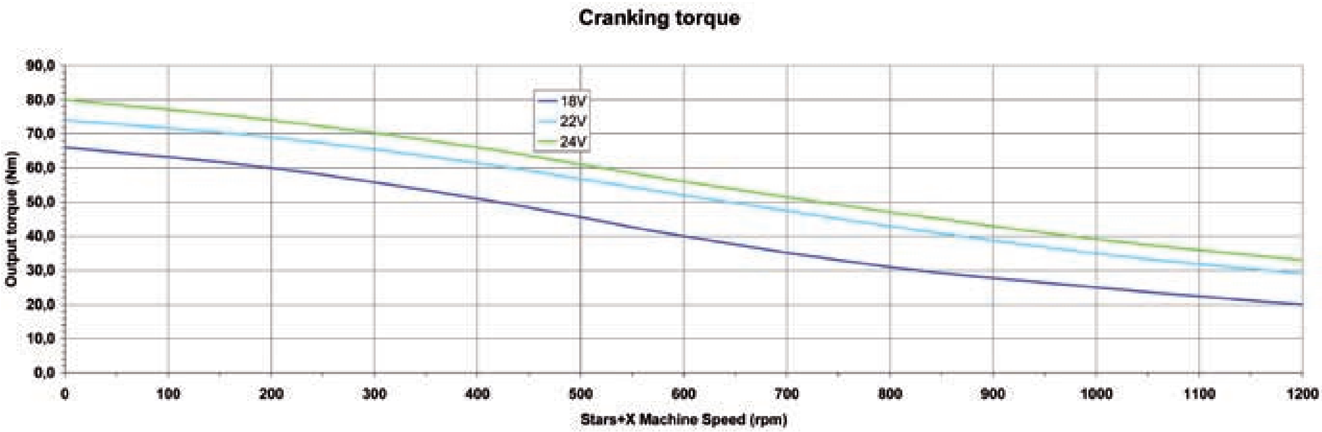

Figure 9: Re-cranking torque

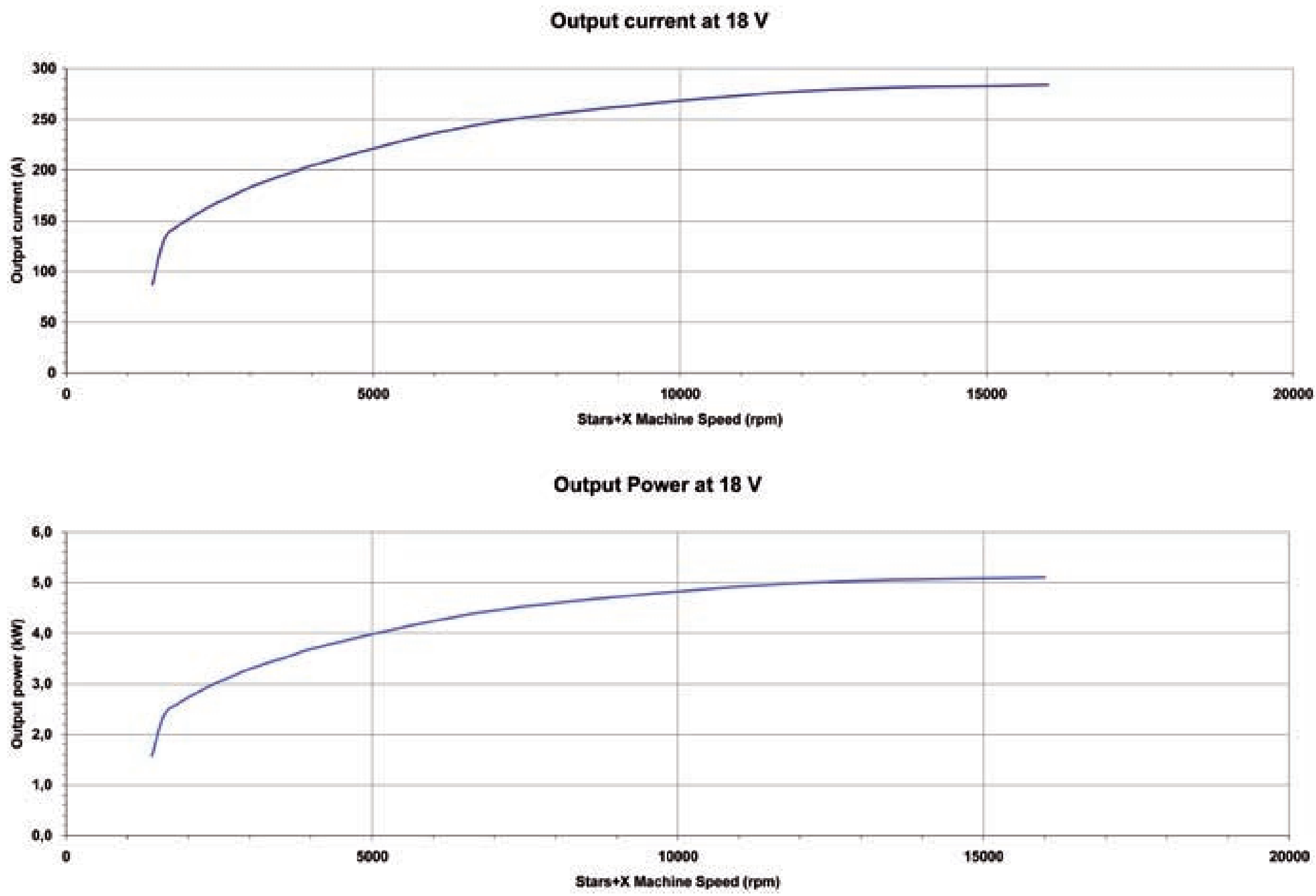

Figure 10: Output current and power versus speed

10 Perspectives and Conclusion

The "StARS+X" micro-mild system can provide up to a 12 % improvement in fuel economy and has been developed to offer a cost efficient solution between micro hybrid systems and mild hybrid systems. It offers all the operation modes of a mild hybrid but at about half the costs. This was achieved by the use of ultra-capacitors for energy storage. Moreover, particular attention has been given to the dimensioning of energy storage elements in order to offer a maintenance free system with no need for storage element replacement during the lifetime of the vehicle.

Ultra-capacitor technology is progressing and higher power densities have already been announced. This opens additional ways to enhance systems like "StARS+X" by either reducing the size of the storage elements or by increasing the energy capacity to offer more torque assistance and increased fuel savings.

References

[1] Dubus, J.-M.; Masson, P.; Plasse, C.; d'Orsay, E.; Dr. Westerholt, E.: A simple Stop&Go Concept for City Cars – Technical Design and Benefits. Aachener Kolloquium Fahrzeug- und Motorentechnik, October 2001

[2] Pfiffer, J.; Rouleau, B.; Morelle, J.-M.: How the need for cost-effective CO_2 emissions reduction through powertrain hybridization pushes for innovative, integrated, and robust mechatronics design. Convergence 2006 06PT-33

[3] Cogo, K.; Dubus, J.-M.; Plasse, C.: The Valeo Belt Driven Starter Alternator Reversible Systems. Société des Ingénieurs de l'Automobile, July 2004

[4] Richard,D.; Armiroli, P.; de Vries, A., Dubel, Y.: Valeo StARS Technology: An Efficient Solution for Hybridization. AVL Engine & Environment Conference 2007

[5] Locment, F.; Bruyere, A.; Semail, E.; Kestelyn, X.; Bouscayrol, A.; Dubus, J. M.: Comparison of 3-, 5- and 7-leg Voltage Source Inverters for low voltage applications. IEEE International Electric Machines and Drives Conference, IEMDC 2007, Antalya, Turkey, pp.1234-1239, May 2007

Torque Vectoring with Electro-hydraulic Actuation

The importance of electronically controlled systems in the chassis and drivetrain is increasing. The associated products have the aims of improving not only safety aspects but also driving pleasure, with end customers laying not inconsiderable weight on the potential to define the driving experience through the components' influence. Magna Powertrain has developed a torque vectoring System with clearly demonstrable improvement of agility and high availability, and brought it into series production.

1 Introduction

To enjoy success in the marketplace, torque vectoring systems should not only offer the fundamental possibility of variable torque distribution between the wheels on one axle but also offer the customer a new form of driving experience. The challenges facing the components, given restrictions on packaging, weight increase and intolerability of efficiency losses and raised fuel consumption, require new solution concepts.

The application of appropriate torque distribution between the two wheels on one axle generates a yaw moment about the vertical axis of the vehicle. This yaw moment can influence vehicle dynamics directly if it can be adjusted independently of the forward propelling force. Using torque vectoring in the drivetrain, delayed or even counteractive reactions of the vehicle to steering input can be influenced without resort to any other control components. For the driver, the vehicle response seems sharper.

At the same time, outward torque transfer can optimize cornering force whilst inward torque transfer can also confer significantly increased stability, damping yaw acceleration. Along with the possibility to ap ply corrective torque transfer at the limit of traction, the result is improvements not only in driving pleasure but also significantly in driving safety under all road conditions.

2 Selection of the Right Overall System and its Sub-systems

The system design is derived from the technical requirements of the components in the complete vehicle and is defined by the functions it must fulfill. The expectations include not only general improvement of agility and the possibility to damp the motion of a vehicle at high rates of yaw, but also complete independence of torque distribution from driving condition, loading and power-on time. The extended functions of the drivetrain should guarantee the highest safety and robustness alongside limited weight increase and minimal loss of efficiency. A further limitation for a system manufacturer is implementability, i.e. the possibility of adapting an existing drivetrain configuration with a reasonable level of investment. Modular construction has enabled simple adaptation, **Figure 1**.

A benchmark comparison of electrical, hydrostatic and mechanical solutions demonstrates absolutely clear packaging and weight advantages for mechanical variants. These consist primarily of superposition units with clutch systems for raising rotation speed. The overall system consists of the final drive, clutch system, power mechanics of the superposition units, hydraulic system and control by means of an ECU and software, **Figure 2**.

3 Basic Final Drive and Differential

Adding variable torque distribution to an axle of an existing drivetrain should only have a limited effect on the existing, proven components like the differential. The pre-existing basic final drive ensures a separation between the superposition function and the fundamental transmission of torque via the differential to the rear axle, thereby offering the conventional standard transmission functional-

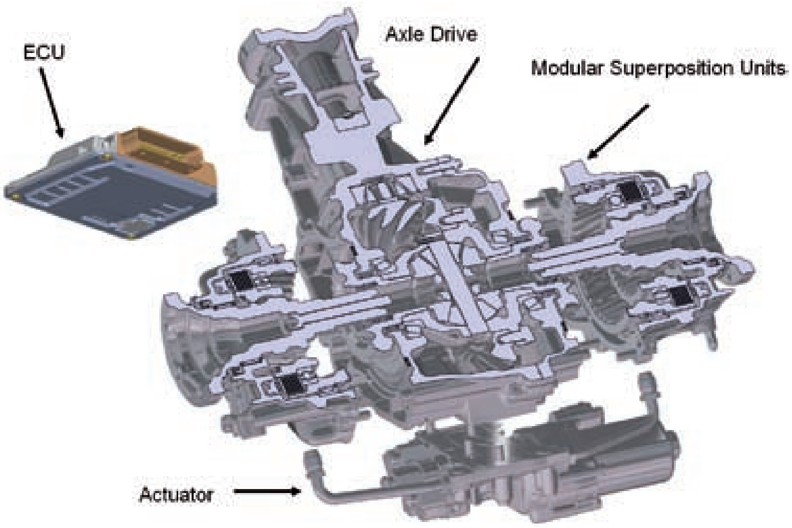

Figure 1: Modular layout

The Authors


Walter Sackl
is Head of Engineering Product Line / Concepts at Magna Powertrain in Lannach (Austria).


Gerhard Eibler
is Development Project Manager at Magna Powertrain in Lannach (Austria).


Thomas Linortner
is System Architect at Magna Powertrain in Lannach (Austria).

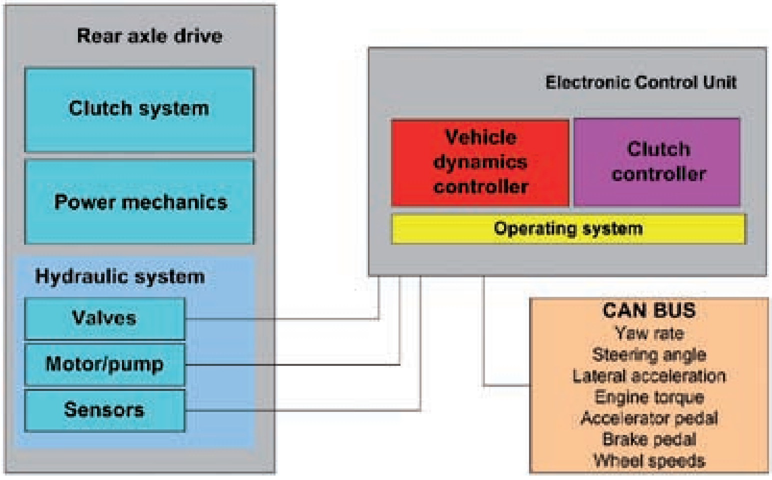

Figure 2: System overview

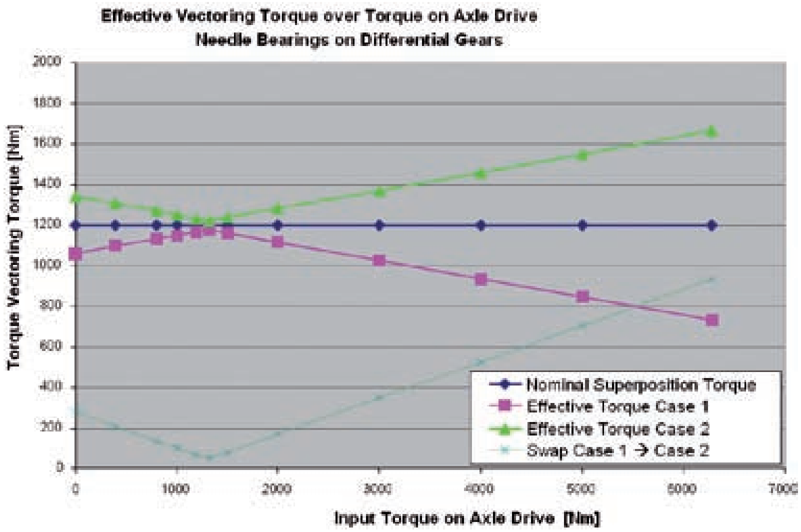

Figure 3: Effective superposition torque

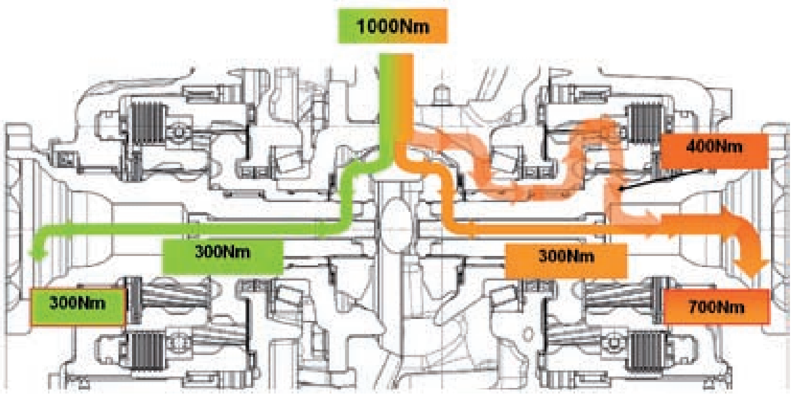

Figure 4: Torque flow

ity as a fallback free of consequent impairment. With its own oil circuit, apart from adaptation of interfaces it remains autonomous. However, the original effect of the locking function of a differential counteracts transfer of torque in the positive direction to the outer wheel in a bend, and is also dependent on the loading on the differential. As shown in **Figure 3**, with a standard differential coasting freely, effectively less torque is transferred outboard in line with the locking level (case 1). If torque is superimposed inboard (case 2) for damping purposes, a correspondingly larger level is distributed.

The absolute magnitude of these influences depends on the torque present on the final drive at any given time and can increase or reduce superposition torque according to evolving yaw rate. Direct measurement of both parameters is involved or, at the lowest rates of rotation, practically impossible, so it is necessary to take reduction measures.

Analysis of the sources of friction shows one of the greatest potentials to lie in the side gear journal bearings. In order to ensure fine control independent of final drive load, differential friction performance was improved through the application of needle roller bearings in place of thrust washers.

4 Superposition Units and Clutch System

The basic concept for influencing vehicle dynamics is the generation of asymmetric or opposing forces on the wheels of one axle. To achieve this, 2 superposition drives are so arranged that engagement of the clutch integrated into each unit accelerates one wheel and brakes the second wheel. These processes have to take place very rapidly as the generation of inertial torques in the drivetrain as a result of control system intervention is undesirable given the need to avoid virtual locking. **Figure 4** shows the basic flow of power. In the presence of a motive torque of 1000 Nm a torque difference of 400 Nm should be generated acting about the yaw axis. To turn the vehicle in to the left, 400 Nm of torque pass through the superposition unit. The differential distributes 2 x 300 Nm approximately symmetrically between the two driveshafts. The resultant is now 700 Nm on the right hand output and 300 Nm of torque on the left.

Figure 5 shows the rotary behavior at the superposition units without and with control active. Parts with accelerations during control are shown in yellow color.

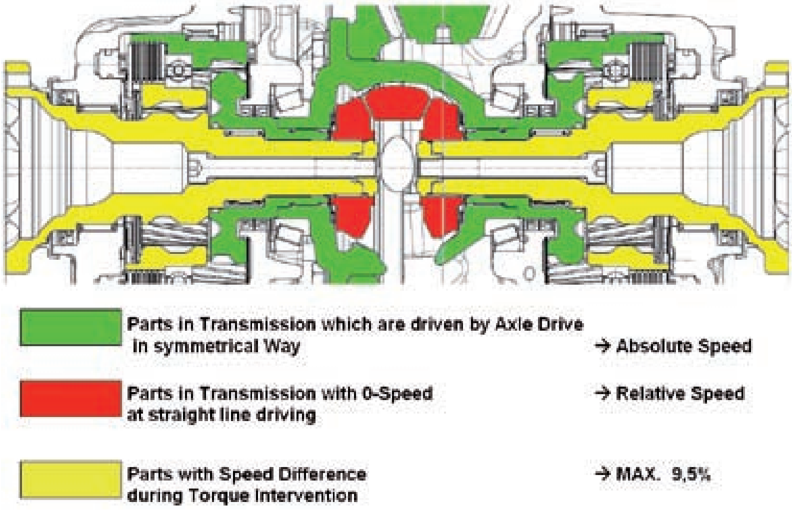

Figure 5: Systematic of speeds

The side required to apply a higher torque is accelerated rapidly, the rotary speed difference reduces but the rotary behavior of the engaged gears changes only slightly.

4.1 Gearing System

The mechanical superposition function consists of a torque-inserting gearing stage directly driven by the differential, the co-rotating clutch and a second gearing stage that acts on the flange shafts. Both gearing stages work at the same distance in one axle, offset from the axis of the differential hypoid gearing. Thus the outer part of the superposition unit is positioned about 7mm off center, **Figure 6**. The ratios are selected in such a way that they impose the smallest possible differential rotation speed on the clutches, essential for good overall efficiency.

4.2 Clutch System and Lubrication

The clutches are positioned directly in the superposition branch and have an absolute rotation speed of 90 % of that of the axle and straight-ahead drag of only 8.5 %. The outer lamellae are connected to the driving outer ring gear, whilst the inner lamellae are connected to the hub, which simultaneously constitutes the driven outer ring gear.

The low level of drag in the clutches in the non-actuated condition yields low drag torques even with narrow clearances and a temperature situation similar to that of a conventional differential. Comprehensive road testing has confirmed this, with temperature levels similar to those of similar differentials.

The entire arrangement of units can be tailored very simply to critical packaging situations, given the diameter and positioning offset from the centerline.

Furthermore, by virtue of direct drive via the differential, the gearing system also guarantees that no additional counterproductive sources of friction compromise the torque superposition function.

With this arrangement, all drag torques are driven via the differential housing and not from the wheel side, Figure 5. As a consequence, there are no reverse influences (virtual locking effect), brought about by the superposition units through reactive torques at high differential rotation speeds that might affect the function of the braking control system.

Care has been taken to ensure that drag torque has no influence on step changes in superposition torque as a result of changing from driving in a straight line to going round a bend. **Figure 7** shows the flow of power through the differential and superposition units. In order to meet the requirements for the highest possible availability, the superposition units were designed and verified on the basis of 8 % duty throughout the entire vehicle life.

The multi-plate system was developed to deliver the highest possible consistency of friction coefficient throughout its lifetime. Through efficient centrifugal lubrication in the units, the oil circuit, which is separate from that of the differential, ensures excellent temperature conditions, even during maximum loading such as on the racetrack.

Figure 8 shows that the change in frictional behavior over the entire lifetime is less than 5 %, and this small level is compensated within the actuation system over the unit lifetime.

5 Hydraulic System

Packaging limitations and the possibility to vary the positioning of the actuator led to selection of an electro-hydraulic system with one motor and one pump without a pressure accumulator.

The concept is based on the direct electro-hydraulic actuator system as used also in other applications for clutch actu-

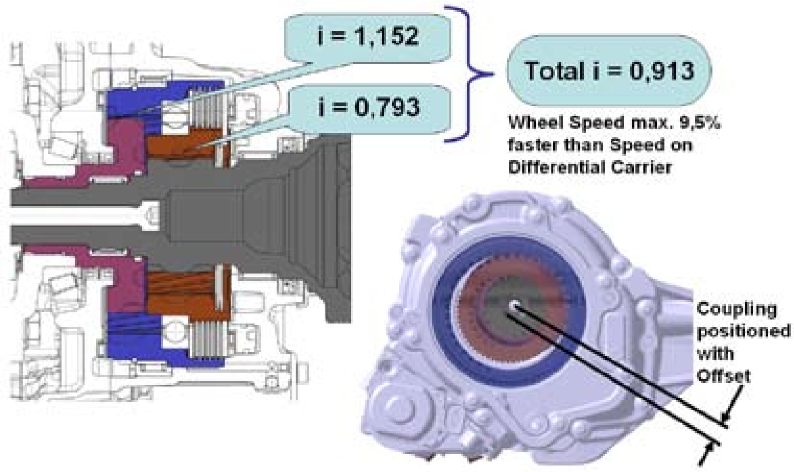

Figure 6: Gear sets and coupling

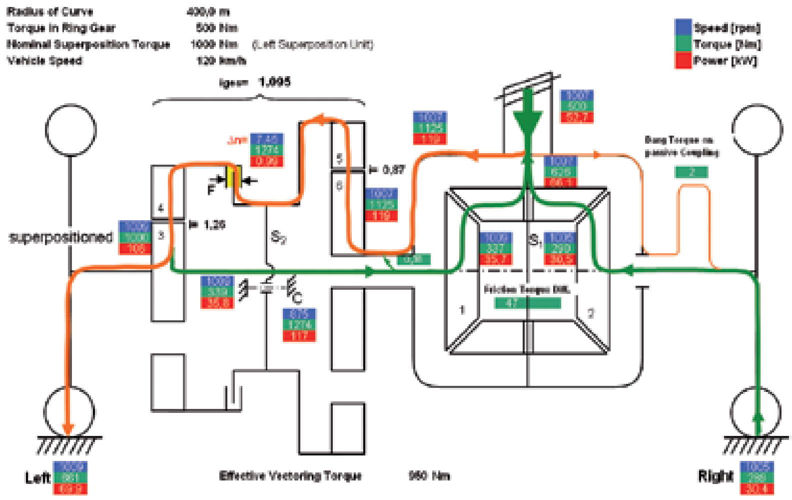

Figure 7: Power flow

ation in the drivetrain, **Figure 9**. It offers the fundamental advantage of controlling two clutches with one actuator. Well-considered system design has also resulted in no significant delay during switching from the first to the second clutch. The motor drives a pump that operates in both directions of rotation and thus delivers pressure to the piston on one torque superposition side at any time. Control is effected directly; the motor is used for pressure generation and reduction, thereby obviating the need for additional control valves. This reduces the number of power line outputs required in the controller.

Two redundant pressure sensors measure the pressures on both clutches via shuttle valves and ensure very high actuation precision. A shut-off valve on each side permits induction from the opposite path in each case and, in addition, a safety shut-off is operated simply through interruption of the power supply.

The exceptionally compact actuator unit, **Figure 10**, with associated oil reservoir is attached to the differential housing and shares an oil volume with the two superposition units. Air bleeding from the system takes place at defined intervals via the passive bleed valves. All components are robust, so no complicated hydraulic circuit filtering is necessary.

Thus the electro-hydraulic design, with its high overall efficiency, allows rapid transition through from the disengaged state alongside high precision of control by virtue of the short tolerance chain.

6 ECU, Sensors and Software

The ECU controls the electric motor and the two switchable valves. The incoming pressure sensor readings constitute the feedback loop in the control circuit, whilst the torque control demand comes from the vehicle bus system. The software is subdivided into basic software, driving dynamics controller and clutch controller. The calculated superposition torque is transferred via a torque interface between the driving dynamics controller and clutch controller.

The driving dynamics controller uses steering input angle, lateral acceleration, yaw rate and other information from the bus system to calculate the torque to be transferred and is networked to other control systems (e.g.: ESP). The clutch controller handles control of the demanded torque and torque vectoring system protection and diagnostic functions. This covers the multi-plate clutches, motor/pump unit, sensors and valves. The basic software handles signal conditioning and diagnostics. This modular design enables straightforward adaptation to different vehicles and bus systems (e.g. CAN or Flexray).

Diagnosis of the torque controller response behavior is achieved by means of tolerance bands. Decisions are made on

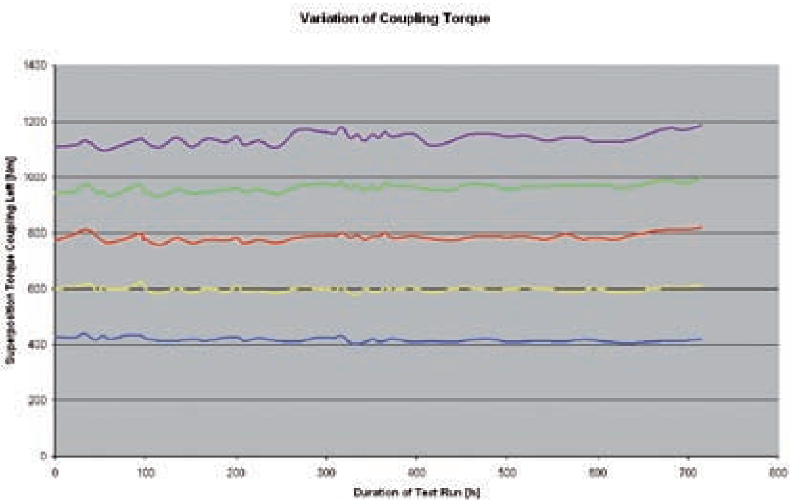

Figure 8: Friction coefficient over lifetime

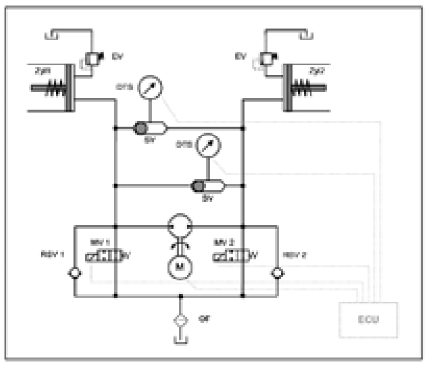

EV	Bleeding Valve	RSV	Check Valve
M	DC-Motor	DTS	Pressure / Temperature Sensor
ECU	Electronic Control Unit	MV	Solenoid Valve
SV	Shuttle Valve	Zyl	Cylinder / Piston
OF	Oil Filter		

Figure 9: Hydraulic system of direct electro-hydraulic actuator

the basis of hard and soft threshold values depending on the magnitude of deviation, in order to ensure that the system is stable and secure over its entire lifetime. The limit values for these diagnostic functions were established on the basis of test drives. **Figure 11** shows an example of a control level with upper and lower "hard" and "soft" tolerance bands. Crossing the "hard" threshold would compromise vehicle safety, so the system must be shut off if it is exceeded. In the "soft" area there is no sudden shut down but rather a calculation of the error integral to check whether response behavior is only briefly outside specification.

7 Overall System Performance and Safety

The entire system was developed in line with the requirements of IEC 61508 – Functional Safety Management. Because this is a steering system achieved by active torque superposition on the rear axle, it is necessary to prevent false actuations with failure probability levels of less then 10^-7 dangerous failures per hour. This applies to all electrical, electronic and programmable electronic components.

In the event of a failure, the transferred axle torque must be reduced to a non-critical value within 100ms. This is achieved through the combination of direct electro-hydraulic actuators with shut-off valves that open when power is interrupted. When a dangerous failure is detected, the power is interrupted immediately with the result that system pressure also reduces immediately, yielding behavior the same as that of a conventional axle. Dangerous failures are detected by means of redundant pressure measurement in combination with tolerance bands for the setpoint and actual torque relationship. A special hardware and software architecture guarantees the required low failure probability.

One central requirement is torque control dynamics. In order to achieve well-defined driving behavior it is necessary that a superposition of torque should be available at the wheels before the onset of strong under or oversteer. Otherwise there would be disquieting transitions between vehicle understeer

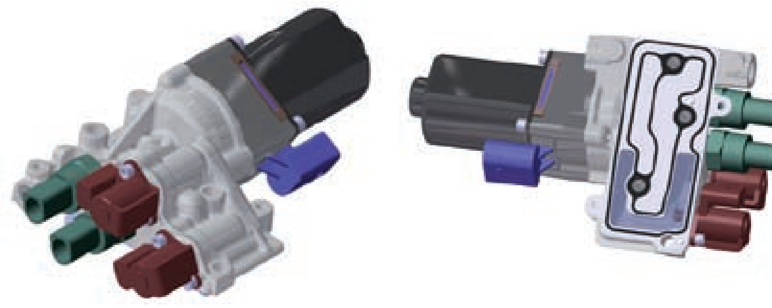

Figure 10: Actuation module

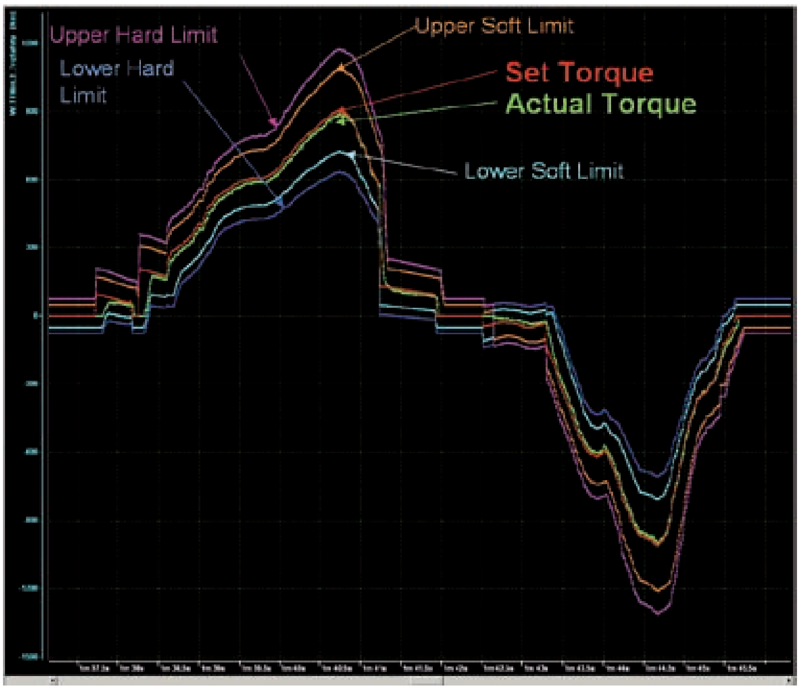

Figure 11: Tolerance zone of controller

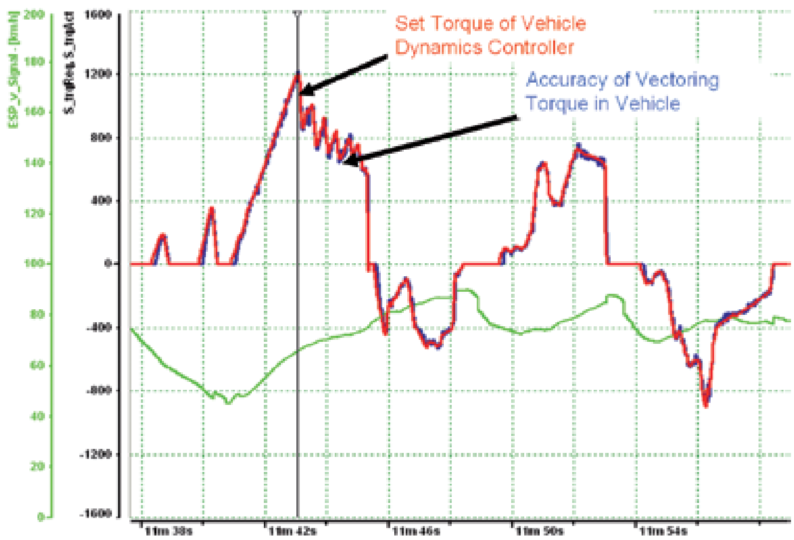

Figure 12: Subsequence to set torque of vehicle dynamics controller

IMPRINT

ATZ WORLDWIDE

www.ATZonline.com

12|2008 · December 2008 · Volume 110
Springer Automotive Media | GWV Fachverlage GmbH
P. O. Box 15 46 · 65173 Wiesbaden · Germany
Abraham-Lincoln-Straße 46 · 65189 Wiesbaden · Germany

Managing Directors Dr. Ralf Birkelbach, Albrecht Schirmacher
Senior Advertising Thomas Werner
Senior Production Ingo Eichel
Senior Sales Gabriel Göttlinger

EDITORS-IN-CHARGE

Dr.-Ing. E. h. Richard van Basshuysen
Wolfgang Siebenpfeiffer

EDITORIAL STAFF

Editor-in-Chief
Johannes Winterhagen (win)
Phone +49 611 7878-342 · Fax +49 611 7878-462
E-Mail: johannes.winterhagen@springer.com

Vice-Editor-in-Chief
Dipl.-Ing. Michael Reichenbach (rei)
Phone +49 611 7878-341 · Fax +49 611 7878-462
E-Mail: michael.reichenbach@springer.com

Chief-on-Duty
Kirsten Beckmann M. A. (kb)
Phone +49 611 7878-343 · Fax +49 611 7878-462
E-Mail: kirsten.beckmann@springer.com

Sections
Body, Safety
Dipl.-Ing. Ulrich Knorra (kno)
Phone +49 611 7878-314 · Fax +49 611 7878-462
E-Mail: ulrich.knorra@springer.com

Chassis
Roland Schedel (rs)
Phone +49 6128 85 37 58 · Fax +49 6128 85 37 59
E-Mail: ATZautotechnology@text-com.de

Electrics, Electronics
Markus Schöttle (schoe)
Phone +49 611 7878-257 · Fax +49 611 7878-462
E-Mail: markus.schoettle@springer.com

Engine
Dipl.-Ing. (FH) Richard Backhaus (rb)
Phone +49 611 5045-982 · Fax +49 611 5045-983
E-Mail: richard.backhaus@rb-communications.de

Heavy Duty Techniques
Ruben Danisch (rd)
Phone +49 611 7878-393 · Fax +49 611 7878-462
E-Mail: ruben.danisch@springer.com

Online
Dipl.-Ing. (FH) Caterina Schröder (cs)
Phone +49 611 7878-190 · Fax +49 611 7878-462
E-Mail: caterina.schroeder@springer.com

Production, Materials
Stefan Schlott (hlo)
Phone +49 8191 70845 · Fax +49 8191 66002
E-Mail: Redaktion_Schlott@gmx.net

Service, Event Calendar
Martina Schraad
Phone +49 212 64 232 64
E-Mail: martina.schraad@springer.com

Transmission, Research
Dipl.-Ing. Michael Reichenbach (rei)
Phone +49 611 7878-341 · Fax +49 611 7878-462
E-Mail: michael.reichenbach@springer.com

English Language Consultant
Paul Willin (pw)

Permanent Contributors
Christian Bartsch (cb), Prof. Dr.-Ing. Peter Boy (bo),
Prof. Dr.-Ing. Stefan Breuer (sb), Jens Büchling (jb),
Jörg Christoffel (jc), Jürgen Grandel (gl),
Erich Hoepke (ho), Prof. Dr.-Ing. Fred Schäfer (fs),
Bettina Seehawer (bs)

Address
P.O. Box 1546, 65173 Wiesbaden, Germany
E-Mail: redaktion@ATZonline.de

MARKETING | OFFPRINTS

Product Management Automedia
Sabrina Brokopp
Phone +49 611 7878-192 · Fax +49 611 7878-407
E-Mail: sabrina.brokopp@springer.com

Offprints
Martin Leopold
Phone +49 2642 9075-96 · Fax +49 2642 9075-97
E-Mail: leopold@medien-kontor.de

ADVERTISING | GWV MEDIA

Key Account Manager
Elisabeth Maßfeller
Phone +49 611 7878-399 · Fax +49 611 7878-140
E-Mail: elisabeth.massfeller@gwv-media.de

Ad Sales
Sabine Röck
Phone +49 611 7878-269 · Fax +49 611 7878-140
E-Mail: sabine.roeck@gwv-media.de

Heinrich X. Prinz Reuß
Phone +49 611 7878-229 · Fax +49 611 7878-140
E-Mail: heinrich.reuss@gwv-media.de

Display Ad Manager
Sandra Reisinger
Phone +49 611 7878-147 · Fax +49 611 7878-443
E-Mail: sandra.reisinger@gwv-media.de

Ad Prices
Price List No. 51

SUBSCRIPTIONS

VVA-Zeitschriftenservice, Abt. D6 F6, ATZ
P. O. Box 77 77, 33310 Gütersloh, Germany
Renate Vies
Phone +49 5241 80-1692 · Fax +49 5241 80-9620
E-Mail: SpringerAutomotive@abo-service.info

SUBSCRIPTION CONDITIONS

The emagazine appears 11 times a year at an annual subscription rate of 269 €. Special rate for students on proof of status in the form of current registration certificate 124 €. Special rate for VDI/ÖVK/VKS members on proof of status in the form of current member certificate 208 €. Special rate for studying VDI members on proof of status in the form of current registration and member certificate 89 €. The subscribtion can be cancelled in written form at any time with effect from the next available issue.

PRODUCTION | LAYOUT

Kerstin Gollarz
Phone +49 611 7878-173 · Fax +49 611 7878-464
E-Mail: kerstin.gollarz@gwv-fachverlage.de

HINTS FOR AUTHORS
All manuscripts should be sent directly to the editors. By submitting photographs and drawings the sender releases the publishers from claims by third parties. Only works not yet published in Germany or abroad can generally be accepted for publication. The manuscripts must not be offered for publication to other journals simultaneously. In accepting the manuscript the publisher acquires the right to produce royalty-free offprints. The journal and all articles and figures are protected by copyright. Any utilisation beyond the strict limits of the copyright law without permission of the publisher is illegal. This applies particularly to duplications, translations, microfilming and storage and processing in electronic systems.

Springer Automotive Media is part of the specialist publishing group Springer Science+Business Media.

and oversteer, perceived in a negative light by the driver. Here the System guarantees controlled torque application and release within <120ms between released, passive state and the maximum possible torque, redistribution can be done within 100 ms. It was therefore necessary to optimize the clutch controller for rapid transition through from the disengaged state and regulation of set-point torque without overshoots. The safety-related release in the event of a failure mentioned above is much faster as a result of the lack of a need for active control and thanks to the potential energy stored in the clutches.

The system precision is another important aspect. Because an excessively high superposition torque can lead to depletion of wheel side force on the limit of traction, it is necessary to control the stabilized torque with an accuracy of +/-10 %. The short tolerance chain and simple relationship between pressure and torque make it possible to achieve the required high precision of control and also the safety requirements.

Figure 12 shows the good response behavior of the effective superposition torque in the vehicle, with no significant overshoot. Because torque vectoring systems are desirable for high-powered, sporty vehicles, thermal demands on the system are very high. For example, if driving quickly on mountain roads or around a circuit, rear axle temperatures can rise to 150°C. So the requirements for accuracy and dynamic response stated above have to be ensured over a very broad range of temperature. Through a modular design and dedicated pursuit of customer wishes it was successful to bring an effective torque vectoring unit into series production.

References

[1] Mohan S.; Sackl W.: Simulation and Definition of an Active Yaw Control Device. Graz, Magna Powertrain, Allradkongress, 2006
[2] Gratzer F.; J.Quehenberger.: Direkte elektrohydraulische Aktuierung [Direct electro-hydraulic actuation], Würzburg, Innovative Fahrzeuggetriebe CTI Symposion 2005


Karriere
Archiv
Events
Wissen
Topmeldung
Aktualität
1500 m
www.ATZonline.de
Optionen
NAVIGON

Torque Vectoring with Electro-hydraulic Actuation

The importance of electronically controlled systems in the chassis and drivetrain is increasing. The associated products have the aims of improving not only safety aspects but also driving pleasure, with end customers laying not inconsiderable weight on the potential to define the driving experience through the components' influence. Magna Powertrain has developed a torque vectoring System with clearly demonstrable improvement of agility and high availability, and brought it into series production.

1 Introduction

To enjoy success in the marketplace, torque vectoring systems should not only offer the fundamental possibility of variable torque distribution between the wheels on one axle but also offer the customer a new form of driving experience. The challenges facing the components, given restrictions on packaging, weight increase and intolerability of efficiency losses and raised fuel consumption, require new solution concepts.

The application of appropriate torque distribution between the two wheels on one axle generates a yaw moment about the vertical axis of the vehicle. This yaw moment can influence vehicle dynamics directly if it can be adjusted independently of the forward propelling force. Using torque vectoring in the drivetrain, delayed or even counteractive reactions of the vehicle to steering input can be influenced without resort to any other control components. For the driver, the vehicle response seems sharper.

At the same time, outward torque transfer can optimize cornering force whilst inward torque transfer can also confer significantly increased stability, damping yaw acceleration. Along with the possibility to ap ply corrective torque transfer at the limit of traction, the result is improvements not only in driving pleasure but also significantly in driving safety under all road conditions.

2 Selection of the Right Overall System and its Sub-systems

The system design is derived from the technical requirements of the components in the complete vehicle and is defined by the functions it must fulfill. The expectations include not only general improvement of agility and the possibility to damp the motion of a vehicle at high rates of yaw, but also complete independence of torque distribution from driving condition, loading and power-on time. The extended functions of the drivetrain should guarantee the highest safety and robustness alongside limited weight increase and minimal loss of efficiency. A further limitation for a system manufacturer is implementability, i.e. the possibility of adapting an existing drivetrain configuration with a reasonable level of investment. Modular construction has enabled simple adaptation, **Figure 1**.

A benchmark comparison of electrical, hydrostatic and mechanical solutions demonstrates absolutely clear packaging and weight advantages for mechanical variants. These consist primarily of superposition units with clutch systems for raising rotation speed. The overall system consists of the final drive, clutch system, power mechanics of the superposition units, hydraulic system and control by means of an ECU and software, **Figure 2**.

3 Basic Final Drive and Differential

Adding variable torque distribution to an axle of an existing drivetrain should only have a limited effect on the existing, proven components like the differential. The pre-existing basic final drive ensures a separation between the superposition function and the fundamental transmission of torque via the differential to the rear axle, thereby offering the conventional standard transmission functional-

The Authors

Walter Sackl
is Head of Engineering Product Line / Concepts at Magna Powertrain in Lannach (Austria).

Gerhard Eibler
is Development Project Manager at Magna Powertrain in Lannach (Austria).

Thomas Linortner
is System Architect at Magna Powertrain in Lannach (Austria).

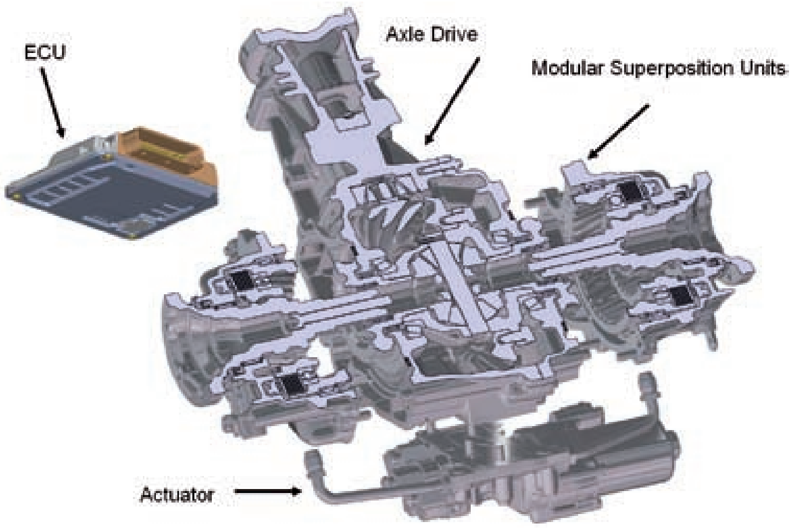

Figure 1: Modular layout

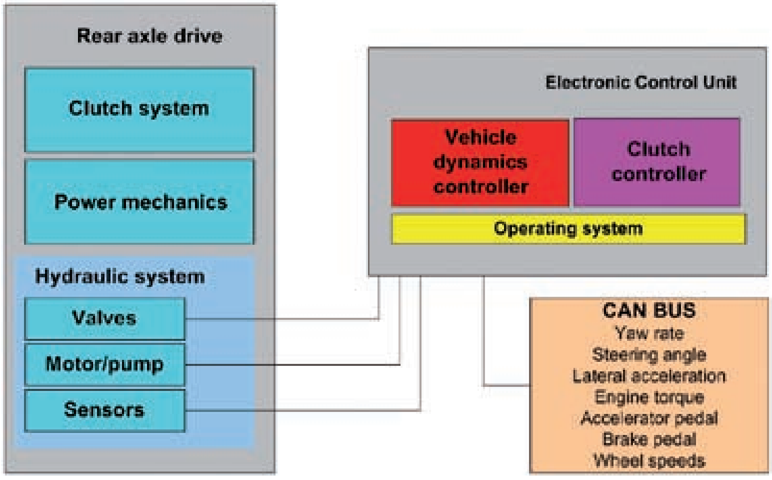

Figure 2: System overview

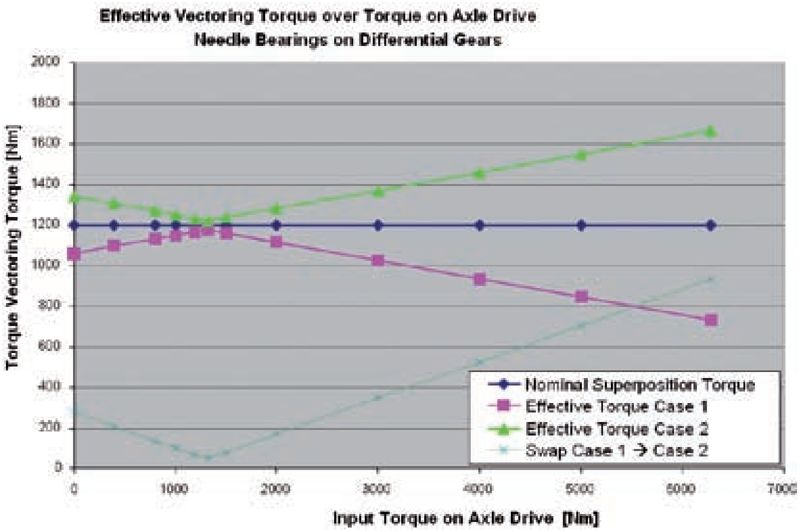

Figure 3: Effective superposition torque

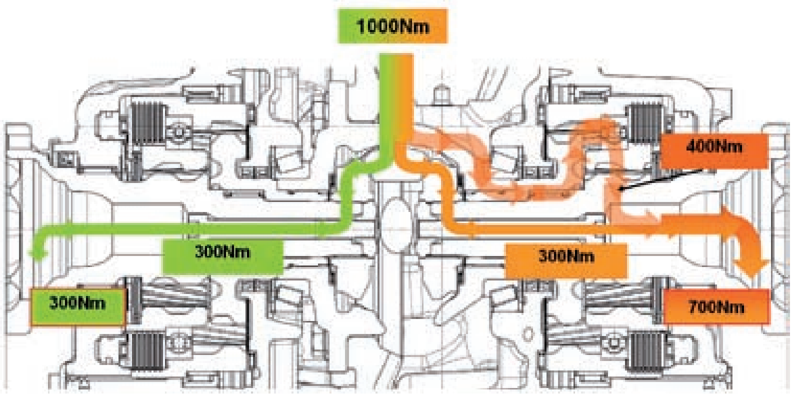

Figure 4: Torque flow

ity as a fallback free of consequent impairment. With its own oil circuit, apart from adaptation of interfaces it remains autonomous. However, the original effect of the locking function of a differential counteracts transfer of torque in the positive direction to the outer wheel in a bend, and is also dependent on the loading on the differential. As shown in **Figure 3**, with a standard differential coasting freely, effectively less torque is transferred outboard in line with the locking level (case 1). If torque is superimposed inboard (case 2) for damping purposes, a correspondingly larger level is distributed.

The absolute magnitude of these influences depends on the torque present on the final drive at any given time and can increase or reduce superposition torque according to evolving yaw rate. Direct measurement of both parameters is involved or, at the lowest rates of rotation, practically impossible, so it is necessary to take reduction measures.

Analysis of the sources of friction shows one of the greatest potentials to lie in the side gear journal bearings. In order to ensure fine control independent of final drive load, differential friction performance was improved through the application of needle roller bearings in place of thrust washers.

4 Superposition Units and Clutch System

The basic concept for influencing vehicle dynamics is the generation of asymmetric or opposing forces on the wheels of one axle. To achieve this, 2 superposition drives are so arranged that engagement of the clutch integrated into each unit accelerates one wheel and brakes the second wheel. These processes have to take place very rapidly as the generation of inertial torques in the drivetrain as a result of control system intervention is undesirable given the need to avoid virtual locking. **Figure 4** shows the basic flow of power. In the presence of a motive torque of 1000 Nm a torque difference of 400 Nm should be generated acting about the yaw axis. To turn the vehicle in to the left, 400 Nm of torque pass through the superposition unit. The differential distributes 2 x 300 Nm approximately symmetrically between the two driveshafts. The resultant is now 700 Nm on the right hand output and 300 Nm of torque on the left.

Figure 5 shows the rotary behavior at the superposition units without and with control active. Parts with accelerations during control are shown in yellow color.

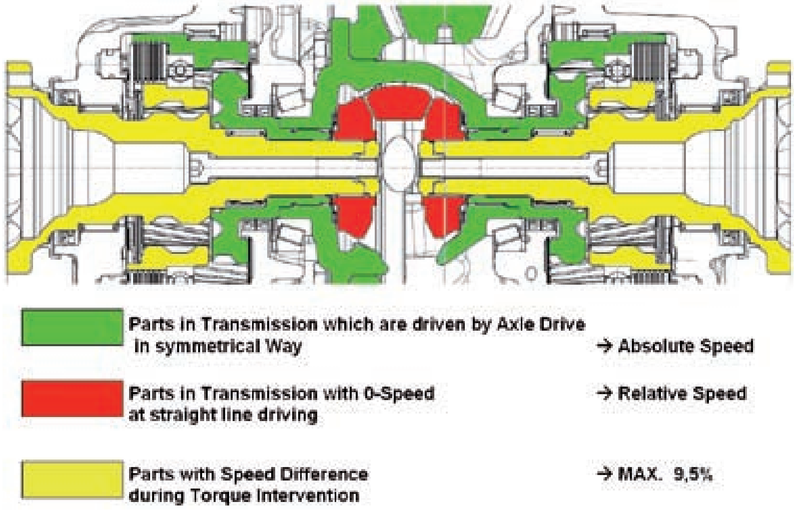

Figure 5: Systematic of speeds

The side required to apply a higher torque is accelerated rapidly, the rotary speed difference reduces but the rotary behavior of the engaged gears changes only slightly.

4.1 Gearing System

The mechanical superposition function consists of a torque-inserting gearing stage directly driven by the differential, the co-rotating clutch and a second gearing stage that acts on the flange shafts. Both gearing stages work at the same distance in one axle, offset from the axis of the differential hypoid gearing. Thus the outer part of the superposition unit is positioned about 7mm off center, **Figure 6**. The ratios are selected in such a way that they impose the smallest possible differential rotation speed on the clutches, essential for good overall efficiency.

4.2 Clutch System and Lubrication

The clutches are positioned directly in the superposition branch and have an absolute rotation speed of 90 % of that of the axle and straight-ahead drag of only 8.5 %. The outer lamellae are connected to the driving outer ring gear, whilst the inner lamellae are connected to the hub, which simultaneously constitutes the driven outer ring gear.

The low level of drag in the clutches in the non-actuated condition yields low drag torques even with narrow clearances and a temperature situation similar to that of a conventional differential. Comprehensive road testing has confirmed this, with temperature levels similar to those of similar differentials.

The entire arrangement of units can be tailored very simply to critical packaging situations, given the diameter and positioning offset from the centerline.

Furthermore, by virtue of direct drive via the differential, the gearing system also guarantees that no additional counterproductive sources of friction compromise the torque superposition function.

With this arrangement, all drag torques are driven via the differential housing and not from the wheel side, Figure 5. As a consequence, there are no reverse influences (virtual locking effect), brought about by the superposition units through reactive torques at high differential rotation speeds that might affect the function of the braking control system.

Care has been taken to ensure that drag torque has no influence on step changes in superposition torque as a result of changing from driving in a straight line to going round a bend. **Figure 7** shows the flow of power through the differential and superposition units. In order to meet the requirements for the highest possible availability, the superposition units were designed and verified on the basis of 8 % duty throughout the entire vehicle life.

The multi-plate system was developed to deliver the highest possible consistency of friction coefficient throughout its lifetime. Through efficient centrifugal lubrication in the units, the oil circuit, which is separate from that of the differential, ensures excellent temperature conditions, even during maximum loading such as on the racetrack.

Figure 8 shows that the change in frictional behavior over the entire lifetime is less than 5 %, and this small level is compensated within the actuation system over the unit lifetime.

5 Hydraulic System

Packaging limitations and the possibility to vary the positioning of the actuator led to selection of an electro-hydraulic system with one motor and one pump without a pressure accumulator.

The concept is based on the direct electro-hydraulic actuator system as used also in other applications for clutch actu-

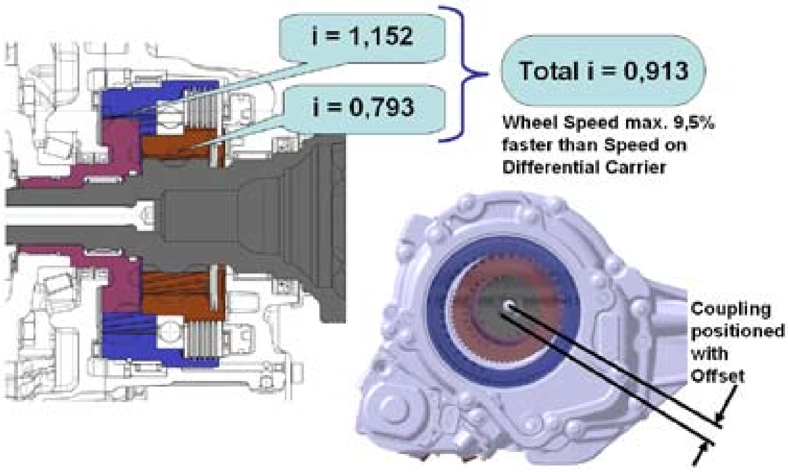

Figure 6: Gear sets and coupling

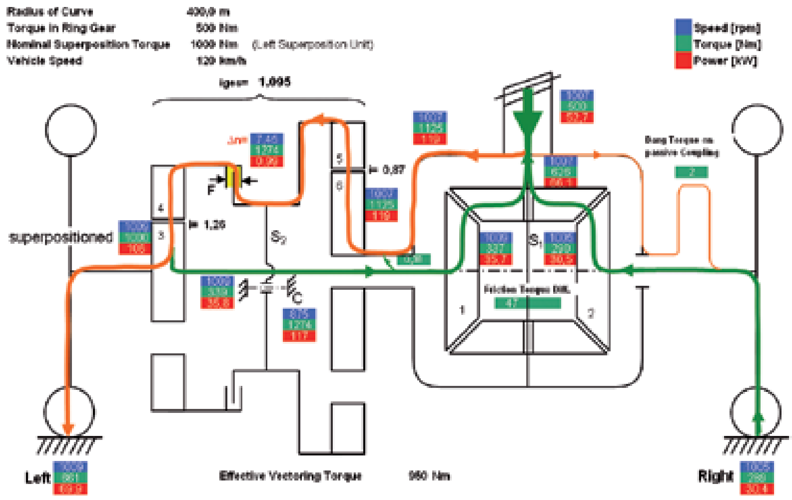

Figure 7: Power flow

ation in the drivetrain, **Figure 9**. It offers the fundamental advantage of controlling two clutches with one actuator. Well-considered system design has also resulted in no significant delay during switching from the first to the second clutch. The motor drives a pump that operates in both directions of rotation and thus delivers pressure to the piston on one torque superposition side at any time. Control is effected directly; the motor is used for pressure generation and reduction, thereby obviating the need for additional control valves. This reduces the number of power line outputs required in the controller.

Two redundant pressure sensors measure the pressures on both clutches via shuttle valves and ensure very high actuation precision. A shut-off valve on each side permits induction from the opposite path in each case and, in addition, a safety shut-off is operated simply through interruption of the power supply.

The exceptionally compact actuator unit, **Figure 10**, with associated oil reservoir is attached to the differential housing and shares an oil volume with the two superposition units. Air bleeding from the system takes place at defined intervals via the passive bleed valves. All components are robust, so no complicated hydraulic circuit filtering is necessary.

Thus the electro-hydraulic design, with its high overall efficiency, allows rapid transition through from the disengaged state alongside high precision of control by virtue of the short tolerance chain.

6 ECU, Sensors and Software

The ECU controls the electric motor and the two switchable valves. The incoming pressure sensor readings constitute the feedback loop in the control circuit, whilst the torque control demand comes from the vehicle bus system. The software is subdivided into basic software, driving dynamics controller and clutch controller. The calculated superposition torque is transferred via a torque interface between the driving dynamics controller and clutch controller.

The driving dynamics controller uses steering input angle, lateral acceleration, yaw rate and other information from the bus system to calculate the torque to be transferred and is networked to other control systems (e.g.: ESP). The clutch controller handles control of the demanded torque and torque vectoring system protection and diagnostic functions. This covers the multi-plate clutches, motor/pump unit, sensors and valves. The basic software handles signal conditioning and diagnostics. This modular design enables straightforward adaptation to different vehicles and bus systems (e.g. CAN or Flexray).

Diagnosis of the torque controller response behavior is achieved by means of tolerance bands. Decisions are made on

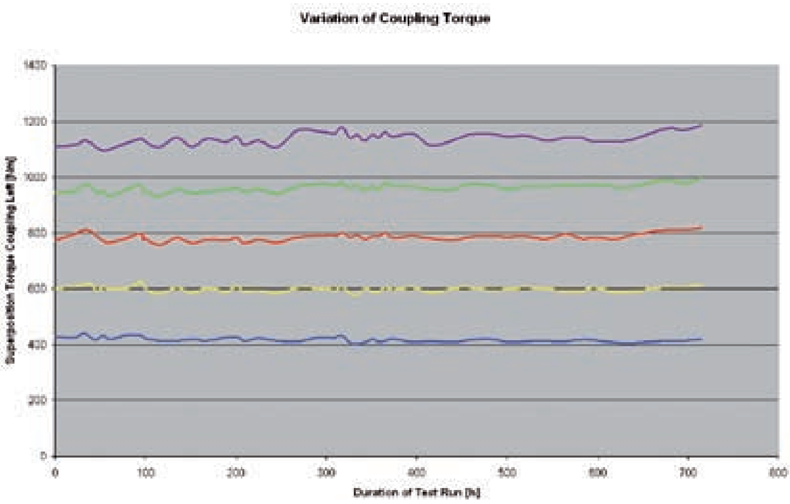

Figure 8: Friction coefficient over lifetime

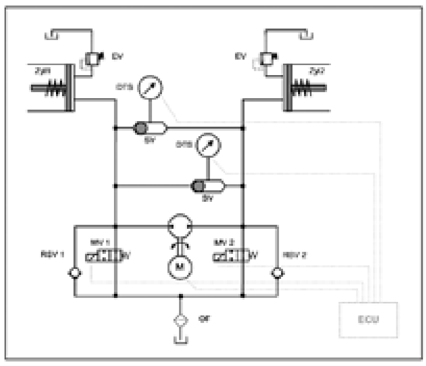

EV	Bleeding Valve	RSV	Check Valve
M	DC-Motor	DTS	Pressure / Temperature Sensor
ECU	Electronic Control Unit	MV	Solenoid Valve
SV	Shuttle Valve	Zyl	Cylinder / Piston
OF	Oil Filter		

Figure 9: Hydraulic system of direct electro-hydraulic actuator

the basis of hard and soft threshold values depending on the magnitude of deviation, in order to ensure that the system is stable and secure over its entire lifetime. The limit values for these diagnostic functions were established on the basis of test drives. **Figure 11** shows an example of a control level with upper and lower "hard" and "soft" tolerance bands. Crossing the "hard" threshold would compromise vehicle safety, so the system must be shut off if it is exceeded. In the "soft" area there is no sudden shut down but rather a calculation of the error integral to check whether response behavior is only briefly outside specification.

7 Overall System Performance and Safety

The entire system was developed in line with the requirements of IEC 61508 – Functional Safety Management. Because this is a steering system achieved by active torque superposition on the rear axle, it is necessary to prevent false actuations with failure probability levels of less then 10^-7 dangerous failures per hour. This applies to all electrical, electronic and programmable electronic components.

In the event of a failure, the transferred axle torque must be reduced to a non-critical value within 100ms. This is achieved through the combination of direct electro-hydraulic actuators with shut-off valves that open when power is interrupted. When a dangerous failure is detected, the power is interrupted immediately with the result that system pressure also reduces immediately, yielding behavior the same as that of a conventional axle. Dangerous failures are detected by means of redundant pressure measurement in combination with tolerance bands for the setpoint and actual torque relationship. A special hardware and software architecture guarantees the required low failure probability.

One central requirement is torque control dynamics. In order to achieve well-defined driving behavior it is necessary that a superposition of torque should be available at the wheels before the onset of strong under or oversteer. Otherwise there would be disquieting transitions between vehicle understeer

Figure 10: Actuation module

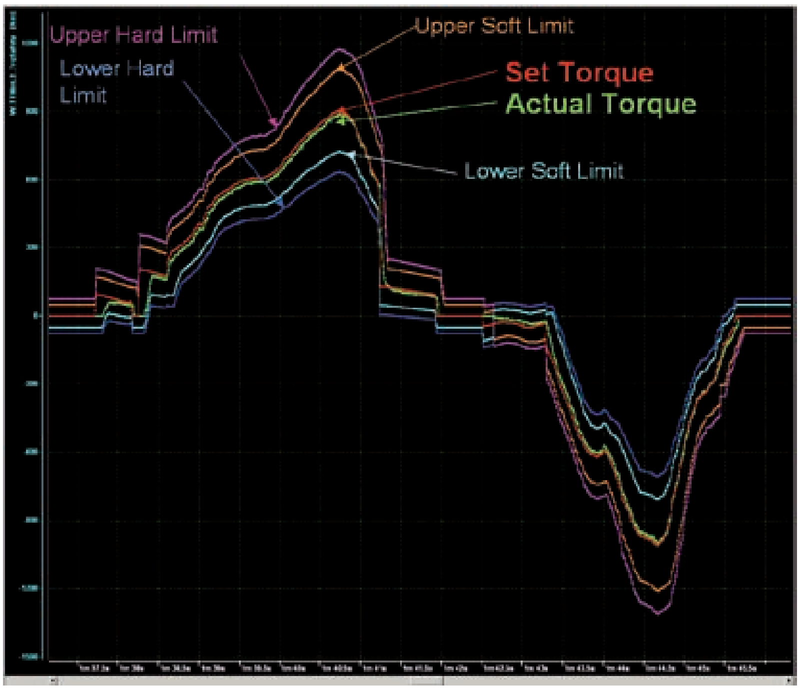

Figure 11: Tolerance zone of controller

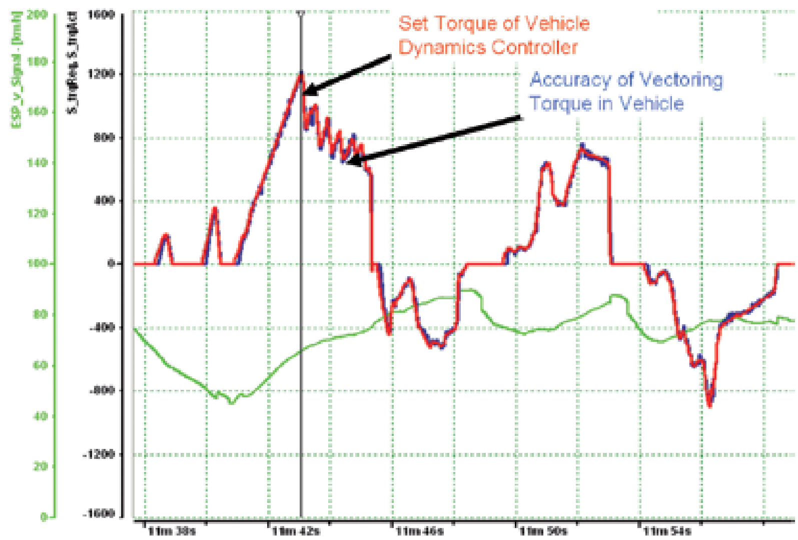

Figure 12: Subsequence to set torque of vehicle dynamics controller

IMPRINT

ATZ WORLDWIDE

www.ATZonline.com

12|2008 · December 2008 · Volume 110
Springer Automotive Media | GWV Fachverlage GmbH
P. O. Box 15 46 · 65173 Wiesbaden · Germany
Abraham-Lincoln-Straße 46 · 65189 Wiesbaden · Germany

Managing Directors Dr. Ralf Birkelbach, Albrecht Schirmacher
Senior Advertising Thomas Werner
Senior Production Ingo Eichel
Senior Sales Gabriel Göttlinger

EDITORS-IN-CHARGE

Dr.-Ing. E. h. Richard van Basshuysen
Wolfgang Siebenpfeiffer

EDITORIAL STAFF

Editor-in-Chief
Johannes Winterhagen (win)
Phone +49 611 7878-342 · Fax +49 611 7878-462
E-Mail: johannes.winterhagen@springer.com

Vice-Editor-in-Chief
Dipl.-Ing. Michael Reichenbach (rei)
Phone +49 611 7878-341 · Fax +49 611 7878-462
E-Mail: michael.reichenbach@springer.com

Chief-on-Duty
Kirsten Beckmann M. A. (kb)
Phone +49 611 7878-343 · Fax +49 611 7878-462
E-Mail: kirsten.beckmann@springer.com

Sections
Body, Safety
Dipl.-Ing. Ulrich Knorra (kno)
Phone +49 611 7878-314 · Fax +49 611 7878-462
E-Mail: ulrich.knorra@springer.com

Chassis
Roland Schedel (rs)
Phone +49 6128 85 37 58 · Fax +49 6128 85 37 59
E-Mail: ATZautotechnology@text-com.de

Electrics, Electronics
Markus Schöttle (schoe)
Phone +49 611 7878-257 · Fax +49 611 7878-462
E-Mail: markus.schoettle@springer.com

Engine
Dipl.-Ing. (FH) Richard Backhaus (rb)
Phone +49 611 5045-982 · Fax +49 611 5045-983
E-Mail: richard.backhaus@rb-communications.de

Heavy Duty Techniques
Ruben Danisch (rd)
Phone +49 611 7878-393 · Fax +49 611 7878-462
E-Mail: ruben.danisch@springer.com

Online
Dipl.-Ing. (FH) Caterina Schröder (cs)
Phone +49 611 7878-190 · Fax +49 611 7878-462
E-Mail: caterina.schroeder@springer.com

Production, Materials
Stefan Schlott (hlo)
Phone +49 8191 70845 · Fax +49 8191 66002
E-Mail: Redaktion_Schlott@gmx.net

Service, Event Calendar
Martina Schraad
Phone +49 212 64 232 64
E-Mail: martina.schraad@springer.com

Transmission, Research
Dipl.-Ing. Michael Reichenbach (rei)
Phone +49 611 7878-341 · Fax +49 611 7878-462
E-Mail: michael.reichenbach@springer.com

English Language Consultant
Paul Willin (pw)

Permanent Contributors
Christian Bartsch (cb), Prof. Dr.-Ing. Peter Boy (bo),
Prof. Dr.-Ing. Stefan Breuer (sb), Jens Büchling (jb),
Jörg Christoffel (jc), Jürgen Grandel (gl),
Erich Hoepke (ho), Prof. Dr.-Ing. Fred Schäfer (fs),
Bettina Seehawer (bs)

Address
P.O. Box 1546, 65173 Wiesbaden, Germany
E-Mail: redaktion@ATZonline.de

MARKETING | OFFPRINTS

Product Management Automedia
Sabrina Brokopp
Phone +49 611 7878-192 · Fax +49 611 7878-407
E-Mail: sabrina.brokopp@springer.com

Offprints
Martin Leopold
Phone +49 2642 9075-96 · Fax +49 2642 9075-97
E-Mail: leopold@medien-kontor.de

ADVERTISING | GWV MEDIA

Key Account Manager
Elisabeth Maßfeller
Phone +49 611 7878-399 · Fax +49 611 7878-140
E-Mail: elisabeth.massfeller@gwv-media.de

Ad Sales
Sabine Röck
Phone +49 611 7878-269 · Fax +49 611 7878-140
E-Mail: sabine.roeck@gwv-media.de

Heinrich X. Prinz Reuß
Phone +49 611 7878-229 · Fax +49 611 7878-140
E-Mail: heinrich.reuss@gwv-media.de

Display Ad Manager
Sandra Reisinger
Phone +49 611 7878-147 · Fax +49 611 7878-443
E-Mail: sandra.reisinger@gwv-media.de

Ad Prices
Price List No. 51

SUBSCRIPTIONS

VVA-Zeitschriftenservice, Abt. D6 F6, ATZ
P. O. Box 77 77, 33310 Gütersloh, Germany
Renate Vies
Phone +49 5241 80-1692 · Fax +49 5241 80-9620
E-Mail: SpringerAutomotive@abo-service.info

SUBSCRIPTION CONDITIONS

The emagazine appears 11 times a year at an annual subscription rate of 269 €. Special rate for students on proof of status in the form of current registration certificate 124 €. Special rate for VDI/ÖVK/VKS members on proof of status in the form of current member certificate 208 €. Special rate for studying VDI members on proof of status in the form of current registration and member certificate 89 €. The subscribtion can be cancelled in written form at any time with effect from the next available issue.

PRODUCTION | LAYOUT

Kerstin Gollarz
Phone +49 611 7878-173 · Fax +49 611 7878-464
E-Mail: kerstin.gollarz@gwv-fachverlage.de

HINTS FOR AUTHORS
All manuscripts should be sent directly to the editors. By submitting photographs and drawings the sender releases the publishers from claims by third parties. Only works not yet published in Germany or abroad can generally be accepted for publication. The manuscripts must not be offered for publication to other journals simultaneously. In accepting the manuscript the publisher acquires the right to produce royalty-free offprints. The journal and all articles and figures are protected by copyright. Any utilisation beyond the strict limits of the copyright law without permission of the publisher is illegal. This applies particularly to duplications, translations, microfilming and storage and processing in electronic systems.

Springer Automotive Media is part of the specialist publishing group Springer Science+Business Media.

and oversteer, perceived in a negative light by the driver. Here the System guarantees controlled torque application and release within <120ms between released, passive state and the maximum possible torque, redistribution can be done within 100 ms. It was therefore necessary to optimize the clutch controller for rapid transition through from the disengaged state and regulation of set-point torque without overshoots. The safety-related release in the event of a failure mentioned above is much faster as a result of the lack of a need for active control and thanks to the potential energy stored in the clutches.

The system precision is another important aspect. Because an excessively high superposition torque can lead to depletion of wheel side force on the limit of traction, it is necessary to control the stabilized torque with an accuracy of +/-10 %. The short tolerance chain and simple relationship between pressure and torque make it possible to achieve the required high precision of control and also the safety requirements.

Figure 12 shows the good response behavior of the effective superposition torque in the vehicle, with no significant overshoot. Because torque vectoring systems are desirable for high-powered, sporty vehicles, thermal demands on the system are very high. For example, if driving quickly on mountain roads or around a circuit, rear axle temperatures can rise to 150°C. So the requirements for accuracy and dynamic response stated above have to be ensured over a very broad range of temperature. Through a modular design and dedicated pursuit of customer wishes it was successful to bring an effective torque vectoring unit into series production.

References

[1] Mohan S.; Sackl W.: Simulation and Definition of an Active Yaw Control Device. Graz, Magna Powertrain, Allradkongress, 2006
[2] Gratzer F.; J.Quehenberger.: Direkte elektrohydraulische Aktuierung [Direct electro-hydraulic actuation], Würzburg, Innovative Fahrzeuggetriebe CTI Symposion 2005


Karriere
Archiv
Events
Wissen
Topmeldung
Aktualität
1500 m
www.ATZonline.de
Optionen
NAVIGON

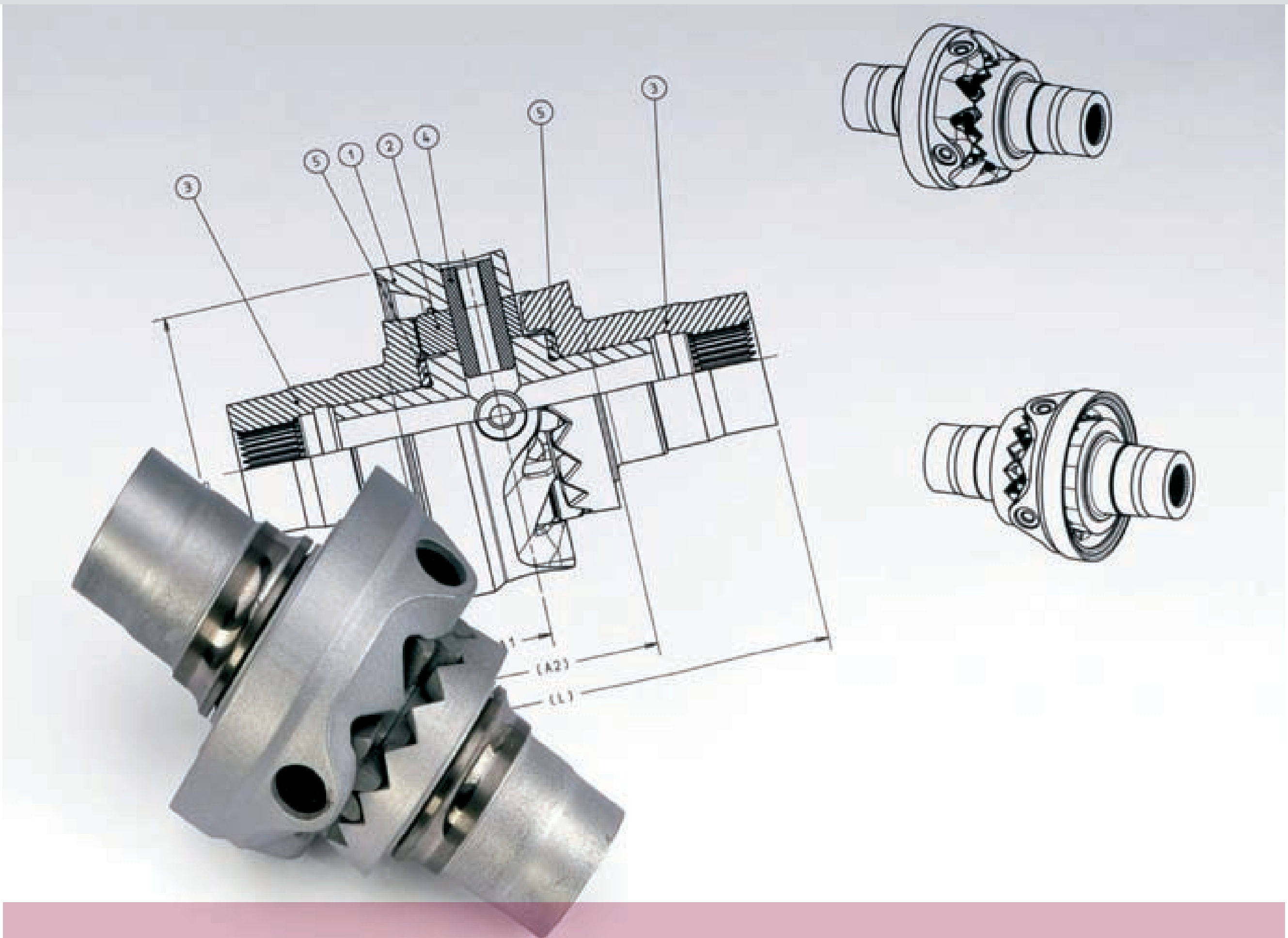

Torque Optimized Spur Gear Differential

Perspective for Reduced Size and Weight

Today's standard vehicles' differentials have a housing, which covers the inner bevel gearing for the torque transmission. With its TPO differential – T/P-O stands for „torque and package optimised" – Tedrive has developed a caseless differential. This new spur gear differential has a decrease in size and weight at the same torque level. A reduction of the required distance between bearings of up to 50 % is possible.

1 Introduction

Reduced CO_2 emissions, new legislation and improved personal protection are the three key requirements, besides costs, for today's vehicles' development. This means package and vehicle weight requirements become important factors in today's vehicle and components design. In order to achieve these reductions, changes can be introduced to components the end customer does not see, for example, in hybrid drives or differentials in front, rear and all wheel drive vehicles.

With its TPO differential – T/P-O means „torque and package optimised" –, Tedrive developed a package-optimized and caseless differential while maintaining the torque transmission. Even allowing for the differentials low weight, all technical performance, noise requirements and price targets of the automotive industry have been achieved.

In the TPO design, the standard differential bevel gears were replaced by spur gears respectively cylinder gears. The TPO differential can be applied to a front-, rear or all wheel drive application. The new TPO design shows a reduction of the required distance between bearings of up to 50 %. Not only the differential will reduce mass inertia, weight and package, but the entire transmission unit. The advantages of the differential lead into advantages for the vehicle itself, **Figure 1**.

2 State of the Art

The vehicles' standard differential today has a housing, which covers the inner bevel gearing for the torque transmission. The differential is placed in the centre of the axle between the wheels to transmit the driving torque, which is introduced by the transmission directly or by the driveshaft. The differential adjusts with low friction losses, for the differences in speed between the drive wheels due to changing road conditions or cornering. Otherwise the powertrain would become locked resulting in tire slip. The pinion gears are free to rotate and thereby balance the torque between both interacting side gears. This ensures that both wheels always transmit the same torque.

The whole differential package is determined by the size of the differential case, which in turn depends on the torque to be transmitted. In this way any increase in the design size of the inner differential gears to carry higher torques, would lead to an increase in the outside diameter and length of the differential case. In many cases the differential package envelope can remain the same even with a torque capacity increase, by changing from a one-piece differential case with two pinions to a two-piece differential case with three or more pinions. But with the more complex case comes a significant increase in production costs and weight.

3 Motivation

The small engine designs within modern vehicles with limited available package space in the engine compartment and underfloor area drives the transmission manufacturers to use more complex differentials. Additional units for electrical steering elements, emission controls as well as components for the improvements in vehicle dynamics, like double clutch transmissions or torque vectoring modules, lead to package conflicts between the individual units. In addition, legal requirements for the improvement in pedestrian protection continue to limit the package available in the frontend. For these reasons plus the need to provide space for bonnet deflection, the entire engine and transmission assembly must be lowered. The long term outcome of all these vehicle requirements is a reduction

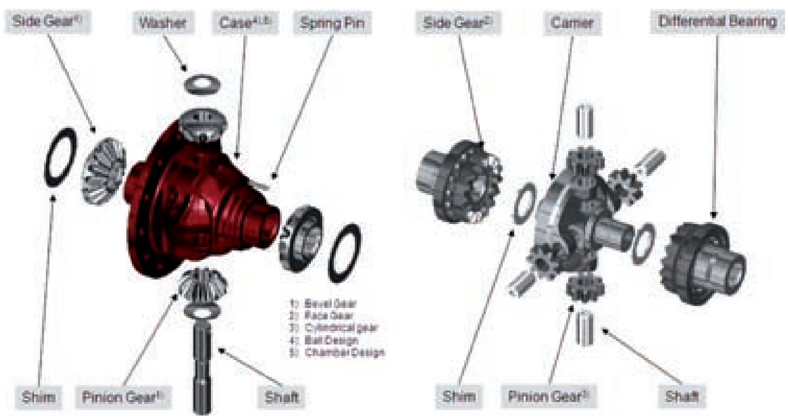

Figure 1: Parts of a traditional bevel gear differential (left) compared to the new TPO differential (right)

The Authors

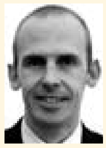

MSc, Dipl.-Ing. (FH) Torge Reinold is manager TPO pursuits and torque management at Tedrive Germany GmbH in Düren (Germany).

Dipl.-Ing. (FH) Christoph Chatenay is engineer PD torque management at Tedrive Germany GmbH in Düren (Germany).

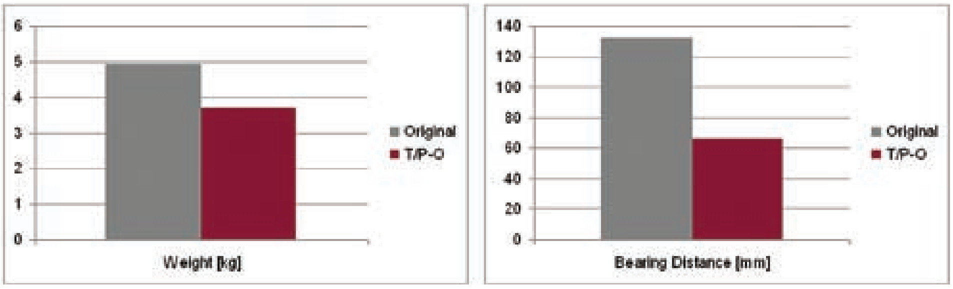

Figure 2: Actual prototype of a TPO differential in weight and bearing distance comparison to a traditional original rear axle housing

in the available space for the gearbox, as there is a minimum ground clearance requirement which cannot be encroached upon. All-wheel drive systems with inline engines intensify the problem of minor available package, because a link shaft has to pass the clutch housing or oil pan.

Alongside the package issues, there is the requirement today to reduce vehicle weight. The drivers are the CO_2 emissions and the vehicle dynamics.

4 TPO Differential – Structure and Advantages

Ever since the end of the 19th Century there have been patents taken out for caseless differentials. The TPO differential picked up on the idea of the caseless differential for the new requirements of package and weight optimization.

The traditional differential case was replaced by a disc-shaped carrier, Figure 1. The two side gears are mounted on each side of the carrier on a central location pin as sleeve bearing. The TPO design has two or more pinion gears similar to the normal bevel gear differential. These are fitted to and can rotate in the simple carrier.

In Figure 1, the standard differential bevel gears were replaced by spur gears. As a result, the torsional lash of the differential gearing need only be adjusted by using shim washers to position the side gears. The straight spur pinion gears do not require axial adjustment.

The final drive is achieved in the form of a bevel or spur gear welded or bolted to the outer diameter of the carrier. The TPO differential can be applied to a front, middle or rear drive application.

The standard option is to use the side gear and the carrier pin as a sleeve bearing. Needle roller bearings can be added for high load applications. Thus, the inner friction of the differential can be minimized, and the efficiency of the TPO differential is increased.

For a limited slip differential application the reverse of the above is required. Suitable wear resistant friction linings would be introduced. The advantage of the limited slip differential is to ensure drive, when the wheels are on unequal friction road surfaces.

4.1 Weight and Package

In a first prototype vehicle a conventional production, bevel gear differential was replaced by a TPO differential in the same housing space. All components of the rear axle housing assembly except the actual differential were carry-over parts. The bevel ring gear was mounted onto the TPO differential and the entire differential assembly mounted into the housing with its original roller bearings. There is a clear package advantage between the original and the TPO differential, **Figure 2**.

The maximum torque capacity of the standard differential is up to 10,000 Nm. With the same peak torque, the TPO design shows a reduction of the required distance between bearings of up to 50 %. Because only the gear geometry of the pinions and side gears determines the distance between bearings, it was possible to make a reduction from 132 down to 66 mm, while the mass of the differential has been cut from 4.92 to 3.69 kg, **Figure 3**. Not only the differential will reduce mass inertia, weight and package, but the entire transmission unit. The advantages of the differential lead into advantages for the vehicle itself.

This freedom in design to create a bigger available space to fill with locking devices or for re-sizing the rear axle housing to an optimized (or required) minimum, enables the designer to find other and new ways of transmission and powertrain concepts. The standardization approach can be realized.

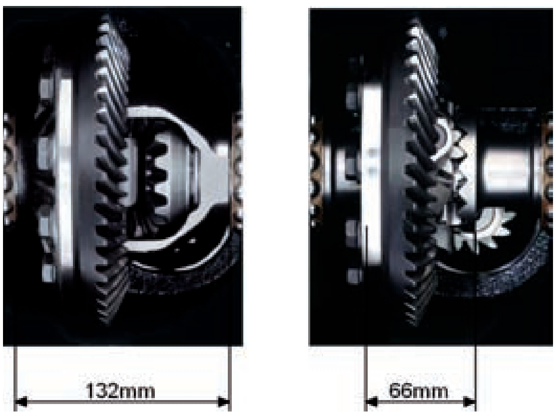

Figure 3: Comparison of mass and bearing distance; traditional bevel gear differential (left) vs. CAE optimized TPO differential (right)

4.2 Performance and NVH Behaviour

The introduction of the TPO differential into the environment of the standard differential shows the same performance as the differential it replaced; torque transfer, ability of speed differentiation and durability in its initial assessment (split-μ-testing and general vehicle road driving) in accordance to specifications.

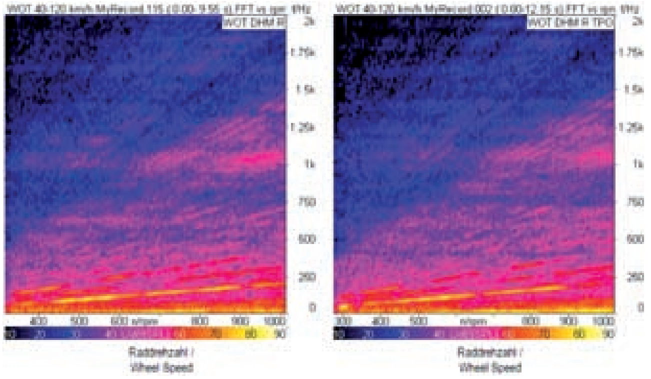

Figure 4: Measurement of sound pressure level: traditional bevel gear differential (left) vs. TPO differential (right) (sound pressure level in passenger's position)

The investigation of NVH behaviour underlined the fact, that there is correct engagement between the pinion and bevel gear within the entire differential operation. The comparable results of the sound pressure level measurements for acceleration from 40 to 120 km/h are shown in **Figure 4**.

4.3 Assembly

Besides the mentioned technology advantages the TPO differential offers at the same time positive effects on the processes in transmission production. The lateral assembly of the side gears allows a straight forward assembly of the differential carrier into the rear differential housing, **Figure 5**. The side gears will be assembled with the pre-mounted differential bearings laterally into the housing bores. The assembly process will be simplified and time consuming operations eliminated.

4.4 Interface Systems

The standard interface between the output shaft assembly and the side gears is a spline connection. These splines are near the centre of the differential in the traditional design, but with the new design the splines can be located at the outer end of the side gears closer to the walls of the differential housing. This allows the vehicle halfshafts to be significantly shorter in its stem length, thereby reducing weight and improving the assembly condition. The halfshaft stem lengths can be reduced to just the spline length, even eliminating the sealing surface on the stem required for the housing sealing ring. Therefore the side gears of the TPO combine the functions of the inner differential gear of transmitting the torque from the pinion gears to the side gears, providing the bearing seat and the sealing surface to seal the entire differential housing.

This raises the possibility of a pre-assembled and oil-filled differential for simple inline handling and testing. The more compact TPO design also allows for longer halfshafts, this reduces the operating angles of the inner and outer board joints.

4.5 Environment

The TPO differential reduces the required package space. This will raise the question, whether the lubricant oil content can also be reduced. Ensuring proper heat dispersion from the fluid to the case and then to atmosphere, will guarantee the oil properties over life time. This will lead to a simple equation, which means: less oil, reduced cost and environmental protection.

5 Summary and Outlook

The TPO differential project started at Tedrive with a basic concept, from which the general feasibility was developed. The team investigated the component loading, the effects on the contact patterns and the manufacturing feasibility. An initial simple hardware concept was built and tested on a rear axle test stand, meeting the requirements.

The positive results encouraged the team to progress to the next phase of the program. New prototypes were built introducing the lessons learned from the first samples. Using production like processes validated their influences on the design. These new variants were evaluated in a vehicle rear axle application. The prototypes passed the comparison to the standard differential in respect to drivability, NVH behaviour and the required torques.

Today, further prototypes are in testing to optimize tribology. Future development targets are to prove out the TPO principle in limited slip differentials, in All-Wheel-Drive differentials and in Torque Vectoring Modules. Also to be investigated is the potential to integrate the halfshaft in board joints with the TPO differential in order to aid assembly and further reduce costs.

Due to its specific carrier design, it is possible to change, with acceptable costs, from a two-pinion design to a design with three or more pinion gears. This is the basis for a cost effective and highly flexible modular design. ■

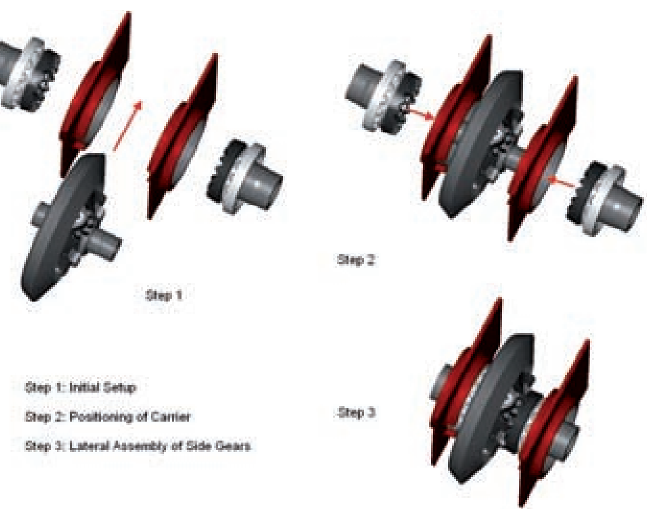

Figure 5: Simplified differential assembly with final drives in threes steps

personal buildup for Force Motors Ltd.

SEA Modelling for Sound Package Development

Inclusion of Simulated Airborne Noise Loads

During the last years, the statistical energy analysis (SEA) has been widely used by vehicle manufacturers and suppliers to analyse the airborne noise on road vehicles. While the basic workflow for the construction of vehicle SEA models is now well established, an accepted specific methodology for the evaluation of the SEA airborne loads to be used in these models is not available yet. In the framework of a joint project between Rieter Automotive and Volkswagen, a hybrid procedure that combines the standard finite element analysis (FEA) with the recently developed energy boundary element analysis (EBEA) was used for the evaluation of such loads and validated obtaining rather satisfactory results.

1 Introduction

When a test vehicle is available, the experimental evaluation of the sound pressure level distribution around the vehicle of interest represents a robust and sensible approach for the definition of the airborne loads to be used in its statistical energy analysis (SEA) model. This approach has been used by many SEA analysts with satisfactory results, and in a first attempt, it was used also for the joint Rieter/Volkswagen SEA simulation project, in cooperation with University Michigan (USA) considered here. Papers [1] to [3] represent just a very small selection of the dozens of papers that have been published on this topic during the last 15 years.

For the evaluation of the airborne loads, the outer panels of the vehicle passenger compartment are subdivided in a way compatible with the subdivision of the SEA model into subsystems. After this, for each panel, a few measurement positions close to the panel surface are defined. The total number of measurement positions can range from 200 to 350, depending on the vehicle's size. The sound pressure level generated by one or more sound sources at each one of these positions is evaluated. The joint activity between Rieter and Volkswagen focused on the acoustic transfer function from the rear tyre as noise source and, for this case, Volkswagen test standards prescribe considering eight different source positions, four around each rear tyre. For each panel, the airborne load to be applied in the SEA model is obtained by energetically averaging both on the microphone positions lying on the panel itself and on all source positions.

As already mentioned, this whole process has proven to be reliable and robust. But in some cases it might represent a weak point in the construction process of the SEA model:

- The necessary testing is timely quite extensive: depending on the number of source positions to be analysed and on the hardware available, it can take from one to three weeks.
- If the SEA model is intended to assist the development of a vehicle sound package, the measurement of the SEA loads assumes the availability of a vehicle prototype.
- Even when the vehicle is available, the measured SEA loads are introduced into the SEA model as "static constraints". This precludes the ability to simulate the effect of design changes related to the external shape of the vehicle, the position of the source and the presence and the positioning of absorbing materials.

As a consequence of all this, SEA analysts have long tried to develop techniques that allow at least to estimate the SEA airborne loads without the need of experimental tests. In most cases, semi-empirical procedures based mainly on „trial-and-error" were used and, for many years, these techniques have remained at the level of „confidential recipes". Only relatively recently have some specific

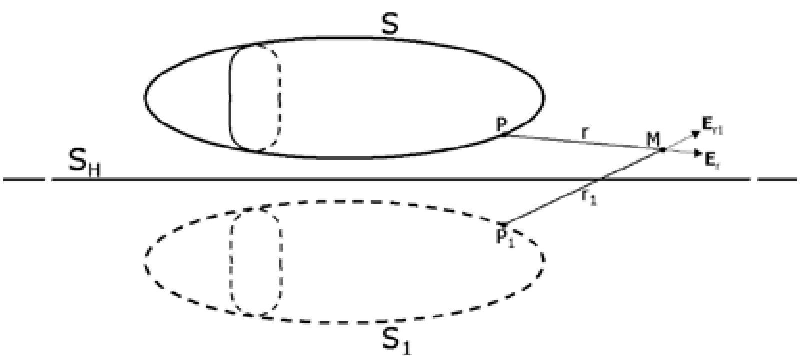

Figure 1: Schematic representation of the radiation from a vibrating body in a half-space (with reflexion panel S_H)

The Authors

Dipl.-Phys.
Boris Brähler
is technical expert for acoustics in the Centre of Excellence for Vehicle Acoustics at Rieter Automotive in Winterthur (Switzerland).

Dipl.-Phys.
Claudio Bertolini
is responsible for NVH tools and methodologies in the Centre of Excellence for Vehicle Acoustics at Rieter Automotive in Winterthur (Switzerland).

works on this topic been published [4, 5]. In particular, a very promising methodology for the efficient analysis of radiation and scattering problems in the mid-high frequency range was proposed by Wang, Vlahopoulos and Wu [6]. This methodology was called energy boundary element analysis (EBEA) by the authors since it essentially consists of an energetic reformulation of the classical integral equations on which the boundary element analysis (BEA) is based.

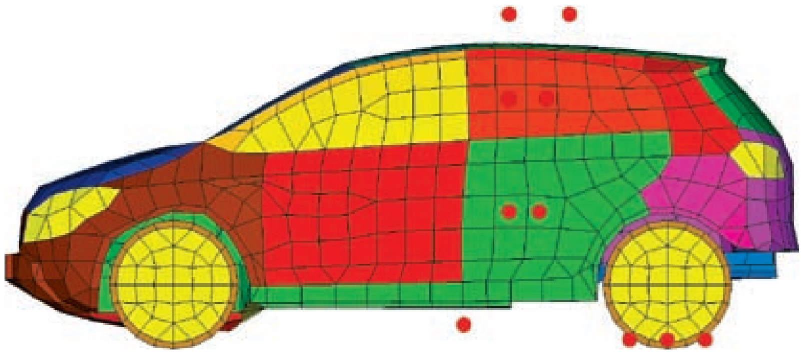

Figure 2: Model used for EBEA simulations; the source positions around the rear left tyre are visible, as well as some response positions around the vehicle's part panels

2 Brief Review of Energy Boundary Element Analysis

EBEA equations are essentially an energetic reformulation of classical BEA equations. Given a vibrating body delimited by a boundary surface S in presence of a rigid halfplane S_H, **Figure 1**, classical BEA integral equations allow to express the acoustic pressure at a receiver point M as Eq. (1):

$$\hat{p}(M) = \int_S A(P)G(P, M)\mathrm{d}S \qquad \text{Eq. (1)}$$

where P is a generic point located on the surface S, A(P) is an unknown complex source strength defined on S, and Eq. (2)

$$g(P, M) = \frac{e^{-ikr}}{4\pi r} + \frac{e^{-ikr1}}{4\pi r_1} \qquad \text{Eq. (2)}$$

is the half-space Green's function (see Figure 1 for the explanation of the notations used in Eq. (2)). Starting from Eq. (1) and under the basic assumption that the spatial correlation between the average acoustic fields in different regions around the vibrating body is zero, it is possible to express the average acoustic energy density and the average acoustic intensity at M as Eq. (3) and Eq. (4):

$$\mathrm{E}[\langle e \rangle] = \int_S \sigma \left(\frac{\rho}{64\pi^2 r^4} + \frac{k^2\rho}{32\pi^2 r^2} + \frac{\rho}{64\pi^2 r_1^4} + \frac{k^2\rho}{32\pi^2 r_1^2} \right) \mathrm{d}S \qquad \text{Eq. (3)}$$

$$\mathrm{E}[\langle \mathrm{I} \rangle] = \int_S \sigma \left(\frac{k^2\rho c}{32\pi^2 r^2}\,\mathrm{E}_r + \frac{k^2\rho c}{32\pi^2 r_1^2}\,\mathrm{E}_{r1} \right) \mathrm{d}S \qquad \text{Eq. (4)}$$

where

$$\sigma = \frac{1}{\rho^2\omega^2} |\mathrm{A}|^2 \qquad \text{Eq. (5)}$$

is defined as the strength density of the energy source and it is a frequency dependent quantity directly linked to A. In Eq. (3) and Eq. (4), E[ ] indicates frequency or space averaging. Comparing to the conventional BEA integral Eq. (1) for half-space problems to Eq. (3) and Eq. (4), it turns out that, in a formal way, EBEA is similar to BEA in the sense that it makes use of surface integral equations for the evaluation of the primary quantities of interest. In the case of EBEA, differently from BEA, such quantities are of an energetic nature, being given by the acoustic energy density and intensity. The half-space Green's functions for the acoustic energy density and intensity are given by Eq. (6) and Eq. (7):

$$G = \frac{\rho}{64\pi^2 r^4} + \frac{k^2\rho}{32\pi^2 r^2} + \frac{\rho}{64\pi^2 r_1^4} + \frac{k^2\rho}{32\pi^2 r_1^2} \qquad \text{Eq. (6)}$$

$$\mathrm{H} = \frac{k^2\rho c}{32\pi^2 r^2}\,\mathrm{E}_r + \frac{k^2\rho c}{32\pi^2 r_1^2}\,\mathrm{E}_{r1} \qquad \text{Eq. (7)}$$

In order to develop a numerical solution, the surface S of the model is divided into n quadrilateral or triangular elements. The source strength density σ_j on each element is assumed to be a constant. Eq. (3) and Eq. (4) are rewritten in a discrete form as Eq. (8) and Eq. (9):

$$\mathrm{E}[\langle e \rangle]_\mathrm{Y} = \sum_{j=1}^{n} \left[\sigma_j \int_{Sj} G(\xi, \mathrm{Y})\mathrm{d}S \right] \qquad \text{Eq. (8)}$$

$$\mathrm{E}[\langle \mathrm{I} \rangle]_\mathrm{Y} = \sum_{j=1}^{n} \left[\sigma_j \int_{Sj} \mathrm{H}(\xi, \mathrm{Y})\mathrm{d}S \right] \qquad \text{Eq. (9)}$$

Here, n is the number of the elements over the surface S, ξ is an arbitrary point on the element j, Y indicates the location of an arbitrary field point exterior to the structure in the half space. The outward radiated acoustic power on each element constitutes the boundary conditions of the EBEA formulation, which is described as Eq. (10):

$$\int_{Si} \langle \mathrm{I} \rangle \cdot \mathrm{n}_i \mathrm{d}S = \bar{P}_i,\ \mathrm{i} = 1, 2, \ldots, \mathrm{n} \qquad \text{Eq. (10)}$$

Substituting Eq. (10) in Eq. (9) results in Eq. (11):

$$K_{ij}\sigma_j = \bar{P}_i, \quad \mathrm{i} = 1, 2, \ldots, \mathrm{n}, \quad \mathrm{j} = 1, 2, \ldots, \mathrm{n} \qquad \text{Eq. (11)}$$

Eq. (11) is solved numerically. Then by employing Eq. (3) and Eq. (4), the acoustic energy density and intensity are determined at any field point in the half space exterior to the BEA model.

3 Description of Hybrid FEA/EBEA Methodology for the Evaluation of SEA Loads

In the application described in this article, a combination of standard FEA (for the mid-low frequency range) and EBEA (for the high-frequency range) is used to evaluate the input value of airborne loads for a SEA model. The use of a deterministic FEA simulation methodology for the mid-low frequency range is related to the fact that EBEA is intrinsically well suited for the high-frequency range. When working on a discretised surface model, the methodology basically assumes that the (average) acoustic fields on different surface elements that constitute the model are uncorrelated. It is intuitive that this assumption tends to be more and more satisfied as the frequency increases and, correspondingly, the wavelength becomes smaller.

Among the various possibilities, for the calculations in the mid-low frequency range standard FE were preferred over BEA and infinite elements because of their higher computational efficiency

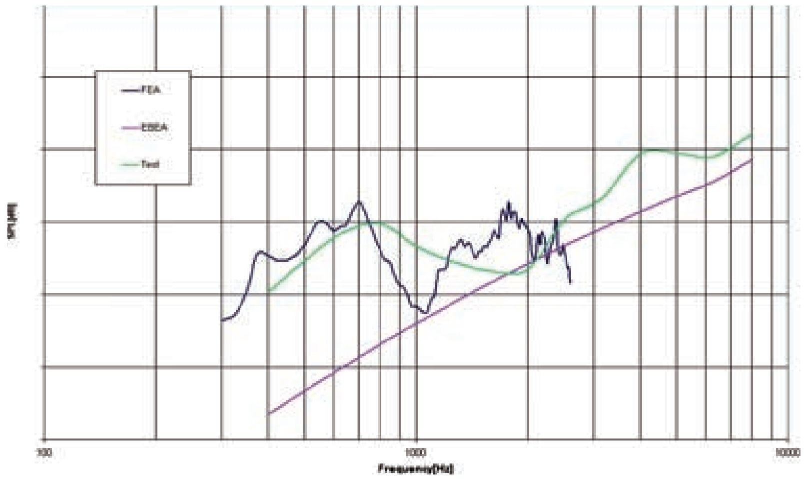

Figure 3: Sound pressure level on the rear left door window panel (spatial and source average); comparison between measured and FEA/EBEA simulated data

and easiness in the preparation of the model. For the FE model, the acoustic space around the vehicle was meshed with four-node tetrahedral elements, up to a distance of about 0.65 m (that is about one wavelength at 500 Hz) from the vehicle external surfaces (roof, side, front and back). On the outer boundary of the FE box so obtained, a boundary impedance equal to the characteristic impedance of air was imposed. It is clear that this boundary condition is able to represent only approximately the infinite acoustic space around the vehicle, in particular at low frequency. Nevertheless, it has to be emphasised that the primary interest here lies in the evaluation of the sound pressure level at points that are very close to the vehicle surface and these points are not likely to feel strongly the details of the boundary conditions imposed on the outer surfaces of the model. A mesh size of 25 mm was chosen, resulting in an upper frequency limit of about 2200 Hz for the validity of the model results. Overall, the resulting model is huge: it includes about 600,000 nodes and about 2.7 millions of elements.

For each one of the panels of interest around the vehicle, a set of response nodes was defined. On average, about 25 points per panel were taken. For each of the eight prescribed positions around the rear tyres, a unit volume velocity source was defined. Calculations were run from 300 up to 2500 Hz, with a frequency step of 25 Hz (this guarantees at least five response frequencies for each third octave band above 500 Hz). All calculations were run using MSC/Nastran on an HP-Itanium machine having 4 GB RAM and a 1.5 GHz processor. The total computational effort is quite remarkable: the solution of the model takes about 45 min per frequency and the total calculation time is about 65 h.

Figure 2 shows the EBEA model used for the evaluation of the airborne loads for the SEA Model of the analysed Volkswagen vehicle. The model includes 2245 nodes and 2436 elements, the average mesh size being about 150 mm. In Figure 2, some of the sources around the rear left tyre are visible, modelled as small spheres. Furthermore, also some of the response points used for the evaluation of the exterior sound pressure level are also marked. Since the computational effort for EBEA calculations is rather small, the model was run also in the mid-low frequency range. The set of response frequencies for the EBEA consisted of the 1/3 octave centre frequency bands, starting from 400 up to 8000 Hz. The computational time for the entire frequency range is approximately 10 min for each source position, on a usual desk-top PC.

4 Validation Results

Figure 3 reports the measured sound pressure level on the rear left window, together with the simulation results obtained both with FEA and with EBEA. To allow a better understanding of the data, FEA results are plotted in narrow-band. As one can see, in the mid-low frequency range, FEA results are able to catch the general trend of the test data and also the corresponding absolute level. The same is true for the EBEA results, but only above 2 kHz. The frequency region around 2 kHz looks ideal for a merging of the FEA and the EBEA results: this is why, for the calculation of the SEA airborne loads, the FEA results were used, after converting them into third-octave bands, up to the 2 kHz frequency band

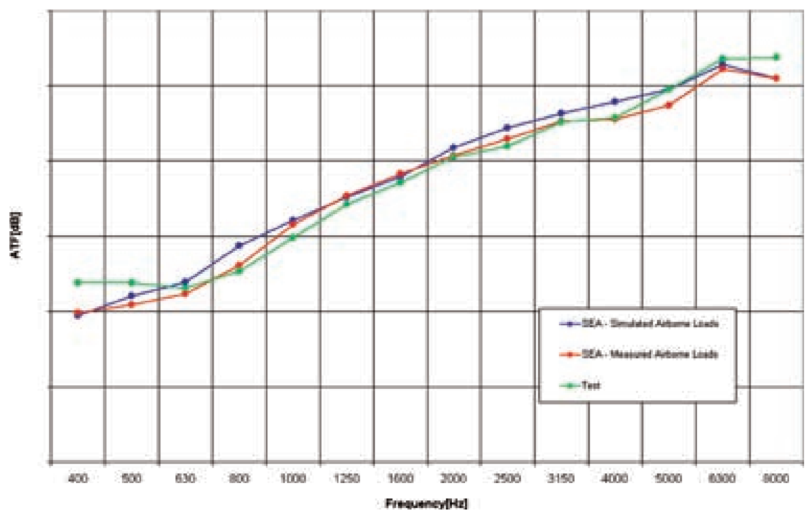

Figure 4: Rear tyre acoustic transfer function for the rear left passenger's head cavity; comparison between measurements, SEA results obtained with experimental airborne loads and SEA results obtained with simulated airborne loads

included. Starting from the 2.5 kHz band, EBEA results were used.

For most panels around the rear part of the vehicle, this allowed obtaining discrepancies lower than 3 dB between the measured and the simulated loads in third-octave bands. The SEA airborne loads obtained from the FEA/EBEA simulations were input into the SEA model of the Volkswagen vehicle under study and the results were compared with the ones obtained using the measured airborne SEA loads. Such comparison is reported in **Figure 4** for the rear passenger's head cavity, which is the cavity of main interest here. As one can see from this figure, the discrepancies between the SEA results obtained with the measured airborne loads and the SEA results obtained with the simulated airborne loads are more than acceptable, being generally lower than 1.5 dB.

5 Conclusions

The combination of standard FEA calculations with special EBEA (energy boundary element analysis) calculations allowed Rieter Automotive and Volkswagen to estimate the airborne statistical energy analysis (SEA) loads with an acceptable accuracy. The results of the SEA model obtained with the introduction of the simulated airborne loads compare rather well with those obtained with the experimental loads.

The employment of such a model to support the acoustic vehicle development process is meaningful as therefore to judge. Some discrepancies are observed but these discrepancies remain within the limits that make it possible to use the model for design decisions. The proposed procedure still has a weak point in the computational effort needed for the FE calculations in the mid-low frequency range. Some further work would be advisable to develop numerical and experimental procedures that allow extending the use of EBEA as far as possible into the mid-low frequency range.

References

[1] Powell, R.; Zhu, J.; Manning, J. E.: SEA Modeling and Testing for Airborne Transmission Through Vehicle Sound Package. SAE Paper 971973, USA, 1997

[2] Parrett, A.; Hicks, J. K.; Burton, T. E.; Hermans, L.: Statistical Energy Analysis of Airborne and Structure-Borne Automobile Interior Noise. SAE Paper 971970, USA, 1997

[3] Bertolini, C.; Gigante, L.: An SEA-Based Procedure for the Definition of Sound Package Component Targets Starting From Global Vehicle Targets. VibroAcoustics Users' Conference Europe, Leuven, Belgium, 2003

[4] Blanchet, D.; DeJong, R.; Fukui, K.: Development of a Modeling Technique for Vehicle External Sound Field Using SEA. Proceedings of Internoise 2004, Prag, Czech, 2004

[5] Venor, J.; Burghardt, M.: SEA Modeling and Validation of Sound-Fields and Seals in Automobiles. Proceedings of EuroPam Conference 2005, Potsdam, Germany, 2005

[6] Wang, A.; Vlahopoulos, N.; Wu, K.: Development of an Energy Boundary Element Formulation for Computing High-Frequency Sound Radiation From Incoherent Intensity Boundary Conditions. Journal of Sound and Vibration, Vol. 278, pp 413-436, Elsevier, Amsterdam, Netherlands, 2004

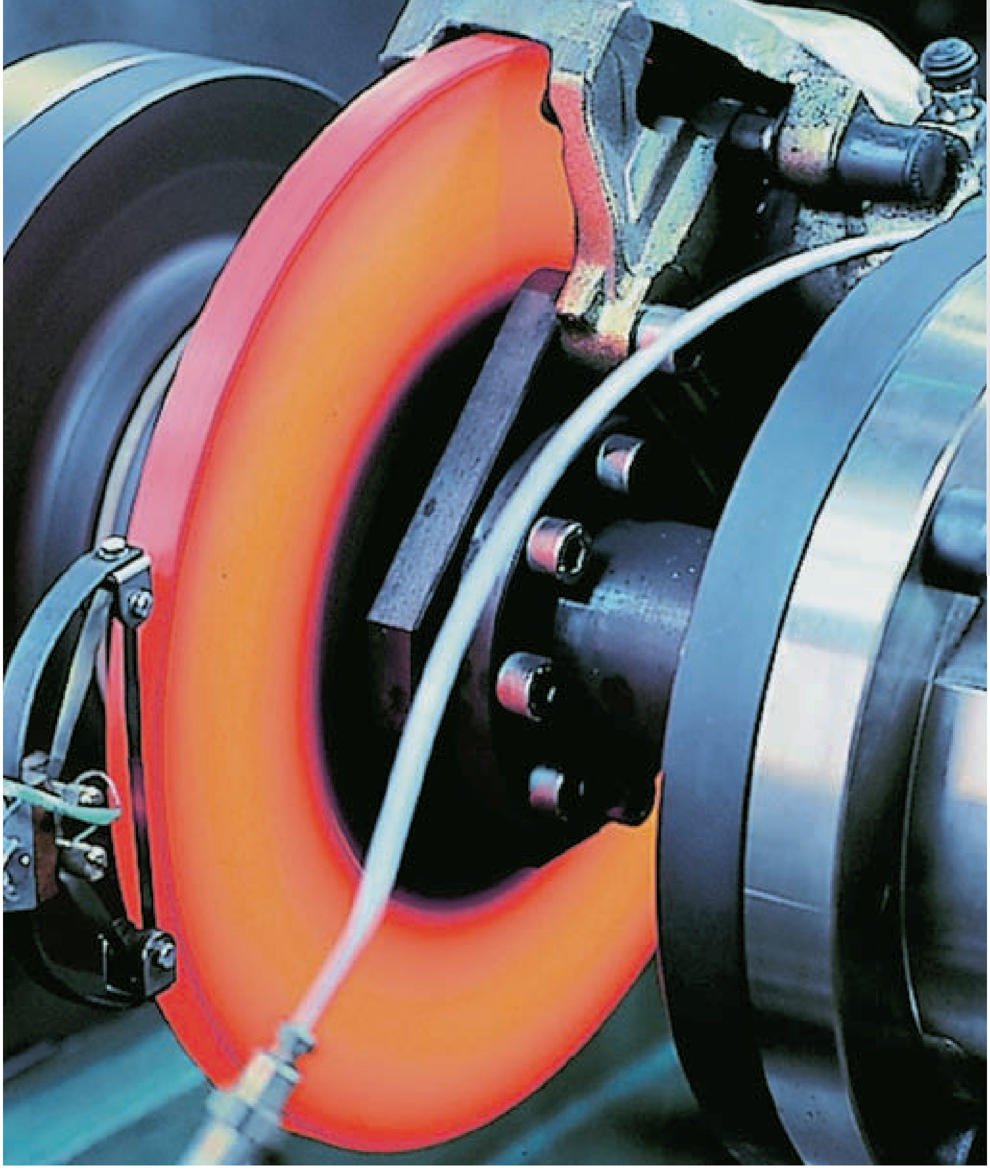

TÜV SÜD Automotive

Choose certain. Add value.

brake.tech 2008

Congress with accompanying trade exhibition

December 9 and 10, 2008

Kempinski Hotel Munich Airport, Germany

More Information: www.ATZlive.de

In cooperation with

ATZ UNIVERSITÄT MÜNCHEN

TÜV SÜD Automotive GmbH

TÜV®

Peer Review ATZ|MTZ

Peer Review Process for Research Articles in ATZ and MTZ

Steering Committee

Prof. Dr.-Ing. Stefan Gies	RWTH Aachen	Institut für Kraftfahrwesen Aachen
Prof. Dipl.-Des. Wolfgang Kraus	HAW Hamburg	Department Fahrzeugtechnik und Flugzeugbau
Prof. Dr.-Ing. Ferit Küçükay	Technische Universität Braunschweig	Institut für Fahrzeugtechnik
Prof. Dr.-Ing. Stefan Pischinger	RWTH Aachen	Lehrstuhl für Verbrennungskraftmaschinen
Prof. Dr.-Ing. Hans-Christian Reuss	Universität Stuttgart	Institut für Verbrennungsmotoren und Kraftfahrwesen
Prof. Dr.-Ing. Ulrich Spicher	Universität Karlsruhe	Institut für Kolbenmaschinen
Prof. Dr.-Ing. Hans Zellbeck	Technische Universität Dresden	Lehrstuhl für Verbrennungsmotoren

Advisory Board

Prof. Dr.-Ing. Klaus Augsburg	**Prof. Dr.-Ing. Martin Meywerk**
Prof. Dr.-Ing. Bernard Bäker	**Prof. Dr.-Ing. Werner Mischke**
Dr.-Ing. Christoph Bollig	**Prof. Dr.-Ing. Klaus D. Müller-Glaser**
Prof. Dr. sc. techn. Konstantinos Boulouchos	**Dr. techn. Reinhard Mundl**
Prof. Dr.-Ing. Ralph Bruder	**Dipl.-Ing. Sascha Ott**
Dr. Gerhard Bruner	**Dr.-Ing. Lothar Patberg**
Prof. Dr. rer. nat. habil. Olaf Deutschmann	**Prof. Dr.-Ing. Peter Pelz**
Dr. techn. Arno Eichberger	**Prof. Dr. techn. Ernst Pucher**
Prof. Dr. techn. Helmut Eichlseder	**Dr. Jochen Rauh**
Dr.-Ing. Gerald Eifler	**Prof. Dr.-Ing. Konrad Reif**
Prof. Dr.-Ing. Wolfgang Eifler	**Dr.-Ing. Swen Schaub**
Prof. Dr. rer. nat. Frank Gauterin	**Prof. Dr. rer.-nat. Christof Schulz**
Prof. Dr. techn. Bernhard Geringer	**Prof. Dr. rer. nat. Andy Schürr**
Prof. Dr.-Ing. Uwe Grebe	**Prof. Dr.-Ing. Ulrich Seiffert**
Prof. Dr.-Ing. Horst Harndorf	**Prof. Dr.-Ing. Hermann J. Stadtfeld**
Prof. Dr. techn. Wolfgang Hirschberg	**Prof. Dr. techn. Hermann Steffan**
Univ.-Doz. Dr. techn. Peter Hofmann	**Dr.-Ing. Wolfgang Steiger**
Prof. Dr.-Ing. Günter Hohenberg	**Prof. Dr.-Ing. Peter Steinberg**
Prof. Dr.-Ing. Bernd-Robert Höhn	**Prof. Dr.-Ing. Christoph Stiller**
Prof. Dr. rer. nat. Peter Holstein	**Dr.-Ing. Peter Stommel**
Prof. Dr.-Ing. habil. Werner Hufenbach	**Prof. Dr.-Ing. Wolfgang Thiemann**
Prof. Dr.- Ing. Roland Kasper	**Prof. Dr.-Ing. Helmut Tschöke**
Prof. Dr.-Ing. Tran Quoc Khanh	**Dr.-Ing. Pim van der Jagt**
Dr. Philip Köhn	**Prof. Dr.-Ing. Georg Wachtmeister**
Prof. Dr.-Ing. Ulrich Konigorski	**Prof. Dr.-Ing. Henning Wallentowitz**
Dr. Oliver Kröcher	**Prof. Dr.-Ing. Jochen Wiedemann**
Dr. Christian Krüger	**Prof. Dr. techn. Andreas Wimmer**
Univ.-Ass. Dr. techn. Thomas Lauer	**Prof Dr. rer. nat. Hermann Winner**
Dr. Malte Lewerenz	**Prof. Dr. med. habil. Hartmut Witte**
Dr.-Ing. Markus Lienkamp	**Dr. rer. nat. Bodo Wolf**
Prof. Dr. rer. nat. habil. Ulrich Maas	

Scientific articles in ATZ Automobiltechnische Zeitschrift and MTZ Motortechnische Zeitschrift are subject to a proofing method, the so-called peer review process. Articles accepted by the editors are reviewed by experts from research and industry before publication. For the reader, the peer review process further enhances the quality of ATZ and MTZ as leading scientific journals in the field of vehicle and engine technology on a national and international level. For authors, it provides a scientifically recognised publication platform.

Therefore, since the second quarter of 2008, ATZ and MTZ have the status of refereed publications. The German association "WKM Wissenschaftliche Gesellschaft für Kraftfahrzeug- und Motorentechnik" supports the magazines in the introduction and execution of the peer review process. The WKM has also applied to the German Research Foundation (DFG) for the magazines to be included in the "Impact Factor" (IF) list.

In the ATZ/MTZ Peer Review Process, once the editorial staff has received an article, it is reviewed by two experts from the Advisory Board. If these experts do not reach a unanimous agreement, a member of the Steering Committee acts as an arbitrator. Following the experts' recommended corrections and subsequent editing by the author, the article is accepted. *rei*

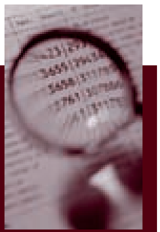

ATZ Peer Review

The Seal of Approval for scientific articles in ATZ.

Reviewed by experts from research and industry.

Received ....

Reviewed ....

Accepted ....

Seal of Approval – this seal is awarded to articles in ATZ/MTZ that have successfully completed the peer review process

Analysis of Driver Behaviour for Presentation of Adaptive Implementation Strategies of Assistance Systems

Assistance systems, whose intervention strategies are based on average expected values, give away potential both in terms of driving safety as well as the expected user acceptance, since they neither meet the expectations nor the support needs of all drivers. One approach to comply with the intra- and inter-individual differences in driver behaviour is the analysis of the driving style and the derivation of situation and driver-oriented assistance. At the Department of Automotive Engineering at the Berlin Institute of Technology an approach was developed that shows the potential of driver-adaptive support using a brake assist system as example. The diploma thesis to this topic won the German award "Hermann Appel Preis 2007", which is powered by the IAV GmbH.

1 Motivation

Many research projects, meetings and symposia have been dealing with the development of assistance systems to enhance active safety and the related expectation to reduce accidents or at least minimize their severity for many years. Innovative assistance systems intervene actively, which means they are perceptible for the driver, so they can warn in critical situations or take over parts of the driving task. But what from the engineers' point of view seems to be a matter of course is subjectively for ordinary drivers still far away – it is treated reluctently by the market: only a few advertising campaigns or sales offensives can be found. Furthermore, user-friendly descriptions of the latest systems are also often missing.

Regarding brake assist systems, determining factors and related difficulties become clear: suitable environment recognition allows to additionally judge the situation and to initiate a warning or, in case of a physically unavoidable collision, to intervene with a partial or even full braking. However, exactly this intervention is seen critically from different points of view: from the vehicle manufacturers point, functionality under even the most rare and worst conditions must be guaranteed to avoid product liability issues. From the drivers point, it is both the concern of being hold responsible in case of a system failure and the lack of experience with the operation of such an intervening system leading to limited confidence. In addition, change in general leads to resistance and therefore the driver needs a motivation to accept a new system and to overcome his concerns about loosing his freedom of choice and the influences on his driving habits [1].

It can be seen that a critical element of success is customer acceptance. However, this requires consideration of the customers‘ wishes and needs in the development process. But the latter are due to the large inter-individual differences in the drivers' expectations hardly to reduce to a common denominator. Age, driving experience, personality, vehicle use and many other aspects lead to a wide variety of perceptions when and how a system should intervene. This makes the implementation of adaptive operation strategies in assistance systems mandatory. Currently, the intervention thresholds of assistance systems are implemented in a way that they work with a statistical optimum. This means the majority of drivers feel adequately comfortable in most situations and only rarely disturbed. However, the further market penetration of assistance systems in all vehicle classes will reach target groups in which more drivers may have the feeling of unsuitable system behaviour.

Crucial for the implementation of such an adaptive intervention strategy is the recognition of the individual driving style by the assistance system. Measurable variables are required, which allow a classification according to proven correlations with the driver type: in particular, these are accepted or desired acceleration levels, braking behaviour and

Table 1: Driving styles and their distribution among men and women [7]

Driving style	Men	Women
Comfort-oriented	27 %	42 %
Active-dynamic	32 %	30 %
Drivers with less accidents and regulatory offences	**59 %**	**72 %**
Sportive-ambitioned	15 %	10 %
Affective-unbalanced	11 %	9 %
Insecure-unskilled	6 %	6 %
Aggressive-heedless	9 %	3 %
Drivers with more accidents and regulatory offences	**41 %**	**28 %**

The Authors

Dipl.-Ing. Alexandra Schulz is scientific assistant at the Department of Automotive Engineering at the Berlin Institute of Technology (Germany).

Dr.-Ing. Robert Fröming received his PhD thesis at the Department of Automotive Engineering at the Berlin Institute of Technology (Germany) and since November 2007 he is working about development of driver assistance systems at Daimler AG in Stuttgart (Germany).

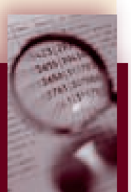

ATZ Peer Review
The Seal of Approval for scientific articles in ATZ.
Reviewed by experts from research and industry.

Received .... August 13, 2008
Reviewed .... August 29, 2008
Accepted........... September 16, 2008

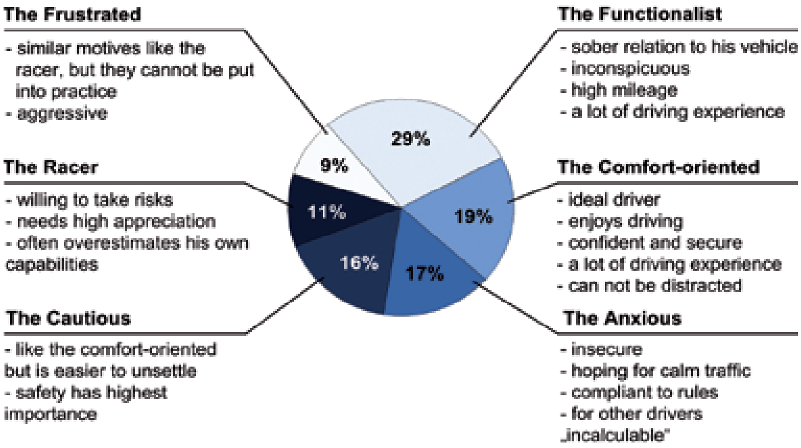

Figure 1: Different types of drivers with their distribution and properties [6]

transient follow-up distances. In addition the speed chosen on routes without speed limit, lateral dynamics in the lane and during lane changes, number of rule violations etc. could be valuable. The driving style is not invariably defined for a specific driver: depending on driving conditions such as with or without a passenger, on vacation or on the way to work, tired or wide awake the driving behaviour scatters strongly intra-individually. If the driving style can be identified successfully, it would be possible to set the warning and intervention thresholds accordingly. The individual variation of the warning time will expand the scope of possible assistance and be a benefit to all drivers.

2 Driving Styles and Driver Types

The basic motive of the driver is to reach his destination quickly, smoothly and with minimum effort. But a vehicle is capable to satisfy needs beyond its transportation function: on the one hand hedonistic needs as driving pleasure are met; on the other hand positive emotions are produced, such as experiencing feelings of competence when driving, an increase of power and self-esteem or the sense of independence [2].

In surveys of depth psychology two basic emotions were identified to derive the different driving styles, which partially include the above-mentioned subjects: the pleasurable experience and the fear of risks [3]. In studies regarding the safety belt and speed limit these basic images of „enjoying" and „securing" as well as related attitudes and behaviours were demonstrated quantitatively [4, 5].

The third basic motive with respect to the distinction of driving styles is autonomy. It describes the wish to arrange one's mobility independent of others and thereby to experience the feeling of having control over what is happening. It also finds expression in the resistance against external constraints such as speed restrictions and no parking or no passing areas. This motive is, according to several surveys on German roads, very widespread and reflected for example in the slogan „Free travel for free citizens", which is based on a campaign initiated by the German drivers' club ADAC in 1974 against the speed limit "Tempo 100" on German motor ways.

2.1 Driving Styles

Based on the two basic motives a risky-offensive and a defensively-avoiding driving style can be defined. In the former the pleasure of driving mostly outweighs feelings of uncertainty and anxiety. From the other road users point of view this style is often perceived as risky and aggressive, whereas both attributes are often classified differently by the subjective perception of the driver himself. Safety systems are often perceived as a restriction by risky-offensive drivers and therefore rejected. In contrast, safety has a high priority for defensively-avoiding drivers. Their fear of being involved in dangerous situations makes driving a means to an end [6]. A distribution of different driving styles shows **Table 1**.

In previously mentioned studies [6, 7] only qualitative data was analysed. It has not been proven that an identified style of driving is connected with driver-individual behaviour like choice of speed or acceleration. This assumption was confirmed by a study [16] investigating the correlation between different driving styles (calm to dynamic) and values such as speed, acceleration and frequency of override of a speed control system. Furthermore, the analysis shows that drivers can assess their own driving style very well regarding the achieved acceleration.

Table 2: Parameters for the derivation of the driving style (normal driving and emergency brake manoeuvres)

Normal driving		
	Unit	**Characterises**
Deceleration	m/s^2	driving style
Course of braking pressure	–	driving style
Distance	m	need for safety / driving style
Time gap	s	need for safety
TTC_{min}	s	situation
Emergency braking (test data)		
Reaction time	s	driver
Maximum deceleration	m/s^2	driver
TTC_{min}	s	criticality
TTC_{br}	s	situation from drivers point of view
Time gap	s	situation from drivers point of view

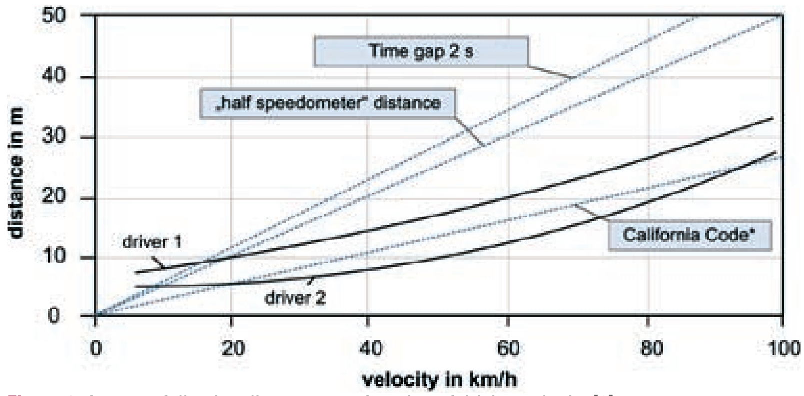

Figure 2: Average following distance as a function of driving velocity [9]
(* California Code: distance of one vehicle length per 10 mph (miles per hour))

2.2 Types of Drivers

The classification of driver types has its origins in the accident research: Theories of transport psychology assume that it is possible to derive traffic behaviour, starting from the personal lifestyle, leisure style to professional status. Such typological approaches in particular provide the possibility to identify and quantify large amounts of drivers especially those with high potential risk, so that appropriate measures for traffic safety can be derived. This results in a type classification, which often uses known patterns and terms that are already associated with a particular type or character.

A well-known classification was the result of a study [6] that carried out an extensive survey with over 1600 drivers. The identified six types of drivers are shown in **Figure 1**, depicting distribution and properties.

Extensive analysis about self-assessment (aggression, respect for others, etc.), details on driving behaviour (for example choice of speed and distance) as well as compliance with the road traffic regulations (StVO) and life style are also part of the type division [6].

2.3 Sub-Conclusion

For the development of adaptive driver assistance systems, type classification is rather inappropriate, especially since the current driving behaviour is of interest and the responsible motives and personal settings move into the background. Shall assistance systems fulfill monitoring functions and reduce risks due to an aggressive driving at the same time, a consideration of various types may be useful in order to increase acceptance and find opportunities to place the systems effectively onto the market.

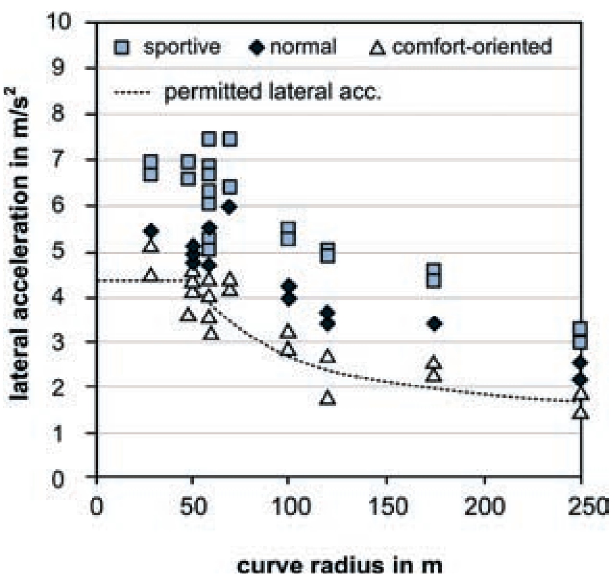

Figure 3: Accepted lateral accelerations of different driver types depending on curves radius [13]

3 Onboard Analysis

The variables for the classification of driver behaviour must be recorded in the vehicle permanently during a trip. Ideally it should be possible to link normal driving with the expected behaviour in emergency situations to derive appropriate warning strategies. Regarding collision avoidance, for example with a brake assist system, the focus is on two possible accident scenarios: approaching a standing or very slowly moving obstacle (traffic jam end, pedestrians etc.) and the sudden deceleration of a vehicle ahead during a follow scenario, whereas the initial velocity of both vehicles can be the same (for example bound travel on the highway). In both cases there are situations where the use of an adaptive system for reasons of acceptance and increasing protection potential is promising.

Parameters that can provide information on the individual driving style from normal driving behaviour as well as in emergency situations are shown in **Table 2**. In addition, also lateral acceleration, speed choice for free travel or the number of rule violations can allow a conclusion about the respective driving style.

3.1 Following Behaviour and Time Gap

The reaction of a driver on a vehicle ahead and his behaviour during following this one are according to Wiedemann [8] depending on the individual safety needs of the driver and his capability of estimating speeds and distances. Both safe distance and perception thresholds are driver individual values that allow the definition of different driver characters. As an appropriate size for assessing the following behaviour the time gap has been proven of value. The time gaps determined in field studies and simulator tests spread very strongly. In many cases distances are accepted that would lead to collision in case of an emergency brake of the vehicle ahead since the time gaps are less than or near the expected response times [9].

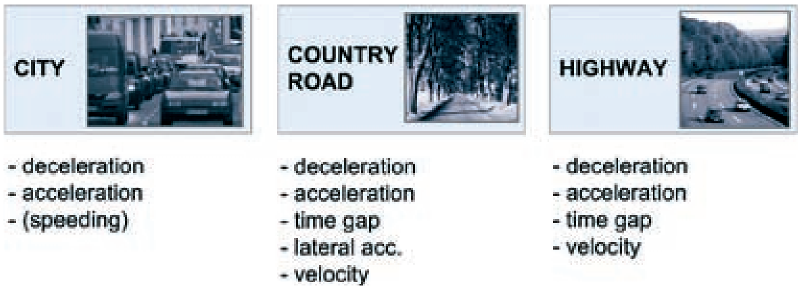

Figure 4: Analysed driving situations and input values for driver classification

The fact that chosen distances often do not match the recommended minimum distances to ensure collision avoidance has already been known for a few decades: within a study from 1971 drivers were observed in a speed range of up to 100 km/h. Their behaviour was compared afterwards with values emerging from known distance rules, **Figure 2**. Both depicted drivers chose a distance, in particular with increasing speed, well below the limits of a "half speedometer" value or a time gap of 2 s [9]. Numerous other studies [see 10] show that these values are representative.

The following behaviour is determined by several factors: by the driver himself (age, sex, alcohol influence, his own situation assessment, risk-taking) and from his driving behaviour (velocity choice, braking behaviour, selected time gap). In addition, different situations affect the sense of safety of the driver: especially poor visibility and a high traffic density have an influence on the choice of distance. Other factors include road conditions, speed limits and number of lanes [11].

The question of how far time gaps are intra-individually constant and whether or not they classify a particular driving style reliably can only be answered by extensive test series with preferably unaffected drivers. A field study carried out at the TU Darmstadt resulted in the identification of three different driving styles and their specific time gaps. However, as the results are very close together, they must be confirmed by further tests before they can be used in the development of driver assistance systems [12].

3.2 Lateral and Longitudinal Acceleration

Within the development of an optimised gear change for automatic transmissions the dependence on accepted lateral acceleration and driving style was analysed. The results are shown in **Figure 3**. The marked permitted lateral acceleration was defined based on the experimental data set and served later in the transmission design [13].

Again, the much higher accepted acceleration of sportive drivers becomes apparent what identifies it as appropriate for driver classification [13]. Even for systems that are not directly related to lateral driver assistance this could be proven as a valuable source of information. Assuming that it is possible to use other parameters in addition, which correlate with the defined driving style as well, it is irrelevant which measured value is responsible for the characterisation in the end. Also for roundabouts different accepted accelerations were found depending on the individual driving style [14].

Longitudinal accelerations in regular driving following traffic lights, stop signs or on slip roads are also appropriate characterization sizes for the analysis of the driving style [14]. First detailed studies promise a high stability and allow the assumption this may be the key indicator for a change of the intra-individual driving style.

3.3 Transformation of Driving Style Recognition

The onboard-recognition is based on the recording of relevant data and analysis of achieved maximum values and thresholds. At the Department of Automotive Engineering (Berlin Institute of Technology) a tool with Matlab Stateflow was developed, which allows the recognition of the driving style on the basis of tracked vehicle parameters.

Input data is taken from the analysis of new experimental data and from the re-evaluation of tests documented in the literature. The analysis of emergency braking tests provides information about reaction time, time to collision (TTC) and reached maximum deceleration. The former allows the identification of the actual driving style, whereas the recognition reacts also on intra-individual variations. Analysed driving situations and input values are shown in **Figure 4**. An environment sensor system with distance measuring is assumed.

In driving tests with various normal and emergency braking manoeuvres large differences in TTC at the beginning of braking and achieved deceleration were observed, **Figure 5**. Using a cluster analysis, average values for the expected maximum deceleration and the intervention time in a braking manoeuvre could be determined for a comfortable and a sportive driver. After successful

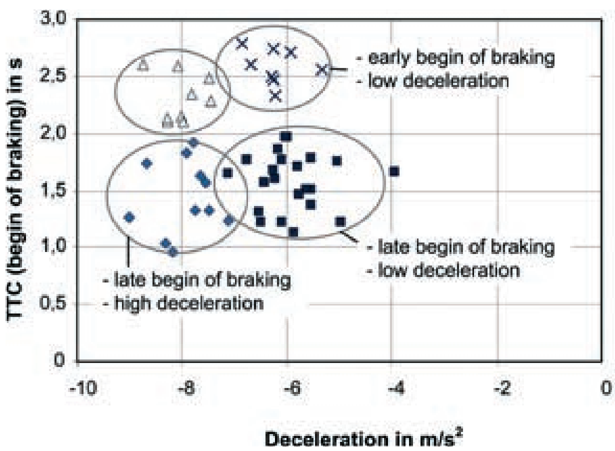

Figure 5: Correlation between time to collision at the beginning of braking (TTCbr) and maximum vehicle deceleration – presentation in four clusters all analysed from data from full brake manoeuvres (n = 52)

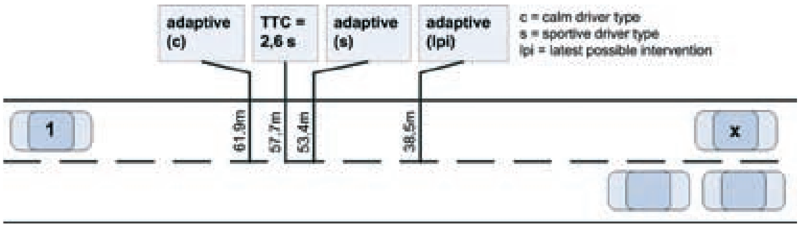

Figure 6: Distance and time to collision (TTC) between vehicle (1) and obstacle (x) at the moment a warning is initiated – different warning strategies depending on the driver type (distances not to scale)

identification of the style of driving, these values can be integrated in threshold values for adaptive driver assistant systems of longitudinal dynamics.

4 Driver-adaptive Intervention in Brake Assist Systems

For the study of potential benefits using a driver-adaptive brake assist system an algorithm is used that initiates a warning in emergency situations or, in case of passive driver behaviour, a partial braking. It is based on a calculated minimum distance to the vehicle ahead taking a driving-style dependent point of intervention and maximum deceleration into account. The application on simulated routes as well as on test data allows a conclusion about warning points and remaining stopping distances for different drivers. Two situations were chosen for further analysis, which appear very often in reality: approaching a vehicle standing still or moving very slowly (for example the end of a traffic jam) and the collision during a following scenario when the vehicle ahead makes an unexpected emergency braking.

Figure 6 shows an example for different points of warning for the first situation (velocity of approaching vehicle v = 80 km/h). The latest possible intervention was defined assuming a reaction time of 0.5 s (includes moving the foot to the brake pedal) and an average deceleration of 9 m/s^2.

The basic idea of driver-adaptive intervention becomes clear: a comfort oriented driver, who will in general intervene sooner in a braking situation, is also warned earlier than the average driver with a TTC of 2.6 s. Regarding sportive drivers it is necessary to accept that warnings especially at high velocities cannot be collision avoiding but only collision mitigating in order to allow undisturbed normal driving. This guarantees higher system acceptance and assures distribution and use.

Beyond the study of the effects on different driving styles, the algorithm allows the analysis of various intervention strategies such as the influence of reduced response times due to improved sight or information systems. **Table 3** shows a simulated braking scenario with rear-end collision (v = 40 m/s). The in this example sportive driver has chosen an overcritical time gap (t_G = 0.7 s). The calculated collision velocities refer to an unexpected full brake manoeuvre of the vehicle ahead. A notable reduction of the collision velocity for a sportive driver regarding different intervention strategies can be shown.

For all manoeuvres a benefit as a result of the adaptive design was found compared to the conventional strategy, both regarding the safety (especially for following scenarios) as well as a higher expected acceptance (when approaching a standing obstacle). Also for pedestrian protection high potentials for collision mitigation could be identified for future assistance strategies [15]. Using driver adaptive specifications an increased customer acceptance can be expected as well.

5 Conclusion

In the following years driver-adaptive systems will be the key to user-friendly assistance. However, all theoretical considerations, the summary of findings in recent decades and also the use of driving simulators or field tests should not obscure the view of the fact, that the events in the last seconds before a real accident (in fact the basis for the development of appropriate intervention strategies) are not sufficiently clarified in detail. The knowledge about circumstances of an accident derived from accident analysis may reflect only a part of what the driver actually experienced. Therefore, it is difficult to make a serious assessment of the benefits warning systems may have without having observed the relevant systems in real traffic and finding out whether they are helpful for the drivers

Table 3: Collision velocities as results of a simulated braking scenario (sportive driver) for different intervention strategies with and without brake assist system (BAS)

	Reaction time	Deceleration	Collision Velocity v_c	Reduction of Collision Velocity Δv_c
Unit	s	m/s^2	m/s	m/s
Passive driver	0	0	19.8	–
Passive driver, partial braking after 1 s	0	3.0	13.1	6.7
Driver reaction without assistance	0.8	8.4	7.9	10.9
Driver reaction and BAS	0.8	9.0	6.3	13.5
driver reaction 0,2 s earlier and BAS	0.6	9.0	0	collision avoided

with regard to their specific deficits. Nevertheless the Department of Automotive Engineering at the Berlin Institute of Technology could show that the use of adaptive strategies in comparison to conventional thresholds has a significant potential regarding the increase of driving safety and user-acceptance. The importance of adaptation of these systems will come to the fore with increasing optimisation of the current systems.

References

[1] Oltersdorf, K. M.: Wie kommen die Fahrerassistenzsysteme zum Fahrer? 4. CTI-Fachkonferenz Fahrerassistenzsysteme, Stuttgart, 2006

[2] Bliersbach, G.; et al.: Gefühlswelten im Straßenverkehr. Schriftenreihe Verkehrssicherheit, Hrsg.: Deutscher Verkehrssicherheitsrat e.V., Bonn, 2002

[3] Klebelsberg, D.: Verkehrspsychologie. ISBN 354011713X, Springer-Verlag, Berlin, 1982

[4] Berger, H. J.; et al.: Psychologische Grundlagen für das Verständnis von Pkw-Fahrern zum Sicherheitsgurt. In: Bundesanstalt für Straßenwesen (Hrsg.): Psychologische Forschung zum Sicherheitsgurt und Umsetzung ihrer Ergebnisse. Köln, 1974

[5] Utzelmann, H. D.: Tempowahl und -motive: Merkmale des Fahrerverhaltens und ihre Zuordnung zu motivationalen Bedingungen. In: Faktor Mensch im Verkehr, Heft 24, Darmstadt, 1976

[6] Adelt, P. J.; et al.: Autofahrertypen auf Deutschlands Straßen. In: Sicher-Direct-Studie 1997, ISBN 3-89701-412-2, Wirtschaftsverlag NW, Bremerhaven, 1999

[7] Jöri, H.: Ruhig bis aggressiv – Sechs Typen am Steuer. In: punktum. Zeitschrift des Schweizerischen Berufsverbands für Angewandte Psychologie, Ausgabe April, Zürich, Schweiz, 2002

[8] Wiedemann, R.: Simulation des Straßenverkehrsflusses. Schriftenreihe des Instituts für Verkehrswesen der Universität Karlsruhe, Nr. 8, Karlsruhe, 1974

[9] Hartwich, E.: Längsdynamik und Folgebewegung des Straßenfahrzeugs und ihr Einfluss auf das Verhalten der Fahrzeugschlange. Dissertation D17, Technische Hochschule Darmstadt, 1971

[10] Schulz, A.: Analyse des Fahrerverhaltens zur Darstellung adaptiver Eingriffstrategien von Assistenzsystemen. Diplomarbeit, Technische Universität Berlin, 2007

[11] Shresta, D.; Chang, G.: A Monitoring and Alert System for Tailgating Behaviour of Drivers. ISBN 0-7803-9152-7, Vehicular Technology Conference, 25–28 September 2005, Dallas, Texas, USA, 2005

[12] Abendroth, B.: Gestaltungspotentiale für ein PKW-Abstandsregelsystem unter Berücksichtigung verschiedener Fahrertypen. Bericht aus dem Institut für Arbeitswissenschaft der TU Darmstadt. Ergonomia-Verlag, Stuttgart, 2001

[13] Hamberger, W.: Verfahren zur Ermittlung und Anwendung von prädiktiven Streckendaten für Assistenzsysteme in der Fahrzeugführung. Fortschritt-Berichte VDI (Reihe 12), Berichte aus dem Fachgebiet Kraftfahrwesen der TU Berlin, Düsseldorf 1999

[14] Deml, B.; Freyer, J.; Färber, B.: Ein Beitrag zur Prädiktion des Fahrstils. In: Tagung Fahrer im 21. Jahrhundert. Human Machine Interface. Braunschweig, 14. und 15. November 2007, VDI-Berichte 2015 (S. 47–60), VDI-Verlag, Düsseldorf, 2007

[15] Fröming, R.: Assessment of Integrated Pedestrian Protection Systems. VDI-Fortschritt-Berichte, Reihe 12, Nr. 681, ISBN 978-3-18-368112-9, Dissertation, TU Berlin, 2008

[16] Marstaller, R.; et al.: Akzeptanzuntersuchungen zu einer automatischen Geschwindigkeitsregelung im Automobil. In: Bedienen und Verstehen. 4. Berliner Werkstatt Mensch-Maschine-Systeme, Berlin, Oktober 2001, ZMMS, VDI-Fortschritts-Berichte, Reihe 22, Düsseldorf, 2002


International
Surface
Technology
IST

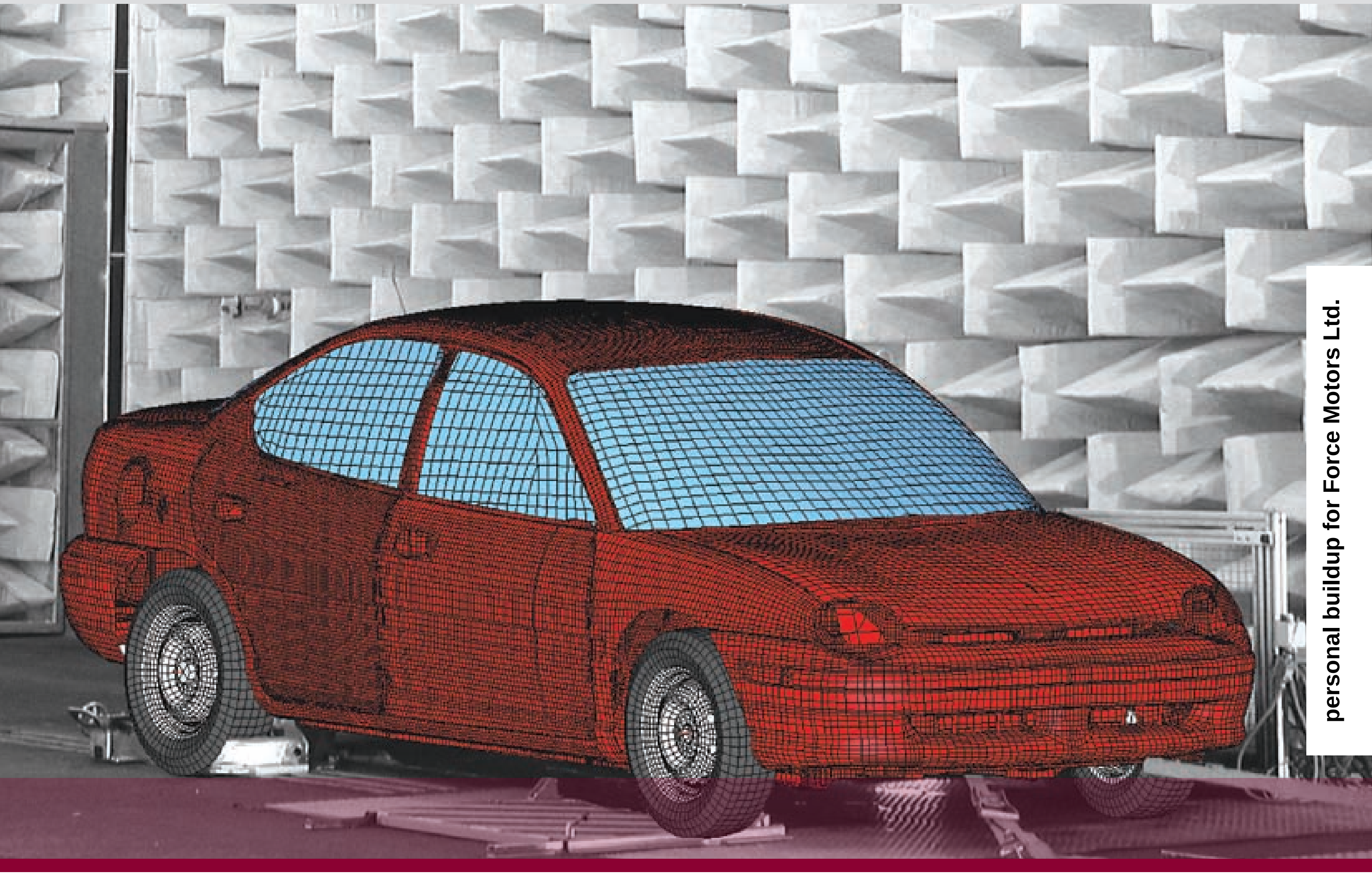

Prediction of Virtual Interior Noise

Optimisation of the Vehicle Body

The overall impression that a vehicle creates is strongly influenced by its acoustic behaviour. In addition to the various excitation mechanisms, the transfer behaviour of the body in particular has a critical influence on the character of the interior noise. During the vehicle development process, key decisions need to be taken with regard to the vehicle body before the first prototypes exist as hardware. To support this process, a virtual noise prediction system has been developed at FEV that combines the established experimental method of interior noise simulation with an FE calculation for the vehicle body.

1 Introduction

As development times become ever shorter, virtual noise prediction can be used to achieve target-oriented acoustic development. This involves extending the established method of interior noise simulation, which is based on experimentally determined excitations and transfer functions: measured excitations are combined with the calculated transfer behaviour of the body.

The airborne and structure-borne noise excitation characteristics of the engine are determined via measurements on the test bench, or can be taken from a database. The transfer behaviour of the body is calculated on the basis of a finite element (FE) model. This makes it possible to predict the impression created by a vehicle's interior noise even before the body exists as hardware. In addition, different versions or modifications of the body can be assessed with regard to their influence in terms of noise. This allows acoustic criteria, including a subjective evaluation of the overall noise, to be incorporated at an earlier stage into the vehicle development process, on the basis of which important decisions can be taken.

2 FE Calculation for the Body

In recent years, the virtual vehicle has become an integral element in the development of new vehicle models. This development is partly the result of external influences. These influences include ever-decreasing development times in a tough competitive environment; the need to save time and money by reducing the number of prototypes built; additional, tighter legal requirements with regard to vehicle safety; and the increasing need to build weight-optimised vehicles in order to reduce fuel consumption. At the same time, thanks to the wide availability of high-performance computer systems and general advances in the field of CAE, new possibilities have emerged for making the virtual vehicle a reality.

In the area of body development, the CAE-based development process is driven forward by vehicle safety requirements. The focus of this work is on crash simulation, but aspects of, for example, pedestrian protection, and the need to achieve the most favourable possible insurance classification, also play a role. Here, highly-detailed models are constructed, which are used for the implicit transient calculations typical in the field of crash simulation. At the same time, these models form the basis for the creation of special FE models for use in structural stability, structural dynamics and acoustics calculations. For this, they are given additional properties and adapted to the respective requirements. In this way, integrated into an interdisciplinary development and decision-making process, the best possible solutions for the widely-varying and sometimes contradictory requirements applicable to a vehicle body can be found in good time and without the need to build hardware.

Using a vehicle model supplemented with interior trim and an FE mesh representing the air space, the various measurement variables, relevant for noise, vibration, harshness (NVH), such as accelerations and sound pressure levels, can be determined. The engine, drivetrain and chassis are taken into account here as sources of structure-borne noise. This allows calculation of the interior noise level and the vibrations resulting from engine and road surface excitations. In addition, critical transfer paths and vibration surfaces (panels) can be identified and effective countermeasures developed.

One restriction associated with this method is the limited frequency range for which statements can be made about acoustic values, due to the time and expense involved in modelling and calculation. This limits the application to phenomena that can be represented within a frequency range up to approximately 200 Hz (for example the second engine order for a four-cylinder in-line engine). Furthermore, only the structure-borne noise components of the interior noise are taken into account. This is not sufficient to adequately evaluate the character of the noise in the interior.

3 Interior Noise Simulation

In order to work with vehicle acoustics in a target-oriented way, a thorough qualitative and quantitative understanding of the causes of noise is necessary. To achieve this, the "VINS" (Vehicle Interior Noise Simulation) method is used at FEV for the simulation of interior noises and vibrations [1]. VINS is based on an analytical method that divides all interior vehicle noise into the audible components from the various individual paths, **Figure 1**. In addition, each path is broken down into noise source and multiple-unit transfer function. A typical example here is the path assigned to a power train mount, starting with the acceleration of the power train mount, going via the mount transfer function and body transfer function, through to the corresponding component of the interior noise. In addition to the calculation of engine-induced noise components, an extended method [2] means that noises from the chassis can also be taken into account. In

The Authors

Dr.-Ing. Georg Eisele
is Senior Technical Specialist in the department Vehicle Physics/Acoustics at FEV Motorentechnik GmbH in Aachen (Germany).

Dipl.-Ing.
Klaus Wolff
is Chief Engineer Vehicle Physics/Acoustics at FEV Motorentechnik GmbH in Aachen (Germany).

Dipl.-Ing.
David Völlmecke
is Development Engineer in the department Vehicle Physics/ Acoustics at FEV Motorentechnik GmbH in Aachen (Germany).

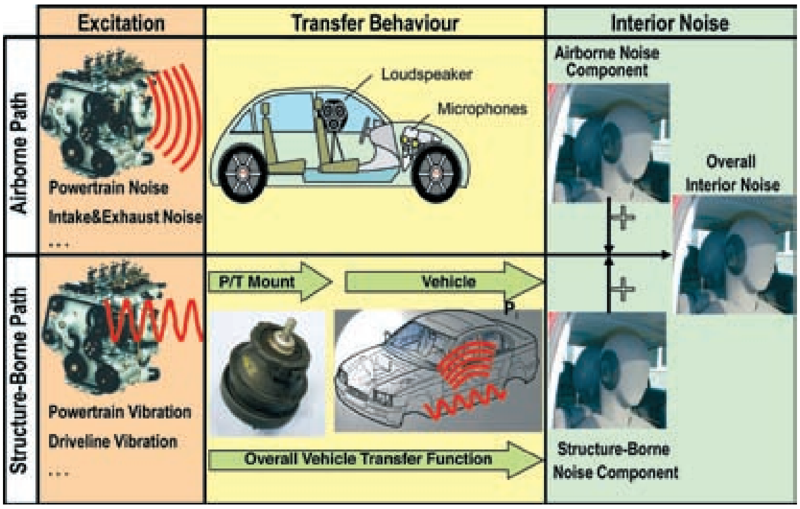

Figure 1: Interior noise simulation (VINS) allows interior noise to be broken down into the individual airborne and structure-borne noise paths, and the individual paths to be broken down into excitations and transfer functions

a modified form, the same methodology can be applied to the calculation of vehicle exterior noise [3].

4 Principle of Hybrid Simulation

The input data for interior noise simulation consist of the excitations of the individual sources, and the transfer behaviour of the vehicle components of the individual paths. Both the excitation data and the transfer functions that describe the transfer behaviour are, depending on the stage of the development process and the availability of hardware, generated in various ways. By combining measurement and calculation data in a hybrid interior noise simulation, virtual interior noise prediction is possible at all phases of the development process.

In the analysis of vehicles and engines that exist completely as hardware, for example in the case of competitor and predecessor vehicles and the various prototypes stages, all input data are obtained via direct measurement.

In the early phases of the development process, where many of the vehicle components exist only virtually, measured data can be replaced by calculation data and used for a hybrid simulation of the interior noise. Thus, in an engine development process, the engine excitations can be simulated, as described in [4], using multibody and finite element calculations.

As a third possibility, instead of via measurements and calculations, the input data – particularly the transfer functions in the frequency range – can be derived from previously-determined target curves. Thus, for example, the airborne noise transfer function necessary for the VINS calculation can be generated from the target curve for the airborne noise transfer behaviour.

This paper looks at the situation in a vehicle development process where, for an extended period, the vehicle body only exists as a CAE model. All essential decisions relating to the body must be made during this phase because, once the body exists as a component, any changes made will be very cost-intensive. In this situation, the transfer behaviour of the body can be calculated by means of FE simulation and used for interior noise simulation.

As already mentioned, the current state of the art means that, due to the calculation times and degree of detail of the model that would be necessary for higher frequencies, FE calculation of the vibroacoustic body transfer functions is only feasible up to a maximum frequency of around 200 Hz. This is sufficient to determine the characteristics of the ignition order for a four-cylinder engine, but does not provide any realistic impression of the noise that would be produced.

A possibility to extend the calculation to higher frequencies is SEA (Statistical Energy Analysis). This is relative complex, does not cover the medium frequency range and does not directly give audible results. Here an alternative method will be presented which additionally allows higher frequencies to be considered, and thereby enables a realistic acoustic impression to be obtained. This has two advantages. Firstly, it means that the characteristics of the ignition order can be assessed within the context of the overall noise. Secondly, it provides access to the higher-frequency components for an evaluation, although it is important to take into account the way in which these components were obtained.

The higher-frequency components of the structure-borne noise paths considered in the FE simulation are incorporated through addition of the transfer functions for the higher frequency range. This is done on the basis of measurements from competitor or predecessor vehicles, empirical values, or targets. The function determined from the FE calculation is used up to a transition frequency of approximately 200 Hz, while above 200 Hz for example the function for the predecessor vehicle is used. This method is visualised in **Figure 2**. Alternatively, for the higher frequency range, an average transfer function found on the basis of scatter bands can be used. A combination is also possible: here, the transfer function for the predecessor vehicle is adapted to take into account the targets for the vehicle development project – for example, undesired peaks whose causes are known can be eliminated or reduced. When combining and adapting transfer functions, it should be borne in mind that these will subsequently be used for interior noise simulation as filters in the time range, and must therefore have a finite impulse response.

In addition to the higher-frequency components of the structure-borne noise paths observed in the FE simulation, it is specifically the engine-induced airborne noise components that determine the high-frequency interior noise above approximately 1 kHz. These, too, are often available from the interior noise simulation of the predecessor vehicle, and can be added to the previously-calculated structure-borne noise components.

In addition to the high-frequency components, the rather low-frequency intake and exhaust orifice noise components

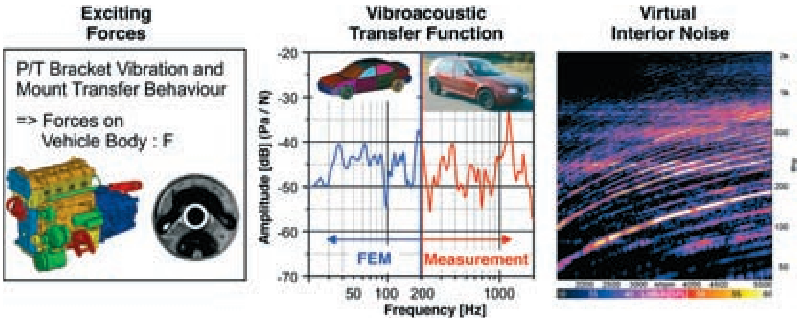

Figure 2: Combination of measured and calculated data in hybrid interior noise simulation

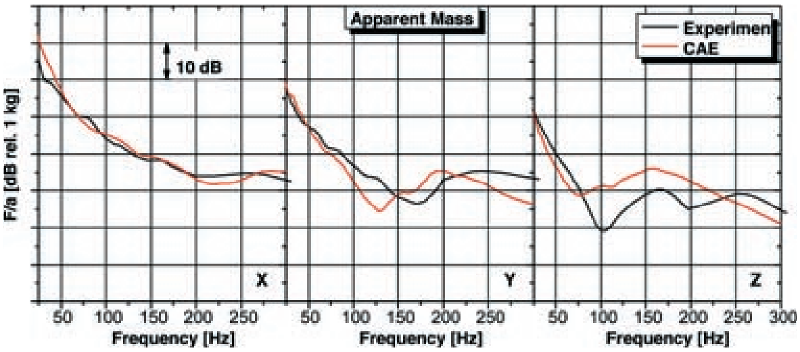

Figure 3: Comparison of measured and calculated apparent mass at a power train mount connection point

can also be added, whose excitations are determined via measurements or 1D CFD simulations. This possibility will, however, not be discussed any further here.

During the vehicle development process, this virtual interior noise prediction method is used to optimise the vehicle body in those situations where it only exists as a CAD model. In the example considered in this paper, the body exists as hardware, so that the potential and limitations of the method can be revealed by comparing calculated and measured data. The FE model was not adapted on the basis of measured data for the body, as this would not be possible in the actual development process, and thus would not provide a realistic impression of the method.

5 Calculation of Transfer Functions

Dynamic input stiffness is an important variable in the calculation of a vehicle's NVH properties. Input stiffness is determined at the coupling points between the chassis, drivetrain, engine and exhaust system and the body, by experimental means via impact or shaker tests, or by calculation via excitation with a sinusoidal unit force in the frequency range. The dynamic input stiffness is represented as the relationship between the excitation force F and the path response s against frequency. Representations of mobility (v/F) and apparent mass (F/a) are also used.

Figure 3 presents a comparison of the measured and calculated apparent mass at a power train mount connection point over a frequency range from 25 to 300 Hz. The consistency across the whole frequency range can be considered here to be good. Individual deviations can arise very easily as a result of non-matching measurement/excitation locations in the simulation and the experiment. Aside from this, the calculation process essentially provides results of an equal quality to that of the measured data, provided that the model is of sufficient quality.

By supplementing the structural model with the acoustically active vehicle interior in the form of an FE model, using the structure-fluid coupling method, the interior noise at predetermined positions can be calculated. In this way, transfer functions between the point of excitation and the local interior noise can also be generated, and can be used for a subsequent VINS.

Figure 4 shows a vibroacoustic transfer function obtained via experiment and calculation. Correlation is very good particularly at low to medium frequencies, while at higher frequencies above approximately 200 Hz the results deviate increasingly from one another. Here, the limitations of vibroacoustic interior noise simulation using the FE method become apparent. At present, the pure structural model can be used to predict effectively the dynamic behaviour of the vehicle body throughout the frequency range observed, whereas this is only possible to a limited extent for the coupled model.

6 Virtual Interior Noise Prediction

As described above, if the transfer functions derived from FE calculations are combined with measured or standard transfer functions, a vibroacoustic transfer function is created that describes the entire frequency range, and can be used as a filter in interior noise simulation. Here this was done for the paths from the power train mounts to the vehicle interior, in all three spatial directions in each case. The respective forces acting on the body which were previously determined experimentally and which lie within the time range are used here as excitations.

For purposes of comparison, the corresponding interior noise components

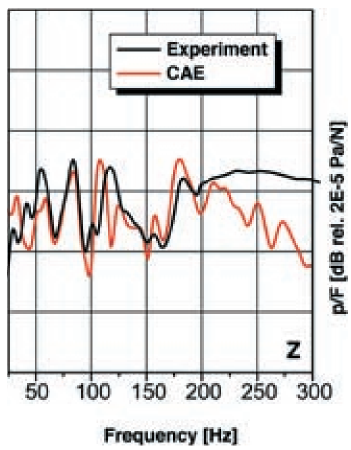

Figure 4: Comparison of the vibroacoustic transfer function from experiment and calculation

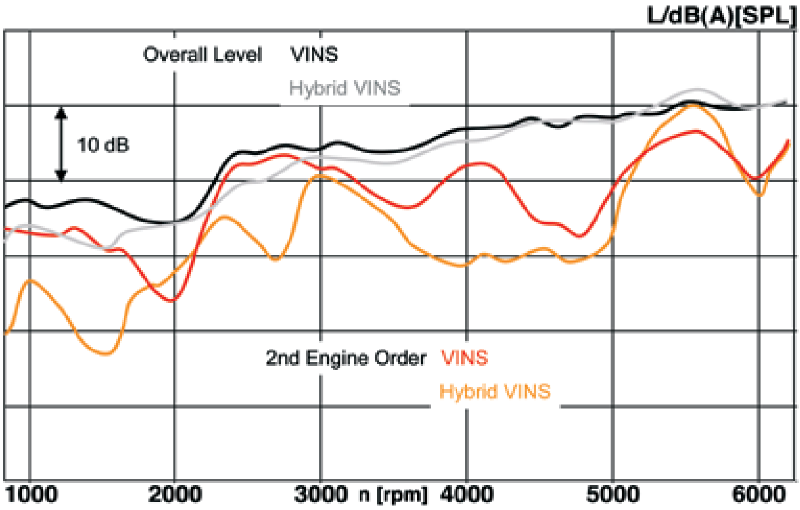

Figure 5: Comparison of the interior noise components originating from the power train mounts, determined once via VINS (measured transfer functions) and once via hybrid VINS (combination of FE and measured transfer functions)

were also calculated using the transfer functions determined purely experimentally, via impact tests. In the real development process this is not possible, because at the time of the virtual calculation the body does not yet exist as hardware.

Figure 5 shows a comparison of the interior noise components for a full load run-up, calculated once via VINS (measured transfer functions) and once via hybrid VINS (combined FE and measured transfer functions), with the sum of all components originating from the power train mounts being presented. The curve for the overall level is similar in both cases. In the detailed observation of the second engine order, both correlations in the peaks and clear deviations could be noted. The deviations are partly attributable to the fact that here, as explained above, the FE model was not adapted to take account of measured data for the body.

In **Figure 6** and in **Figure 7**, the path from the body transfer functions derived from the FE calculations through to an interior vehicle noise is presented in several stages. Usually, as a result of the FE calculation, the curve of the ignition order against engine speed, Figure 6 (a), is presented. Through combination of the FE transfer functions with the excitations in the time range, an audible interior noise covering the frequency range observed in the FE calculation, Figure 6 (b), is generated. In Figure 6 (c), the FE transfer functions are extended, via measured values, to cover the higher frequency range. The noise determined in this way already provides a realistic acoustic impression, and allows the ignition order to be evaluated within the context of overall noise.

The interior noise components induced by the engine airborne noise can also be added, Figure 7 (a). This is also possible during the real development process, on the basis of engine airborne noise measurements from the engine test bench, and using adapted airborne noise body transfer functions from the predecessor vehicle. For purposes of comparison, the actual interior noise measured is presented in Figure 7 (b). In the real development process, this comparison can naturally only take place once the first prototypes have been constructed. The differences that can be seen here are caused, on the one hand, by differences between predicted and actual interior noise components. On the other hand, the actual interior noise measured also contains components which the simulation does not take into account, for example rolling noises and a number of engine-induced noises from, for example, the intake and exhaust orifices, the exhaust system suspension, and the drive shafts.

By combining the FE calculation with interior noise simulation, the causes of individual noise phenomena can be de-

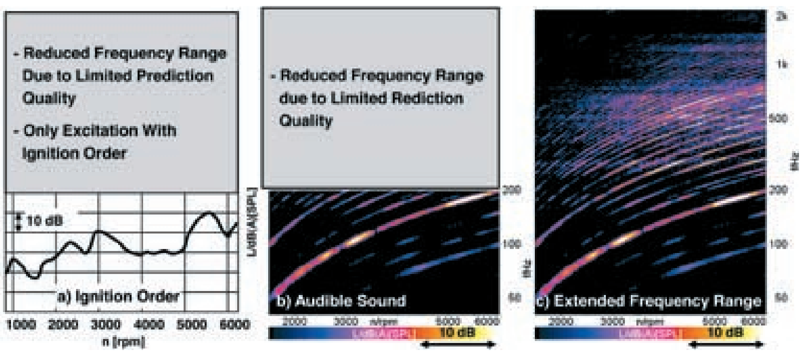

Figure 6: (a) Ignition order curve as a standard result of the FE calculation, (b) Audible interior noise obtained via combination with the excitations in the time range, (c) Extension of the frequency range of the transfer functions.

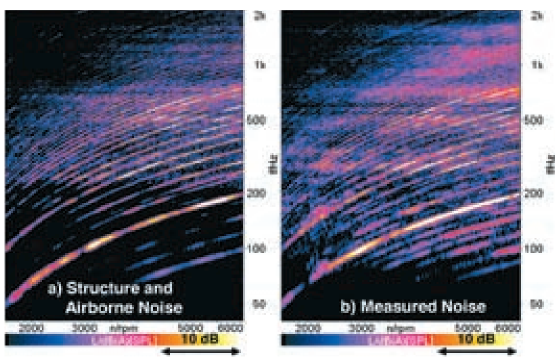

Figure 7: (a) Supplementing of the structure-borne noise with airborne noise, (b) Measured interior noise

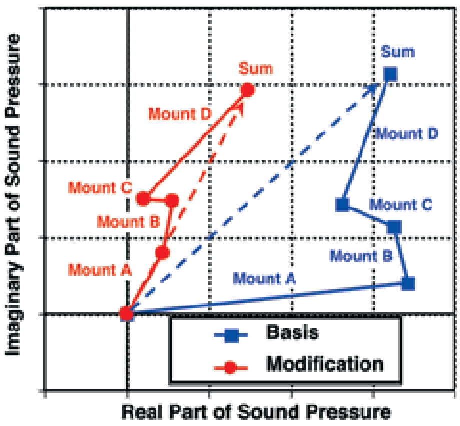

Figure 8: Vectorial sum of the interior noise components from the individual P/T mounts for two different FE-body variants

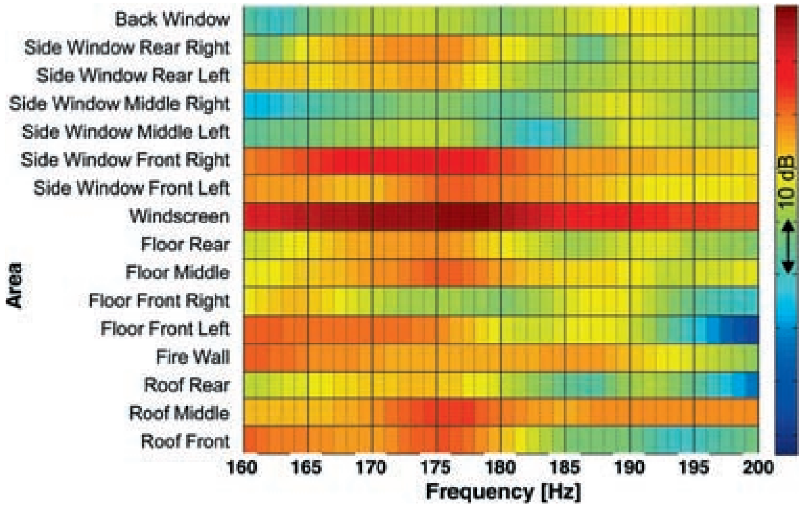

Figure 9: Shares of the individual passenger compartment boundary surfaces in the second engine order peak between 5000 and 6000 rpm

personal buildup for Force Motors Ltd.

termined, and possible hardware modifications can be inferred. For example, an analysis of the interior noise components determined via VINS reveals that the peak in the second engine order between 5000 and 6000 rpm, Figure 6, is essentially caused by the noise path from a single power train mount. This allows possible improvements to be inferred with regard to power train mount position, excitation level and transfer function, and local dynamic input stiffness in the body.

Figure 8 exemplarily shows the potential effect of a greatly increased local dynamic stiffness at the power train mount location identified as being especially important. The amplitudes and phases of individual structure-borne noise shares are plotted in the complex plane. A graphical vector addition is performed by connecting the individual components, giving the total level. The given case clearly shows that an increased local stiffness at mount A can greatly reduce the level of this singular structure-borne noise path. However, if all of the individual mount shares are summed with correct phase relations, the reduction of the total level is lower than the reduction of the structure-borne noise share of mount A. The effectiveness of a local modification must therefore always be regarded in context with its global effects.

The transfer properties of the body can be more precisely analysed using FE calculations with a special focus on radiating panels. **Figure 9** shows the shares of the individual passenger compartment boundary surfaces in the second engine order peak. In particular, the windscreen and side windows contribute significantly to the peak, as do the firewall and roof. These vehicle components represent areas where possible modifications could be made, for example in terms of their mounting/integration into the surrounding body structure, local reinforcements and acoustically insulating heavy material layers.

7 Summary

In the early phases of the vehicle development process, before the body exists as hardware, virtual interior noise prediction is used in optimising the vehicle body. This hybrid method by FEV combines FE calculation results for the body with measured data, thereby generating an interior noise in the time range. This allows the interior noise of a vehicle to be heard before the vehicle is constructed.

The FE body transfer functions for the structure-borne noise paths observed are, above a transition frequency of approximately 200 Hz, supplemented by empirical data or measurements from comparable or predecessor vehicles, and used to calculate the entire structure-borne noise component of the interior noise. In addition, engine-induced airborne noise components which are known from the interior noise simulation for a comparable vehicle can also be incorporated, and usually determine the interior noise above approximately 1 kHz.

On the one hand, this method allows the ignition order based on the FE calculation to be evaluated within the context of the overall noise, and on the other hand, it also allows the higher-frequency components to be accessed for an assessment. Thus the hybrid method allows acoustic criteria to be incorporated into important decisions at an early stage in the vehicle development process.

References

[1] Alt, N.; Wiehagen, N.; Schlitzer, M. W.: Vehicle Interior Noise Simulation for Evaluating Prototype Powertrains in the Vehicle. (Part 1 and 2). In: ATZ Worldwide 103 (2001), No 5 and 6, pp 14-16 and 23-25

[2] Eisele, G.; Wolff, K.; Dohm, M.; Abtahi, R.; Hüser, M.: Optimierung des Fahrwerksgeräusches. In ATZ 110 (2008), Nr. 3, S. 256-261

[3] Alt, N.; Wolff, K.; Eisele, G.; Pichot, F.: Fahrzeugaußengeräuschsimulation. ATZ 108 (2006), Nr. 10, S. 832-836

[4] Steffens, C.; Nussmann, C.; Pilath, C.: Virtuelle Produktentwicklung zur Verbesserung der Motor- und Getriebeakustik. Vortrag auf dem 14. Aachener Kolloquium Fahrzeug- und Motorentechnik, 4. bis 6. Oktober 2005